THESIS APPROVAL

GRADUATE SCHOOL, KASETSART UNIVERSITY

Master of Science (Chemistry)
DEGREE

Chemistry	Chemistry
FIELD	**DEPARTMENT**

TITLE: Structures and Reactivity of Propane over Nanostructured Zeolites: A Newly Developed DFT Approach

NAME: Mr. Sarawoot Impeng

THIS THESIS HAS BEEN ACCEPTED BY

....	**THESIS ADVISOR**
(Mr. Somkiat Nokbin, Ph.D.)	
....	**COMMITTEE MEMBER**
(Professor Jumras Limtrakul, Ph.D.)	
....	**COMMITTEE MEMBER**
(Mr. Pipat Khongpracha, Ph.D.)	
....	**DEPARTMENT HEAD**
(Assistant Professor Noojaree Prasitpan, Ph.D.)	

APPROVED BY THE GRADUATE SCHOOL ON ....

.... **DEAN**

(Associate Professor Gunjana Theeragool, D.Agr.)

THESIS

STRUCTURES AND REACTIVITY OF PROPANE OVER NANOSTRUCTURED ZEOLITES: A NEWLY DEVELOPED DFT APPROACH

SARAWOOT IMPENG

A Thesis Submitted in Partial Fulfillment of
the Requirements for the Degree of
Master of Science (Chemistry)
Graduate School, Kasetsart University
2010

Sarawoot Impeng 2010: Structures and Reactivity of Propane over Nanostructured Zeolites: A Newly Developed DFT Approach. Master of Science (Chemistry), Major Field: Chemistry, Department of Chemistry. Thesis Advisor: Mr. Somkiat Nokbin, Ph.D. 106 pages.

The hydrogen exchange reactions of propane adsorbed over H-FAU zeolite were studied by the ONIOM(B3LYP/6-31G(d,p):UFF) approach. The H/H exchange reactions occur via both primary- and secondary hydrogen exchange mechanisms at the primary- and secondary carbon atoms of the propane molecule, respectively. These two exchange processes proceed via the carbonium ion-like transition state which is in agreement with the experiment study in literature. The corresponding apparent activation energies are calculated to be 27.3 and 26.5 kcal/mol for primary- and secondary hydrogen exchange reactions, respectively, which are close to the previous available experimental study of H/H exchange reaction over H-ZSM-5 zeolite. Our results suggested that the primary- and secondary hydrogen exchange of propane over acidic zeolite are competitive reactions.

Propane cracking over different types of zeolites was investigated using the realistic nanocluster of 120T performed at the M06-L/6-31G(d,p)//ONIOM(M06-L/6-31G(d,p):UFF) level of theory. The adsorption energies of propane for cracking reaction are predicted to be -7.6 and -9.9 kcal/mol for H-FAU and H-MOR, respectively. Using the experimental adsorption energies as the benchmark, our combined ONIOM scheme is found to represent the interaction of propane with zeolites. After adsorption, the zeolite's proton inserts into a C-C bond of a propane molecule, yielding a methane and ethoxide intermediate. Subsequently, the methane molecule is desorbed before the deprotonation of the ethoxide intermediate, resulting in the formation of the ethylene product. The protonation step is found to be rate-determining with the actual activation energies of 43.7 and 41.3 kcal/mol for H-FAU and H-MOR, respectively. The activation energies for the deprotonation step are 24.7 and 18.5 kcal/mol for H-FAU and H-MOR, respectively. Our findings suggest that the propane cracking was insensitive to the zeolite structure.

____________________________ ____________________________ ___ / ___ / ___

Student's signature Thesis Advisor's signature

ACKNOWLEDGMENTS

First, I would like to thank my advisor, Dr. Somkiat Nokbin for his helpful comments, excellent advice, discussion and support throughout the duration of my graduate study and research. Professor Jumras Limtrakul, my co-advisor, is gratefully acknowledged for the excellent opportunity given me, valuable assistances, exceptionally helpful comments, direction and support during these years. I also thank my co-advisor, Dr. Pipat Khongpracha, for his helpful advice, comments and suggestions to fulfill this thesis work.

I would like to acknowledge the National Science and Technology Development Agency (2009 NSTDA Chair Professor funded by the Crown Property Bureau under the management of the National Science and Technology Development Agency and NANOTEC Center of Excellence funded by the National Nanotechnology Center), the Commission on Higher Education, Ministry of Education, under the Postgraduate Education and Research Programs in Petroleum and Petrochemicals, and Advanced Materials, as well as the Thailand Research Fund (TRF) for financial support. The Laboratory for Computational and Applied Chemistry (LCAC), Kasetsart University, Kasetsart University Research and Development Institute (KURDI) are gratefully acknowledged for use of their research facilities. The Kasetsart University Graduate School is also acknowledged.

I would also like to thank all of my friends and colleagues at LCAC, especially Mr. Thana Maihom and Mr. Teeranan Nongnual, for their advice, help and support during these years.

Finally, I wish to thank my caring parents for their encouragement and support.

Sarawoot Impeng
April, 2010

TABLE OF CONTENTS

Page

LIST OF TABLES

LIST OF TABLES (Continued)

LIST OF FIGURES

Figure **Page**

LIST OF FIGURES (Continued)

Figure **Page**

LIST OF FIGURES (Continued)

Figure **Page**

LIST OF FIGURES (Continued)

LIST OF FIGURES (Continued)

LIST OF ABBREVIATIONS

B3LYP = Becke’s three parameters hybrid functional using the Lee-Yang-Parr correlation functional
BEA = Beta zeolite
BH&HLYP = Becke’s half-and-half (BH&H) non-local exchange with Lee–Yang–Parr (LYP) correlation functional
CBS-QB3 = Quadratic complete basis set with B3LYP density functional theory geometry
DFT = Density functional theory
DZPV = Double-zeta plus polarization
FAU = Faujasite zeolite
HF = Hartree-Fock
K = Kelvin
kcal/mol = Kilocalories/mol
LDA = Local density approximation
M05 = Minnesota 2005
M06 = Minnesota 2006
MAS = Magic-Angle-Spinning
MM = Molecular mechanics
MOR = Mordenite zeolite
MP2 = The second-order Møller-Plesset perturbation theory
NMR = Nuclear magnetic resonance
ONIOM = Our-own N-layered Integrated molecular Orbital and molecular Mechanics
QM = Quantum mechanics
QM/MM = Quantum mechanics/molecular mechanics
T = Tetrahedral
UFF = Universal force field
ZSM-5 = Zeolite socony mobil 5

STRUCTURES AND REACTIVITY OF PROPANE OVER NANOSTRUCTURED ZEOLITES: A NEWLY DEVELOPED DFT APPROACH

INTRODUCTION

Nowadays, zeolite is one of the most important heterogeneous catalysts. Zeolites are a fascinating, nanostructured material with three-dimensional framework structures. They are broadly used as catalysts in the modern oil refining and petroleum industry. There are many types of zeolites available, they are found in nature and they can also be synthesized. Thus, the different structural topologies in various kinds of zeolite provide different properties such as size-shape selectivity, ion-exchange and catalysis. Furthermore, zeolites are environmentally friendly, have high activity and thermal stability. Because of its interesting catalytic properties, much interest has emerged in the area of zeolite catalysts. As a catalyst perspective, acidic zeolite can be generated by the following steps: Generally, zeolites are composed of Si and O atoms in the structure. The framework structures of zeolites are made from sharing one oxygen atom between two tetrahedral of SiO_4. When Si^{4+} atoms are replaced by Al^{3+} atoms, the negative charges in the framework exist and will be counterbalanced by the by positive charge cations, such as proton (H) or the alkali ions. In the case that the proton is selected to compensate the negative charge of the system, the generation of an acidic hydroxyl group called the Brønsted acid site forms (Figure 1). The Brønsted acid site of zeolites plays an important factor in its catalytic property. In addition, the other factors from different types of zeolite such as pore sizes and channel in each zeolite are also important factors in its catalytic property.

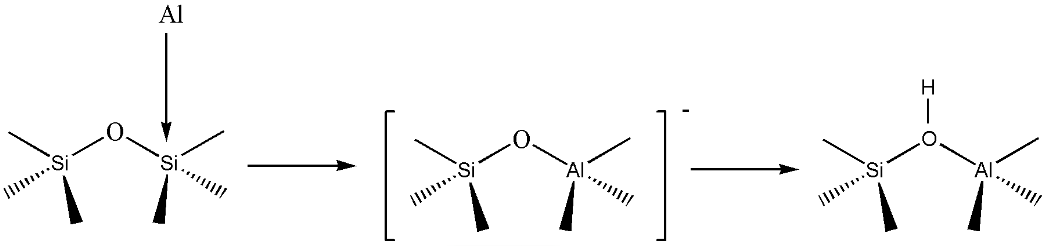

Figure 1 The formation of the Brønsted acid site in zeolite.

Two types of zeolite are used in this study, namely faujasite (FAU) and mordenite (MOR) because of their wide use in cracking processes (Narbeshuber *et al.*, 1995; Babitz *et al.*, 1999; Xu *et al.*, 2006; Jiang *et al.*, 2008). The cracking process is a significant reaction process in the petrochemical industry. Beside the cracking reaction, zeolites are also used in many other petrochemical processes such as dehydrogenation (Narbeshuber *et al.*, 1997; Milas and Nascimento, 2005), alkylation (Becker *et al.*, 1973; Reddy *et al.*, 1993; Corma *et al.*, 2000; Solans-Monfort *et al*, 2002) and isomerization (Klepel *et al.*, 2003; Martin *et al.*, 2005) of hydrocarbons, for example. The faujasite structure is formed by a wide supercage (13 Å) accessed through 12-membered silicate rings with 7.4 Å diameter. This zeolite is a three-dimensional channel (Figure 2a). Mordenite structure consists of the two types of one-dimensional channel: the 12- and 8-membered ring (MR) channels. The straight 12 MR channel (6.5 x 7.0 Å) is perpendicularly interconnected by the 8 MR side pockets (2.6 x 5.7 Å) (Figure 2b).

The conversion reactions of hydrocarbons catalyzed by zeolites are not clearly understood. Because of complicated reaction mechanisms and various simultaneous reaction pathways, the mechanisms of hydrocarbon conversion in acidic zeolites (heterogeneous phase) assumed to have an analogy with traditional organic chemistry in superacidic solution (homogeneous phase) (Poutsma *et al.*, 1976; Olah *et al.*, 1987, 1995). These mechanisms assumed that the proton transfer from Brønsted acid sites of the zeolites to an alkene creates trivalent carbenium ion intermediates. Whereas, the protonation of an alkane at C-C or C-H bonds leads to non-classical pentacoordinated carbonium ions that are unstable in the channel of zeolites which dissociates to form carbenium ions and smaller alkane or hydrogen (Figure 3). The carbenium ions intermediates in the zeolite, in contrast to the superacidic solution, form a covalent bond with the framework of the zeolites resulting in the existence of long-lived alkoxide intermediates (Haw *et al.*, 1989, 1996).

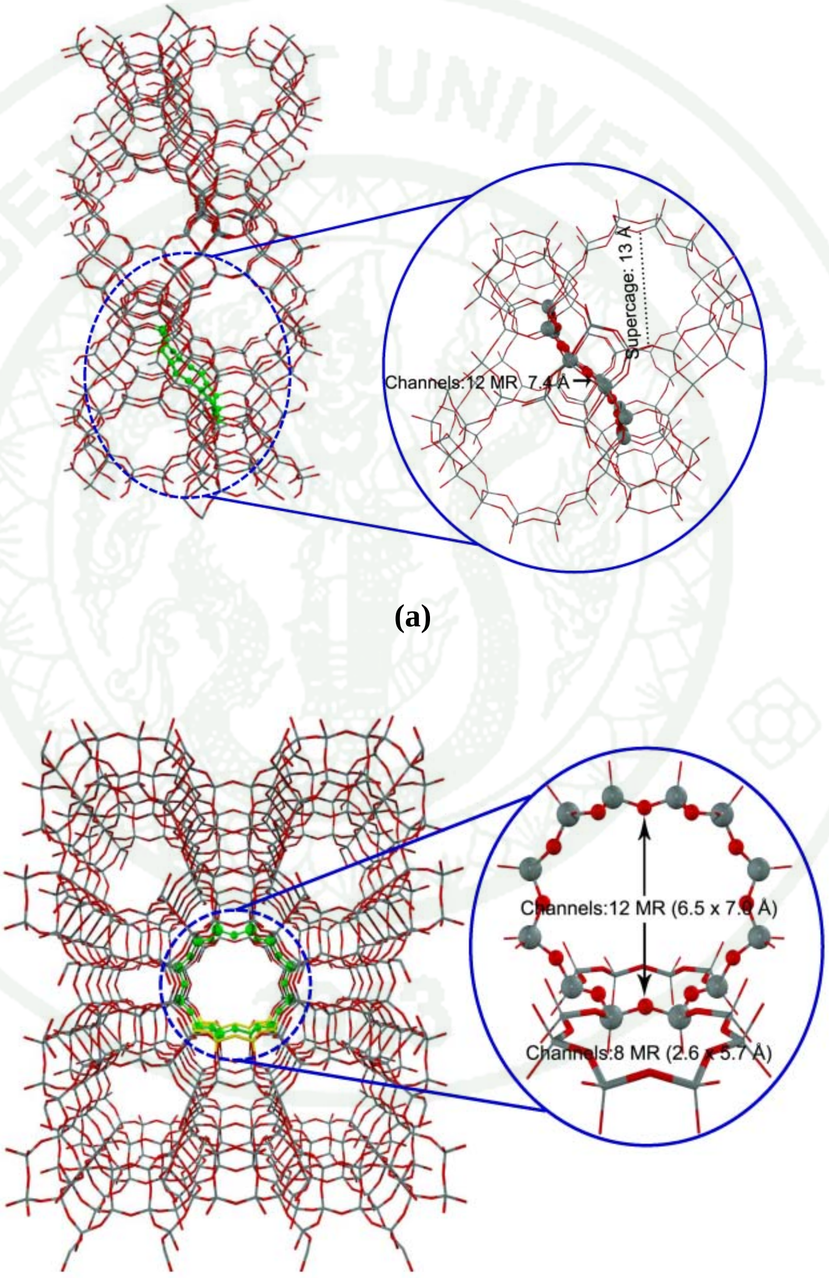

(a)

(b)

Figure 2 The illustration of (a) FAU and (b) MOR zeolites.

Specifically, the proton transfer from the Brønsted acid site of zeolites to an adsorbed hydrocarbon molecule is the major step in acid catalysis by zeolites. However, this step is not clearly understood at the atomic level. In particular, the protonated species are not well characterized and it is not known whether that proton transfer to an alkane molecule produces a carbonium-like ion as a transition state (Blaszkowski *et al.*, 1996; Kazansky *et al.*, 1994, 1996, 1999; Lercher *et al.*, 1994, Zygmunt *et al.*, 2000; Zheng and Blowers, 2005) or a stable intermediate on a reaction coordinate (Boronat *et al.*, 2008; Hunter and East, 2002; Collins and O'Malley, 1995a, 1995b). However, the carbonium ions are very active ions that are difficult to observe with *in situ* study due to their short-lived lifetime and theoretical investigation becomes a practical tool for their study (Hunter and East, 2002).

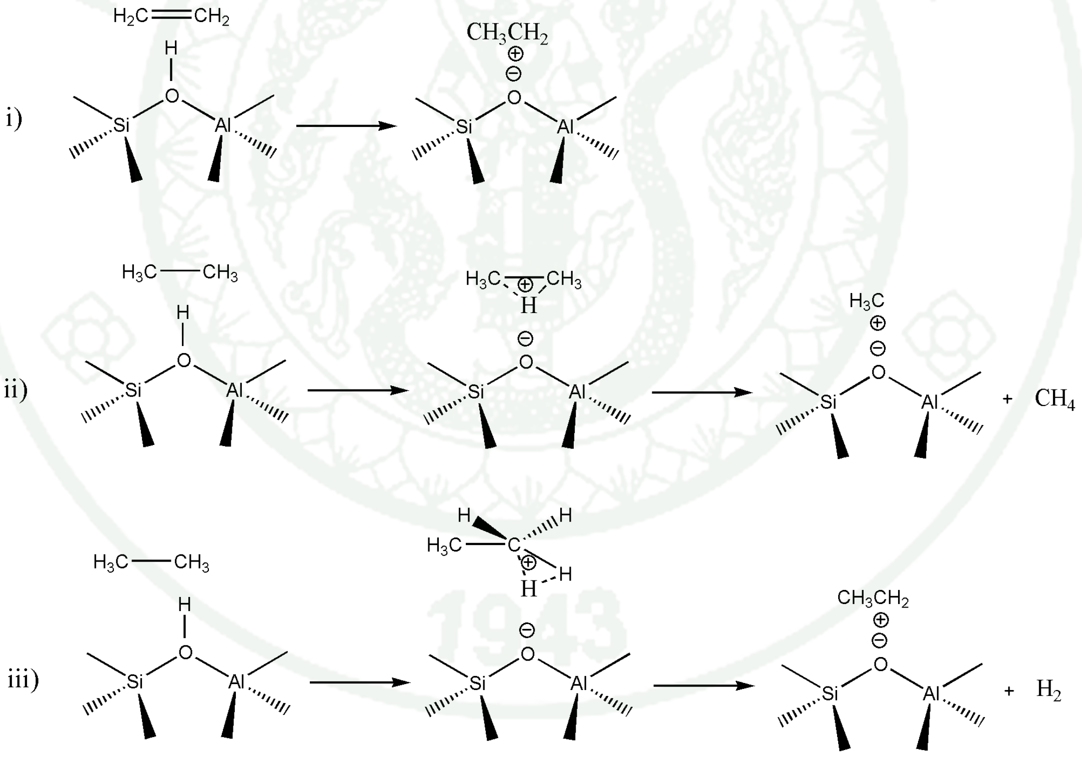

Figure 3 The formation of (i) carbenium ion and (ii, iii) carbonium ion in zeolite.

From the literature, the theoretical study of alkane conversion reactions over zeolites has been investigated using only small clusters (3T, 5T) of zeolite (T=tetrahedral Si or Al atom) (Blaszkowski *et al.*, 1996; Kazansky *et al.*, 1994, 1996, 1999; Zygmunt *et al.*, 2000; Zheng and Blowers, 2005a, 2005b, 2005c, 2006; Hunter and East, 2002; Collins and O'Malley, 1995a, 1995b, Esteves *et al.*, 1999; Ryder *et al.*, 2000). The framework, pore size and shape effect of zeolite were neglected in such a small model. These omissions can significantly change the structure and energy of the system and thus lead to incorrect reaction pathways. In order to include the zeolite framework effect and to reduce the computational cost of calculation, hybrid methods were developed, such as the embedded cluster, combined quantum mechanics/molecular mechanics (QM/MM) methods (Greatbanks *et al.*, 1996; Brandle *et al.*, 1998; Khaliullin *et al.*, 2001; Limtrakul *et al.*, 2001), our-Own-N-layer Integrated molecular Orbital + molecular Mechanics (ONIOM) method (Svensson *et al.*, 1996; de Vries *et al.*, 1999). From our previous study, the ONIOM method has been successfully employed to study the adsorption properties and the reaction mechanisms of organic molecules over different types of zeolite catalysts (Maihom *et al.* 2008; Jansang *et al.* 2007, 2008; Pantu *et al.*, 2007; Namuangruk *et al.*, 2006a, 2006b; Pabchanda *et al.*, 2005; Kasuriya *et al.*, 2003;).

For a small alkane, propane provides good conversion reactions for characterizing and establishing the relationship between their structure and catalytic activity, including clarifications on the mechanism of an alkane conversion on the surface of the zeolites. Three propane conversion reactions are possible, i.e., (i) Cracking, (ii) Dehydrogenation and (iii) Hydrogen exchange reaction. The cracking reaction of propane is the process that breaks propane into methane and ethylene products through C-C bond scission. For the dehydrogenation reaction, the zeolite's proton transfers into the C-H bond of the propane molecule, resulting in the breaking of the C-H bond and the generation of a hydrogen molecule and a propylene product. Beside cracking and dehydrogenation reactions, a propane molecule is exchanged hydrogen (proton) with the Brønsted acid site of zeolite.

In this thesis, two different propane conversion reactions over nanostructured zeolites were investigated, i.e., 1) the hydrogen exchange reaction and 2) the cracking reaction. In the first reaction, we studied the hydrogen exchange reaction of propane adsorbed only over H-FAU zeolite by the ONIOM(B3LYP/6-31G(d,p):UFF) method.

In the second reaction, we investigated the cracking reaction of propane over H-FAU and H-MOR zeolites with the ONIOM method [ONIOM(B3LYP/6-31G(d,p):UFF) and ONIOM(M06-L/6-31G(d,p):UFF)].

The objectives in this thesis are stated below:

1. H/H Exchange Reaction of Propane Adsorbed over H-FAU Zeolite Investigated by the ONIOM method

1) To study the influence of the zeolite topology on structures and energetic profiles of the hydrogen exchange reaction.

2) To investigate the reaction pathways of the H/H reaction between the propane molecule and the Brønsted acid of zeolite in which the H/H exchange takes place at the primary carbon and the secondary carbon of the propane molecule.

2. Propane Cracking Reaction over Different Types of Nanostructured Zeolites: A Newly Developed DFT Approach

1) To investigate the reaction mechanism of the propane cracking reaction over H-FAU and H-MOR zeolites and answer the question whether the mechanism proceeds via a carbonium ion transition state or a stable carbonium ion on reaction coordinates.

2) To investigate the influence of zeolite topology on structures and energetic profiles of the cracking reaction.

3) To compare the efficiency of the density functional between B3LYP and M06-L methods for the propane cracking reaction over zeolite.

LITERATURE REVIEW

1. H/H Exchange Reaction of Propane Adsorbed over H-FAU Zeolite Investigated by the ONIOM method

Zeolite is one of the important heterogeneous catalysts for many industrial processes due to its high activity, selectivity and environmentally friendliness. One of the industrially important zeolites is faujasite (FAU). In particular, its protonic form (H-FAU), which can be used as a catalyst in many reaction processes such as *n*-alkane cracking, dehydrogenation and isomerization of hydrocarbons. However, the reactivity of alkane over the acid zeolite is not clearly understood. The alkane activation is usually accompanied by hydrogen exchange. The hydrogen exchange reaction involves the C-H bond breaking and C-H bond formation between alkanes and the Brønsted acid site of zeolite. Various experimental and theoretical studies were carried out, in order to clarify both the mechanism of the hydrogen exchange itself and its relation to the dehydrogenation and cracking reaction of alkanes.

For small alkanes (methane and ethane), only primary protons are available, the hydrogen exchange reaction proceeds in a concerted step involving a carbonium ion with pentacoordinated carbon atom. The non-classical carbonium ions having a three-center/two-electron bond was first detected in a mass spectrometry experiment (Tal’roze and Lyubimova, 1953:2590), only in the gas phase. The H/H exchange of methane and ethane with the Brønsted acid site of zeolite has been investigated by several groups (Kramer *et al.*, 1993, 1995; Evleth *et al.*, 1994; Blaszkoski *et al.*, 1996; Lins and Nascimento, 1996; Lee *et al.*, 1999). For example, Kramer *et al.* (1993) studied the hydrogen exchange reaction of a methane molecule on acidic ZSM-5 and FAU zeolites by means of IR spectroscopy and ab initio calculations. At the low partial pressure of methane, the mechanism of hydrogen exchange proceeds in a concerted step involving a carbonium ion with pentacoordinated carbon atom. In their study, the apparent activation energy for H-ZSM-5 and H-FAU were reported to be ~31 kcal/mol.

In 1996, Blaszkowski *et al.* studied the hydrogen exchange of ethane catalyzed by a protonated zeolite using a 3T cluster model at the LDA/DZPV level of theory. They found that the carbonium ion is the transition state (on the reaction coordinate). The activation barrier for the hydrogen exchange of ethane with respect to the reactant in the gas phase, including zero point energy (ZPE) corrections, was found to be 28.2 kcal/mol.

For alkanes with three or more carbon atoms, the mechanism of the hydrogen exchange is not clearly reported as to whether the reaction proceeds via the carbonium ion as a transition state or the carbenium ion intermediates. Stepanov *et al.* (1998, 2005) and Arzumanov *et al.* (2005) studied the mechanism of H/D exchange between deuterated propane and the H-ZSM-5 zeolite by *in situ* H^1 and C^{13} MAS NMR spectroscopy in the temperature range of 500-550 K. The hydrogen exchange was found to occur directly between the methyl or methylene group (primary or secondary carbon of propane) of propane and the Brønsted acid site of zeolite via the pentacoordinated carbonium ion transition state. Moreover, regioselectivity between methyl (CH_3) and methylene (CH_2) groups of propane was observed. The exchange process with the methyl group is faster than that of the methylene group. This accounts for the regioselectivity of the exchange propane over acidic zeolites (Sommer *et al.*, 1995). The intramolecular hydrogen transfer between the methyl and methylene groups is one order of magnitude slower than the hydrogen exchange of both the groups with the Brønsted acid site of zeolite. The apparent activation energy for the exchange in the methyl group and methylene group were reported to be 25.8±1.7 and 28.0±1.7 kcal/mol, respectively.

In contrast, Haouas *et al.* (2003) studied the H/D exchange reaction of propane over sulfated zirconia-based catalysts. At low temperature (323 K), the hydrogen exchange process between propane and sulfated zirconia-based catalysts occurred only for the methyl group of propane, but this reaction exists for both the methyl and methylene groups of propane at higher temperature. However, the rate of the H/D exchange in the methyl groups is higher than the methylene group. In their result, an important regioselectivity for the H/D exchange (is that only methyl hydrogen is exchanged) is observed. Finally, they suggested that the hydrogen reaction occurs via the formation of propene and isopropyl carbenium ion intermediates in their proposed catalytic cycle. In addition, the study of the H/D exchange of isobutane over acidic zeolites using different spectroscopy techniques by many research groups (Engelhardt and Hall, 1995; Sommer *et al.*, 1999; Schoofs et al., 2000; Hua et al., 2001) reported that the reaction mechanism proceeds via carbenium ion.

Several theoretical investigations of the H/H exchange reaction of alkane adsorbed over acidic zeolites have been reported. In 1999, Esteves and coworker (Esteves *et al.*, 1999) investigated the H/H exchange reactions of light alkanes such as methane, ethane, propane, and isobutane on the 3T cluster model of acidic zeolite by the B3LYP/6-31G(d,p) and MP2/6-31G(d,p)//HF/6-31G(d,p) methods. In this work, the transition state resembles a pentacoordinated carbonium ion and the corresponding activation barriers for all light alkane exchange reactions, calculated by the B3LYP/ 6-31G(d,p), were similar (ca. 30 kcal/mol). The result implies that the reactivity of the alkanes C-H bonds on the zeolite surface is the same, regardless of being interacted at the primary carbon, secondary carbon (in the case of the propane molecule), or tertiary carbon (in the case of the isobutane molecule). Ryder *et al.* (2000) studied the hydrogen exchange reaction of the propane molecule on a 5T cluster model of zeolite at the BH&HLYP/6-31++G(d,p) level of theory. The apparent activation energies were reported to be 40.5 and 39.2 kcal/mol for the hydrogen exchange reaction at the primary carbon and the secondary carbon, respectively.

Zheng and Blowers (2005a, 2005b, 2005c, 2006) investigated the H/H exchange reaction for methane, ethane, propane, butane, and isobutane using a 3T cluster model of acidic zeolite. All geometries were optimized at the B3LYP/6-31 G(d) level of theory and the energies were calculated with CBS-QB3 using a high-level complete basis set composition energy method. They found that the computed activation barriers decrease slightly with increasing hydrocarbon length starting from 33.5 kcal/mol (for methane) to 29.5 kcal/mol (for the methyl group of butane). Moreover, the activation barriers of the hydrogen exchange reactions at different carbon atoms, between 1° C and 2° C in propane and between 1° C and 3° C in isobutane, were less than 1 kcal/mol.

2. Propane Cracking Reaction over Different Types of Nanostructured Zeolites: A Newly Developed DFT Approach

Because of its great importance in the petroleum industry, the cracking of hydrocarbons has been of immense interest in both the academic and the industrial sectors throughout the 20th century. Acidic zeolites are widely used as solid catalysts for the cracking reaction due to their environmentally friendliness, high activity, size-shape selectivity, and thermal stability. Moreover, microporous structures in zeolite provide a large internal surface and selectivity effect that relate to diffusion of the reactant, steric constraint on intermediates and transition state, and products within the pore system (Corma, 2003; van Santen and Kramer, 1995; Weitkamp and Traa, 1999).

From the experimental studies (Haag *et al.*, 1984: 305, Corma *et al.*, 1985), the mechanisms of alkanes catalytic cracking over the Brønsted acid site in zeolites were suggested to exist either via (1) bimolecular or (2) monomolecular mechanisms, depending on the reaction conditions: High reactant pressure, high conversion, and low temperature favor the bimolecular mechanism. Instead, low reactant pressure, low conversion, and high temperature favor the monomolecular mechanism. In the bimolecular mechanism, an alkane is activated by hydride transfer between the alkane and the adsorbed alkoxide followed by β-scission and the rate limiting step is the hydride transfer (Haag *et al.*, 1991). In the monomolecular mechanism, an alkane is protonated by the Brønsted acid site of acid zeolite at the C-C bond to form non-classical pentacoordinated carbonium ions. This protonation step of the alkane is reported to be the rate limiting step (Narbeshuber *et al.*, 1995). The monomolecular cracking mechanism, also known as the protolytic cracking, Haag-Dessau cracking mechanism, and carbonium ion cracking mechanism, is now of wide research interest, with *in situ* study (Narbeshuber et al., 1995; Babitz *et al.*, 1999; van Bokoven *et al.* 2001, 2004; Xu *et al.*, 2006a, 2006b, 2007) and with several theoretical investigations

(Collins and O’Malley, 1995a, 1995b; Kazansky *et al.*, 1994, 1996; Blaszkowski *et al.*, 1996; Rigby *et al*, 1997; Zygmunt *et al.*, 2000; Hunter and East, 2002; Zheng and Blowers, 2005a; Boronat and Corma, 2008). However, the carbonium ions are very active ions that are difficult to observe with *in situ* study due to their short-lived lifetime and theoretical investigation becomes a practical tool for their study. In order to get a better understanding on the monomolecular cracking mechanism of alkane over zeolites, previous experimental studies as well as previous theoretical investigations available in the literature are discussed to gain understanding of the influence of the local structure of the acid sites, rate-limiting step and intrinsic activity of monomolecular cracking of the alkane molecule over zeolites.

In 1995, Narbeshuber *et al.* studied the monomolecular conversion of C3-C6 alkanes over H-ZSM-5. They found that the alkane is protonated by the Brønsted acid site that is reported to be the rate limiting step. The intrinsic activation energy of the propane cracking reaction is about 48 kcal/mol. Later, the cracking reaction of *n*-hexane on ZSM-5, MOR, and Y zeolites were studied by Babitz *et al.* (1999). They found that the intrinsic activation energy of *n*-hexane cracking is insensitive to the difference in the acid strength among ZSM-5, MOR, and Y zeolites, but, is strongly dependent on the adsorption energies of *n*-hexane in the zeolites.

In 2001, van Bokhoven *et al.* studied light alkane conversion in mild steam dealuminated mordenite (H-MOR). They found that the enhanced activity for alkane cracking over zeolite mordenite was explained in terms of increased sorption of the reactant in the pores of the steamed zeolite. Subsequently, in 2004, van Bokhoven *et al.* studied the alkane cracking reaction on different zeolite structures. In this study, the rate of *n*-hexane cracking increases in the order of H-Y < H-MOR < H-ZSM-5 and the corresponding adsorption energies for *n*-hexane on H-Y, H-MOR and H-ZSM-5 were reported to be 50, 69, 86 kJ/mol, respectively. This suggests that the reaction rate strongly depends on the adsorption energy in the system, which is in good agreement with the report by Babitz *et al.* (1999).

Xu *et al*. (2006a, 2007) studied the catalytic activity of the Brønsted acid site in different zeolite types (H-ZSM-5, H-MOR, H-BEA and H-FAU) by the monomolecular conversion of propane. The intrinsic activation energy of propane cracking reactions were 46.2, 44.5-45.4, 47.3-48.1 and 46.9 kcal/mol for H-ZSM-5, H-MOR, H-BEA and H-FAU zeolites, respectively. They concluded that the activity of the Brønsted acid site depended on the rate-limiting step of the reaction. The cracking reaction of alkane proceeds via protonation of the alkane as the rate-limiting step. Moreover, the size and shape of the pore in the zeolites is reported to play an important role on the heat of adsorption (adsorption energy). They also suggested that zeolites suitable for the propane cracking reaction are in the order of ZSM-5 $\geq$ H-MOR > Beta > FAU. In addition they studied the structure collapse and the reconstruction of Brønsted acid in zeolite Y by the propane cracking reaction. The intrinsic activation energy of the propane cracking reaction over H-Y zeolite was reported to be 49.7 kcal/mol (Xu *et al.*, 2006b).

As for theoretical studies, the monomolecular cracking mechanisms of alkane over acidic zeolites have been investigated by several research groups. Two major different pathways were as a result of the existence of the carbonium species in the system. The carbonium ion species were reported to be the transition state (Kazansky *et al.*, 1994, 1996; Blaszkowski *et al.*, 1996; Zygmunt *et al.*, 2000; Zheng and Blowers, 2005) or as thermodynamically stable intermediated at local minimum on potential energy surface (Collins and O’Malley, 1995a, 1995b; Hunter and East, 2002; Boronat and Corma, 2008).

Collins and O’Malley (1995b) investigated the *n*-butane cracking on the 1T zeolite cluster model with the BLYP/3-21G(d); they found the carbonium-like ion intermediate which directly breaks into smaller alkane and alkene products. Nevertheless, with the 3T cluster model they found such structures to be carbonium-like ion transition states instead. In this work, the zeolite model shows a significant role in the existence of the stable structure on the potential energy surface. In 1996, Blaszkowski and coworker studied the activation of C-H and C-C bonds of ethane by an acidic zeolite. In their study of the ethane cracking reaction on the 3T cluster model of acidic zeolite with LDA/DZPV, they found the two different transition states with the same activation barrier and this transition state is a rather ionic carbenium ion which would crack into a methoxide intermediate formed covalent bond with a surface of zeolites and a methane molecule. Kazansky *et al.* (1999) studied isobutane cracking on a 1T zeolite cluster model with HF/6-31G(d) level of theory. They concluded that the carbonium-like ion is not the real reaction intermediate but is, instead, the high-energy transition state. However, Zygmunt *et al.* (2000) studied ethane cracking using HF/6-31G(d) with a 5T cluster model of H-ZSM-5 zeolite. They found that the carbonium-like ion as the transition state is not a stable species on the potential energy surface, thus this ion breaks in to methane and methoxide intermediates.

In 2008, on the other hand, Boronat and Corma (2008) studied *n*-butane cracking on acidic Theta-1 zeolite using various sizes of zeolite models starting from 3T to 27T (3T → 5T → 11T → 27T) at B3PW91/6-31G(d) level of theory. The 3T, 5T and 11T model clusters were optimized and these models did not represent the pore and framework of the zeolite theta-1. The single point energy calculations for the 27T cluster, including the zeolite's environment by the embedding of the optimized structure of the 11T model into the 27T, was carried out. In their work, the carbonium ion exists as an intermediate species adsorbed on the zeolite active site. From all theoretical study reviews, it is still uncertain whether the formation of the carbonium ion is the transition state or the stable carbonium ion intermediate in the cracking reaction.

In addition, theoretical studies have investigated the propane cracking reaction. The activation energy of the rate-limiting step (protonation step) is about 68.0 kcal/mol by using the 3T cluster model with the MP2/6-31G(d)//HF/3-21G correction method (Rigby *et al*, 1997). In 2005, Zheng and Blowers investigated the propane cracking reaction using the 3T cluster model. All geometries were optimized at the B3LYP/6-31G(d) level of theory, and the energies were calculated with CBS-QB3, a high-level complete basis set composition energy method. The computed activation barriers were 62.1 and 62.6 kcal/mol for two different transition states (the breaking bond C1-C2 of the propane molecule stay in the same plane and perpendicular as the zeolite cluster, respectively).

METHODS OF CALCULATIONS

1. Methodologies

In this thesis, the Density Functional Theory (DFT), the Universal Force Field (UFF) and the Our-own N-layered Integrated molecular Orbital and molecular Mechanics (ONIOM) approaches are selected as the methods used in the investigations of the H/H exchange reaction and the cracking reaction of propane adsorbed over nanostructured zeolite. It is important to understand the background theory of these methods. Thus, the descriptive details of these three methodologies are summarized in this section.

1.1 Density Functional Theory (DFT)

Nowadays, the *Density Functional Theory* (DFT) is a widely used technique for computational chemistry because it provides a good relationship between computational cost and accuracy. The concept of DFT is that the ground-state energy of a system is a functional of the electron density (ρ), $E[\rho]$ and the electron density is a function of position (r), $\rho(r)$. The ground-state energy of an n-electrons system can be written as:

$$E[\rho] = T[\rho] + E_{ne}[\rho] + E_{ee}[\rho] + E_{XC}[\rho] \tag{1}$$

where; $T[\rho]$ is the total electron kinetic energy
$E_{ne}[\rho]$ is the electron-nucleus potential energy
$E_{ee}[\rho]$ is the electron-electron potential energy
$E_{XC}[\rho]$ is the exchange-correlation energy

However, the major problem of DFT is that the exact value of the exchange-correlation energy (E_{XC}) is not known and, therefore, the approximate functional has been implemented. Many types of the E_{XC} functionals are available, such as the local density approximation (LDA), the generalized gradient approximation (GGA), and the hybrid functional.

In the *Local Density Approximation* (LDA) it is assumed that the electron densities are treated as uniform electron gas. This approximation provides large errors for the prediction of the interesting properties in the chemistry system such as bond distances and binding energy. For this reason, the improvement over the LDA approximation is considered by the explanation of electron density in terms of a non-uniform electron gas as described in the *Generalized Gradient Approximation* (GGA). The GGA functionals include the derivation of the electron density. Many GGA functionals are available, such as PBE (developed by Perdew in 1986), BLYP (a combination of the Becke exchange (Becke, 1993) and the correlation developed by Lee, Yang and Parr (Lee *et al.*, 1988)). The *Hybrid functional* has also been proposed. One of the widely used functionals is the B3LYP (Becke, 1993; Lee *et al.*, 1988). However, this functional cannot provide a good result for some systems, e.g., the system consisting of the non-covalent interaction of hydrocarbon in zeolite systems. To overcome such problems, Zhao and Truhlar (2006c) recently introduced the new local functional namely M06-L. The functional is designed to capture the main dependence of the exchange-correlation energy on local spin density, spin density gradient, spin kinetic energy density, and their reduced gradient and it is parameterized to satisfy the uniform electron gas limit. Since the M06-L is included with spin kinetic energy density, this functional may be classified as a meta-generalized gradient approximation (meta-GGA). The details of M06-L functional are explained in Zhao and Truhlar paper (2006c). The very brief details of M06-L functional are described below:

The M06-L exchange-correlation can be written as:

$$E_{XC}^{M06\text{-}L} = E_X^{M06-L} + E_C^{M06-L} \tag{2}$$

where E_X^{M06-L} is the M06-L exchange functional and E_C^{M06-L} is the M06-L correlation functional. In particular, the M06-L exchange functional is given by:

$$E_X^{M06-L} = \sum_{\sigma} \int dr \left[F_{X\sigma}^{PBE}(\rho_\sigma, \nabla\rho_\sigma) f(\omega_\sigma) + \varepsilon_{X\sigma}^{LSDA} h_x(x_\sigma, z_\sigma) \right] \tag{3}$$

In Eq. 3, Zhao and Truhlar alter the PBE exchange, $F_{X\sigma}^{PBE}(\rho_\sigma, \nabla\rho_\sigma)$ and the LSDA exchange, $\varepsilon_{X\sigma}^{LSDA}$ by enhancement functions spin kinetic energy density, $f(\omega_\sigma)$ and the special exchange function which is based on Voorhis and Scuseria's (1998) local exchange functional, $h_x(x_\sigma, z_\sigma)$.

The E_C^{M06-L} is derived from the PBE functional with enhancement functions *g* and *h*

$$E_C^{\alpha\beta} = \int e_{\alpha\beta}^{UEG} \left[g_{\alpha\beta}(x_\alpha, x_\beta) + h_{\alpha\beta}(x_{\alpha\beta}, z_{\alpha\beta}) \right] dr \tag{4}$$

$$E_C^{\sigma\sigma} = \int e_{\sigma\sigma}^{UEG} \left[g_{\sigma\sigma}(x_\sigma) + h_{\sigma\sigma}(x_\sigma, z_\sigma) \right] D_\sigma dr \tag{5}$$

where $E_C^{\alpha\beta}$ and $E_C^{\sigma\sigma}$ in Eqs. (4) and (5) are the UEG (uniform electron gas) correlation energy density for antiparallel spin and parallel spin cases and D_σ is the self-interaction correction factor. The defined enhancement functions *g*, *h* and D_σ explained in Zhao and Truhlar's paper (2006c). Significantly, D_σ vanished for any one-electron system. After the integral process, the total correlation energy of the M06-L correlation functional can be written as:

$$E_C = E_C^{\alpha\beta} + E_C^{\alpha\alpha} + E_C^{\beta\beta} \tag{6}$$

where $E_C^{\alpha\beta}$ is the correlation energy from αβ anti-parallel spin, $E_C^{\alpha\alpha}$ is the correlation energy from αα parallel spin, and $E_C^{\beta\beta}$ is the correlation energy from ββ parallel spin. Note that α and β denotes the spin angular momentum and takes on two values: α(+1/2) and β(-1/2).

The hybrid functional has also been proposed. One of the most popular funtionals is B3LYP (Becke, 1993; Lee *et al.*, 1988) defined by eqs. (7):

$$E_{XC}^{B3LYP} = (1-a)E_X^{LSDA} + aE_X^{exact,HF} + bE_X^{B88} + (1-c)E_C^{VWN} + cE_C^{LYP} \tag{7}$$

where the parameters *a*, *b*, and *c* are determined by fitting to experimental data with typical values being *a* ~ 0.2, *b* ~ 0.7, and *c* ~ 0.8. The exchange energy includes the local spin density exchange E_X^{LSDA}, exact HF exchange energy functional $E_X^{exact,HF}$, and the Becke88 (Becke, 1988) GGA exchange energy functional E_X^{B88}. The correlation energy is obtained by the local Vosko-Wilk-Nusair (Vosko *et al.*, 1980) correlation functional E_C^{VWN}, and the Lee-Yang-Parr (Lee *et al.*, 1988) local and GGA correlation functional, E_C^{LYP}.

1.2 Universal Force Field (UFF)

The *Universal Force Field* (UFF) (Rappé *et al.*, 1992) is one of the force field methods or molecular mechanics (MM). The central idea of the MM is that the electronic motions are ignored and the energy of the system (molecules) is calculated as a function of the nuclear position only. Each atom and bond in molecules is considered as balls and springs, respectively. The force field is utilized to describe the intra- and intermolecular forces of atoms within the system. The force field energy is written as a sum of terms, each describing the energy required distorting a molecule in a specific fashion:

$$E_{total} = E_{intra} + E_{inter} \tag{8}$$

and;

$$E_{intra} = E_{str} + E_{bend} + E_{tors} \tag{9}$$

$$E_{inter} = E_{vdW} + E_{el} \tag{10}$$

where, E_{str} is the energy function for stretching a bond between two atoms, E_{bend} is the energy for bending an angle, E_{tors} is the torsional energy for rotation around the bond, E_{vdW} and E_{el} describe the non-bonded atom-atom interactions (van der Waals and electrostatic interaction, respectively).

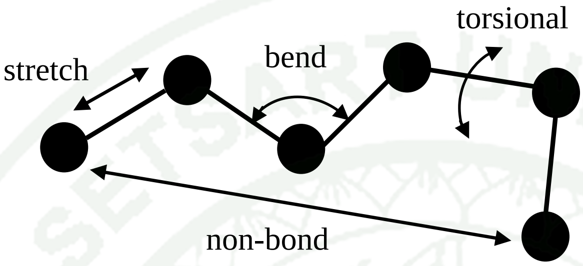

Figure 4 The illustration of the fundamental force field energy terms.

Generally, force fields refer to the mathematic equation or function forms that can represent the interaction of the interesting atom or molecules. In the zeolite system, we require to know the mathematic equation to describe the intra- and intermolecular force of zeolite. Thus, the function form which can explain the distance of Al-O and Si-O bonds, including the Si-O-Si or Si-O-Al bond angle for the intramolecular force of zeolites is required, for example.

Several force fields were developed such as MM2, and MM3 (Allinger *et al.*, 1977, 1989) to describe the general molecules. This force field applying to studies of inorganic material such as zeolite. However, this force field cannot describe the zeolite system. In addition, many force fields were developed, such as Assisted Model Building and Energy Refinement (AMBER) (Cornell *et al.*, 1995) and Chemistry at HARvard Molecular Mechanics (CHARMM) (Brooks *et al.*, 1983) to specifically describe the protein, nucleic acids and carbohydrates system, for example.

The UFF force field was developed by Rappé and co-worker (1992). This force field provides a good description of the dynamic of zeolite and is widely used to represent the environment effect (confinement effect) in the ONIOM method. Since, the calculation of the large model (system) with quantum mechanics (such as DFT, MP2) method is not practical.

1.3 Our-own N-layered Integrated molecular Orbital and molecular Mechanics (ONIOM)

The ONIOM method was developed by Morokuma and co-worker (Svenssen *et al.*, 1996). This is a hybrid method, which can combine any number of quantum molecular orbitals, as well as molecular mechanics methods. In the ONIOM2 approach, the whole system is divided into two layers or parts, so called the inner layer and the outer layer (Figure 5). The inner layer or the active region, presented by a small part of the system, is treated by the high-level of theory (quantum mechanics calculation, QM) to accurately account for the bond breaking and bond forming during the study of the interested system. The outer layer, the rest of system, is described by a computationally less demanding method such as low level of theory QM or MM (molecular mechanics calculation) to account for the environmental effects of the interesting system.

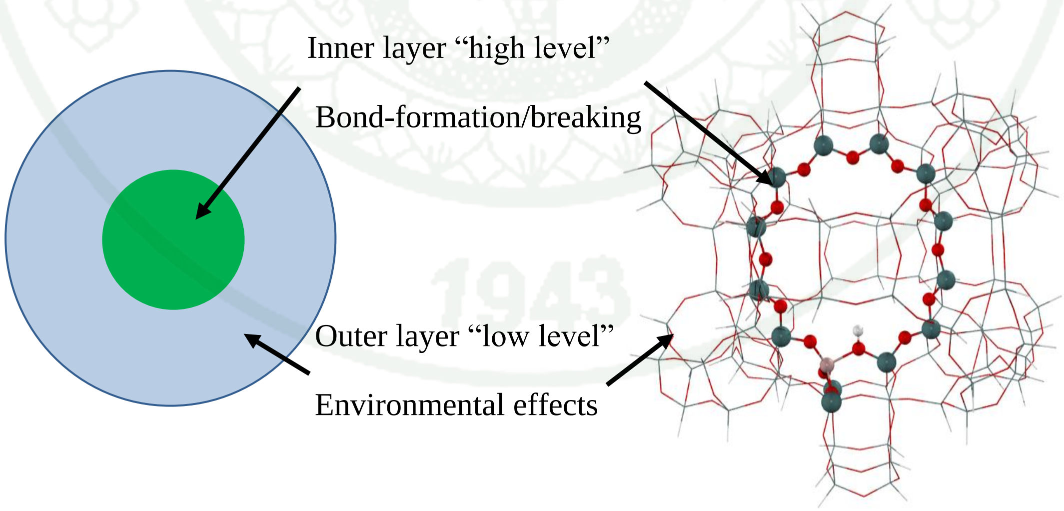

Figure 5 The ONIOM2 model in zeolite structure.

The ONIOM2 approach can be explained most easily when it is considered as an extrapolation scheme in a two-dimensional space, spanned by the size of the system on one of the axis and the level of theory on another axis. Figure 6 shows the extrapolation procedure schematically. Our goal is to describe the real system at the high level of theory, E_4 (point 4).

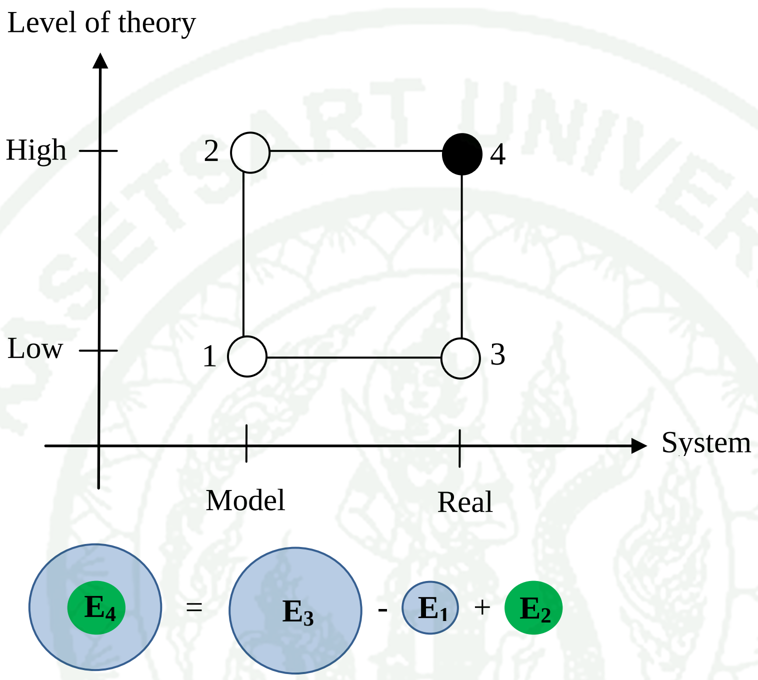

Figure 6 The two-layers ONIOM extrapolation scheme.

The extrapolation of energy at high-level of theory for the real system is estimated as:

$$E_4 = E_3 - E_1 + E_2 \tag{11}$$

or

$$E_{ONIOM\,2} = E_{Low}^{Real} - E_{Low}^{Model} + E_{High}^{Model} \tag{12}$$

where the superscript *Real* (entire) means the whole system and the superscript *Model* means the active region. Subscripts *High* and *Low* mean high- and low-level methodologies. The ONIOM2 approach in this thesis work is generally denoted as

ONIOM(High-level methodology:Low-level methodology), e.g., ONIOM(MP2/6-31 G(d,p):B3LYP/6-31G(d,p)), ONIOM(M06-L/6-31G(d,p):UFF).

The ONIOM3 scheme is also available nowadays. The typical idea of this scheme is that the system of interest is partitioned into three layers, namely the inner-, the middle- and the outer layers and such layers can be treated by the high- middle- and low-level of theories, respectively. More details of ONIOM3 can be found elsewhere (Svenssen *et al.*, 1996; Dapprich, *et al.*, 1999).

2. Models

In this thesis work, two types of zeolites, namely Faujasite (FAU) and Mordenite (MOR) were selected as catalyst supports. Only FAU zeolite was selected to study the H/H exchange reaction of propane. Both FAU and MOR zeolites were used in the propane cracking reaction in order to compare the effects of the zeolite's topology on the reaction mechanisms. Therefore, the details of models used are summarized as follow.

2.1 Faujasite (FAU) zeolite

The 120T cluster model (T=tetrahedral Si or Al atoms) of faujasite (FAU) zeolite is taken from the lattice structure database of faujasite zeolite (Olson and Dempsey, 1969). The model covers the active site, so called the Brønsted acid site, that is located at the 12-membered-ring window connected by the two supercages. The active acid site of the FAU zeolite was represented by the 14T tetrahedral quantum cluster in which the Si atom at the T1 position (Hill *et al.*, 1999) is replaced by an aluminium atom. As a result, a proton is added to one of the bridging oxygen atoms bonded directly to the aluminum atom to compensate for the charge of the system. Generally, the proton will be located at the most stable O1 position (Hill *et al.*, 1999). In this study, the corresponding stable proton site is conventionally labeled as O1 in texts as well as in figures (see Figure 7, drawn as ball and stick). The zeolitic framework environment, the remaining region, was drawn as a line structure.

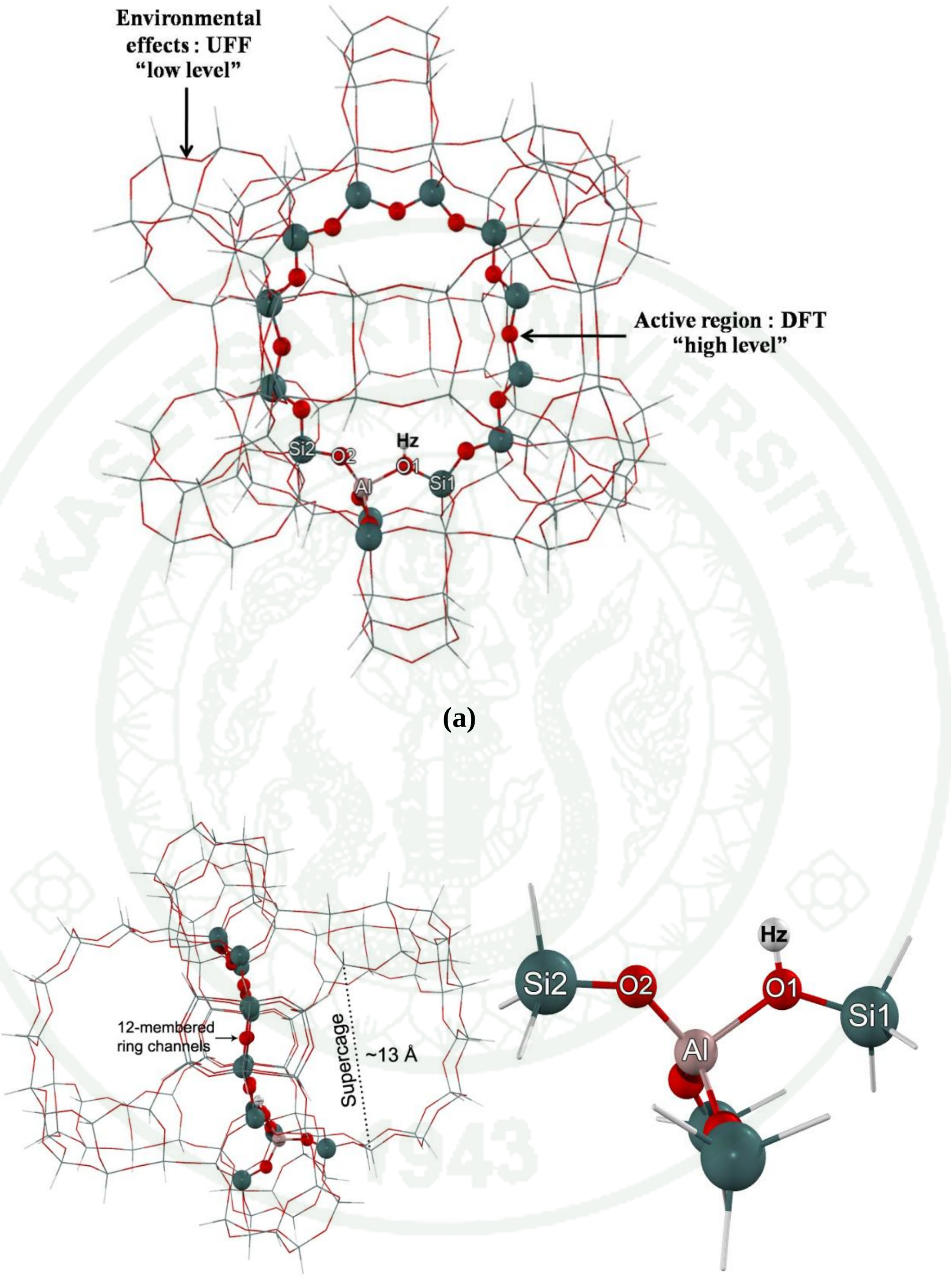

(a)

(b)

(c)

Figure 7 The ONIOM model of 14T/120T cluster of H-FAU. The 14T quantum cluster is drawn as ball and stick and the remaining atoms in the 120T cluster are drawn as line: (a) front view, (b) side view, and (c) focused on 5T/14T relax cluster during optimization.

2.2 Mordenite (MOR) zeolite

The mordenite (MOR) zeolite is represented by the 120T cluster model (T=tetrahedral Si or Al atoms). The crystal structure is taken from the lattice structure database of mordenite zeolite (Alberti *et al.*, 1986). The active site of the MOR zeolites, typically located at the 12-membered-ring window of the straight channel, was represented by the 14T quantum cluster (see Figure 8; drawn as ball and stick) whereas the remainder, represented the zeolite framework environment, was illustrated by line structure. At the 14T active region, one of the silicon atoms is substituted by an aluminum atom at the T2 position (Alberti, 1997). As a result, a proton is added to one of the bridging oxygen atoms bonded directly to the aluminum atom in order to compensate for the charge of the system. The proton will be located at the most stable O2 position (Hill *et al.*, 1999). In this study, the corresponding stable proton site is conventionally labeled as the O1 in texts as well as in figures.

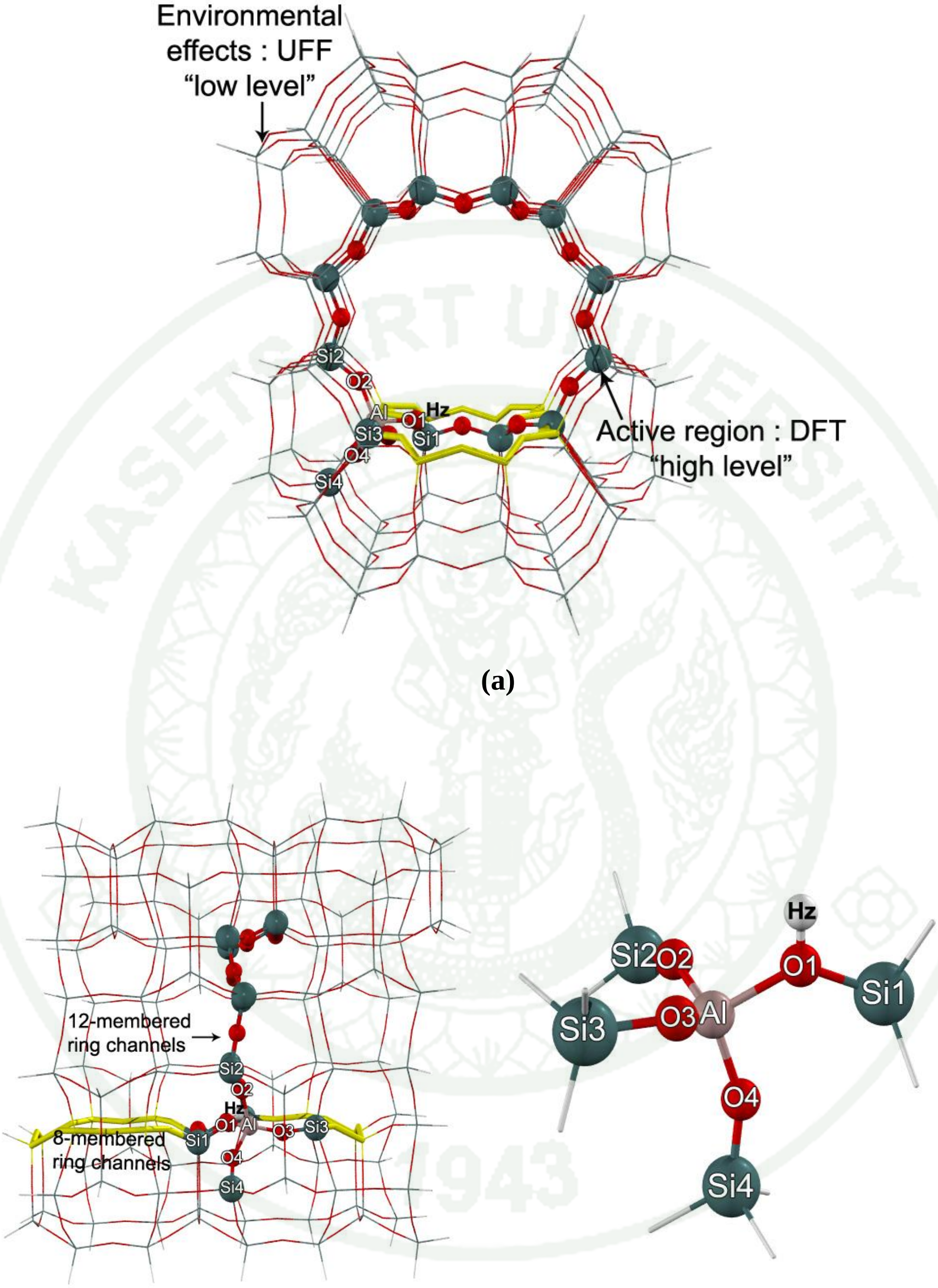

(a)

(b) (c)

Figure 8 The ONIOM model of 14T/120T cluster of H-MOR. The 14T quantum cluster is drawn as ball and stick and the remaining atoms in the 120T cluster are drawn as line: (a) front view, (b) side view, and (c) focused on 5T/14T relax cluster during optimization.

2.3 ONIOM model for zeolites

In the present study, the H/H exchange reaction of propane as well as the propane cracking reaction over nanostructured zeolites was studied within the framework of the ONIOM approach (Svensson *et al.*, 1996). The ONIOM2 scheme was used throughout this work in which the whole system is subdivided into two layers: i) *the inner region* which is presented as the active site of the zeolites and ii) *the outer region* which includes the zeolitic environmental effect (confinement effect) (Derouane, 1986; Zicovich-Wilson *et al.*, 1994). The zeolite active region, for both zeolites, was presented by the 14T cluster and was carried out by means of the selected density functional theory (DFT) approaches (see details later on). While the remainder of the 120T framework connected to the 14T active site was computed with the UFF (Rappé *et al.*, 1992) since this force field has been found to provide a good description of the short-range van der Waals interactions (vdW). All calculations were performed using the Gaussian 03 code (Frisch *et al.*, 2003). During optimization, only the 5T of the 14T active site (Figures 7c and 8c), $\equiv SiO(Hz)Al(OSi\equiv)_2OSi\equiv$, and the probed molecule were allowed to relax while the rest of the active region is fixed at the crystallographic coordinates. Frequency calculations were performed at the same level of the theory to ensure that the obtained transition state structure has only one imaginary frequency that corresponds to a saddle-point of the required reaction coordinates.

2.3.1 ONIOM model for the Faujasite system

The 120T model of FAU zeolite in the ONIOM2 scheme was used to investigate the H/H exchange reaction and the cracking reaction of propane adsorbed over H-FAU zeolite.

The H/H exchange reaction was carried out by the ONIOM (B3LYP/6-31G(d,p):UFF) method. From this approach, the propane molecule and the 14T active site of H-FAU were treated with the high level of theory method, B3LYP/6-31G(d,p) while the remaining atoms were treated by the UFF.

For the cracking reaction, two different combinations of methods for ONIOM2 were used. The 14T active site of H-FAU and the propane molecule were treated with either the B3LYP/6-31G(d,p) and the M06-L/6-31G(d,p) level of theory, while the remaining were calculated using the UFF method. Such combinations of methods are denoted as the ONIOM(B3LYP/6-31G(d,p):UFF) and ONIOM(M06-L/6-31G(d,p):UFF), respectively. In order to obtain more reliable reaction energies, the single point energy calculation at the M06-L/6-31G (d,p)//ONIOM(M06-L/6-31G(d,p):UFF) level of theory was performed for the interactions of all available species over the 120T cluster in the cracking reaction pathway.

2.3.2 ONIOM model for the Mordenite system

Only the propane cracking reaction over the 120T model of MOR zeolites was explored using the ONIOM2 scheme. Two types of DFT calculations, B3LYP/6-31G(d,p) and M06-L/6-31G(d,p), were selected to examine the active site and the adsorbed molecules. The effects of the zeolite framework, the outer region, were treated by the UFF. In order to obtain more reliable reaction energies, the single point energy calculation at the M06-L/6-31G(d,p)//ONIOM(M06-L/6-31G(d,p):UFF) level of theory was performed for 120T cluster for all available species in the cracking reaction pathway.

2.3.3 ONIOM notations in this thesis

Since the ONIOM methods were selected to study reactions in this thesis, the short notations on ONIOM are mentioned here. The ONIOM(B3LYP/6-31 G(d,p):UFF) and ONIOM(M06-L/6-31G(d,p):UFF) are noted as B3LYP:UFF and M06-L:UFF, respectively. Moreover, for the QM calculations, sometimes the B3LYP/6-31G(d,p) and M06-L/6-31G(d,p) are abbreviated as B3LYP and M06-L, respectively.

RESULTS AND DISCUSSION

Reference systems

In this section, the reference systems are discussed. The structures of zeolites (faujasite and mordenite) as well as the adsorbate molecules (propane, ethylene and methane) were examined. The Mulliken charge analysis was also used to calculate the charge corresponding to the specific atoms.

1. Zeolites

1.1 Faujasite (H-FAU)

The selected geometric parameters of H-FAU zeolite at the active site calculated with ONIOM(B3LYP/6-31G(d,p):UFF) and ONIOM(M06-L/6-31G(d,p): UFF) are tabulated in Table 1. From Table 1, the O1-Hz, O1-Al and O1-Si1 bond distances are calculated to be 97.1, 195.4 and 170.8 pm for B3LYP:UFF and 96.7, 196.1 and 170.5 pm for M06-L:UFF, respectively. The bond distances obtained from both methods are slightly different, by less than 1 pm. The Si1-O1-Al bond angle is slightly different, by less than 1^o when calculated with B3LYP:UFF (129.4°) and M06-L:UFF (130.0°) methods. As a result, the structures of the active site obtained from the B3LYP and M06-L functional are very similar. Further support for the reliability of the active site subunit, $\equiv$SiO(Hz)Al(OSi$\equiv$)$_2$OSi$\equiv$, is given by NMR spectroscopy study (Klinowski, 1991) in which the estimated internuclear distances between the aluminum and proton nuclei at the Brønsted acid site, *r*(Al···Hz), of different zeolites are in the range of 234-252 pm. Our computed *r*(Al···Hz) distances are 250.3 and 251.1 pm for B3LYP:UFF and M06-L:UFF methods, respectively, which are in good agreement with NMR experimental value. In conclusion, our results indicated that both combined methods can predict the structure of the active sites for H-FAU zeolite very well.

1.2 Mordenite (H-MOR)

For the H-MOR zeolites, the selected geometric parameters at the active site obtained from the ONIOM(B3LYP/6-31G(d,p):UFF) and ONIOM(M06-L/6-31G (d,p):UFF) methods are documented in Table 1. The corresponding O1-Hz, O1-Al and O1-Si1 bond distances determined from B3LYP:UFF (96.9, 180.1 and 167.7 pm, respectively) and M06-L:UFF (96.5, 180.5 and 167.4 pm, respectively) methods are different by less than 0.5 pm. The Si1-O1-Al bond angle is almost unchanged when comparing the results achieved from the B3LYP:UFF method (127.3°) with the M06-L:UFF method (128.0°). They differ from each other by less than 1^{o}. The computed *r*(Al···Hz) distances are 241.0 and 241.9 pm for B3LYP:UFF and M06-L: UFF, respectively, which are reasonably close to the experimental value from the NMR spectroscopy technique (Klinowski, 1991), 234-252 pm. This suggests that both combined methods can also present the active sites for H-MOR zeolite very well.

Table 1 The optimized geometric parameters of the H-FAU and H-MOR zeolites cluster using ONIOM(B3LYP/6-31G(d,p):UFF) and ONIOM(M06-L/6-31 G(d,p):UFF) methods.

Parameters	H-FAU		H-MOR	
	B3LYP:UFF	M06-L:UFF	B3LYP:UFF	M06-L:UFF
Distances (pm)				
O1-Hz	97.1	96.7	96.9	96.5
O1-Si1	170.8	170.5	167.7	167.4
Al-O1	195.4	196.1	180.1	180.5
O2-Al	171.4	171.0	164.8	164.5
O2-Si2	163.6	163.3	157.2	156.9
Al···Hz	250.3	251.1	242.0	241.9
Angles (degrees)				
∠Si1-O1-Al	129.4	130.0	127.3	128.0
∠Si2-O2-Al	137.5	137.8	149.3	149.0

2. Adsorbate molecules

2.1 Propane

The optimized geometric parameters and the Mulliken charges of the propane molecule calculated with B3LYP/6-31G(d,p) and M06-L/6-31G(d,p) are presented in Figure 9. In Figure 9a, two types of carbon atoms, the primary (1°) carbon (C1 and C3) and the secondary (2°) carbon (C2), are presented. The carbon-carbon bond distances (C1-C2 or C2-C3) of propane molecule obtained from the B3LYP and M06-L methods are calculated to be 153.1 and 151.9 pm, respectively. As for the C-H bond distances, at the primary carbon, the corresponding bond distances of C1-H1(C1-H3) or C3-H1(C3-H3), while H1 and H3 are the primary hydrogen atoms, are calculated to be 109.5-109.6 and 109.4-109.5 pm for B3LYP and M06-L methods, respectively. While at the secondary carbon, the related C2-H2 bond distances are evaluated to be 109.8 and 109.7 pm for B3LYP and M06-L methods, respectively. The bond distances obtained from both methods are slightly different by 1.2 pm. The C1-C2-C3 bond angle is slightly different by 0.4^{o} predicted with B3LYP (113.0^{o}) and M06-L (112.6^{o}) methods, respectively. From our data, the obtained structure of the propane molecule calculated with the popular density functional (B3LYP) and the new local density functional (M06-L) are not different.

The distributions of the Mulliken charge for the propane molecule in its neutral form are shown. The secondary (2°**)** carbon (C2) can keep negative charges of about -0.172 *e* (B3LYP) and -0.211 *e* (M06-L) and, in contrast, the Mulliken charges at the primary (1°) carbon (C1 and C3) are calculated to be -0.310 *e* and -0.374 *e* for B3LYP and M06-L, respectively (see Figure 9b). The Mulliken charges of all hydrogen atoms in the propane molecule are positive charges and divided into three types (H1, H2, and H3). The H1 types are calculated to be 0.101 and 0.120 *e* with B3LYP and M06-L, respectively. The H2 and H3 types are calculated to be 0.095, 0.116 *e* and 0.99, 0.124 *e* with B3LYP and M06-L, respectively.

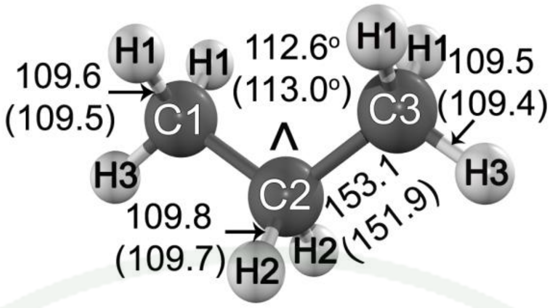

(a)

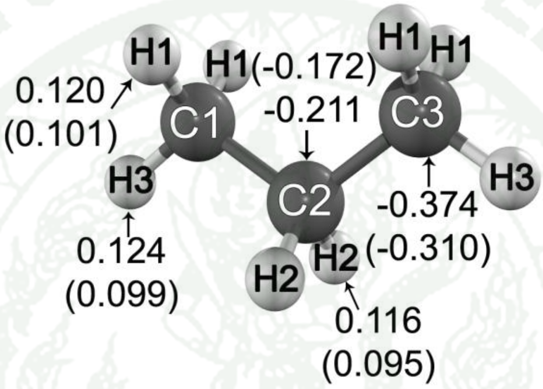

(b)

Figure 9 The optimized geometric parameters (a) and the Mulliken charges (b) of the propane molecule calculated with B3LYP/6-31G(d,p) and M06-L/6-31 G(d,p). Values in parentheses represent the results obtained from B3LYP/ 6-31G(d,p) level of theory.

2.2 Ethylene

Figure 10 shows the optimized geometric parameters and the Mulliken charges of the ethylene molecule obtained from the B3LYP/6-31G(d,p) and the M06-L/6-31G(d,p) calculations. The C1-C2 double bond distances and the corresponding C1-H (or C2-H) bond distances are calculated to be 133.0 and 108.6 pm for B3LYP, and 132.8 and 108.7 pm for and M06-L methods, respectively (see Figure 10a). The deviation of the bond distances obtained from both methods is slightly different by 0.2 pm. The H-C1-H (or H-C2-H) and the C1-C2-H angles are predicted to be very similar; H-C1-H angles are 116.2^{o} (B3LYP) and 116.3^{o} (M06-L) and the C1-C2-H bond angles are computed to be 121.8^o (B3LYP) and 121.9^o (M06-L). Thus, B3LYP and M06-L methods provide an excellent agreement of data.

The corresponding Mulliken charges for the carbon atom (C1 and C2) are -0.202 *e* (B3LYP) and -0.260 *e* (M06-L) (see Figure 10b). The Mulliken charges for all hydrogen atoms are identical with the positive charges of 0.101 *e* (B3LYP) and 1.130 *e* (M06-L).

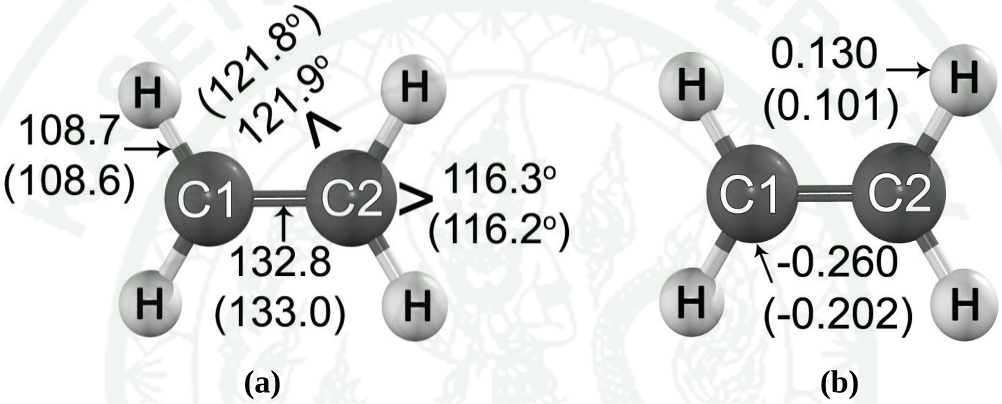

Figure 10 The optimized geometric parameters (a) and the Mulliken charges (b) of the ethylene molecule calculated with B3LYP/6-31G(d,p) and M06-L/6-31 G(d,p). Values in parentheses represent the results obtained from B3LYP/6-31G(d,p) level of theory.

2.3 Methane

The optimized geometric parameters and the Mulliken charges of the methane molecule calculated with B3LYP/6-31G(d,p) and M06-L/6-31G(d,p) are presented in Figure 11. In Figure 11a, the methane bonds (C-H) are 109.2 and 109.0 pm achieved from the B3LYP and M06-L methods, respectively. Methane’s bond angles are not different form the calculation with the B3LYP and M06-L methods (109.5^o).

The Mulliken charges for the carbon atom (C) are -0.472 *e* (B3LYP) and -0.564 *e* (M06-L) (see Figure 11b). The Mulliken charges for all hydrogen atoms are identical with the positive charges of 0.118 *e* (B3LYP) and 0.141 *e* (M06-L).

Figure 11 The optimized geometric parameters (a) and the Mulliken charges (b) of the methane molecule calculated with B3LYP/6-31G(d,p) and M06-L/6-31 G(d,p). Values in parentheses represent the results obtained from B3LYP/ 6-31G(d,p) level of theory.

H/H Exchange Reaction of Propane Adsorbed over H-FAU Zeolite Investigated by the ONIOM method

1. Adsorption of propane over H-FAU zeolite

The adsorption of propane over H-FAU zeolite has been investigated using the ONIOM(B3LYP/6-31G(d,p):UFF) method. The three possible configurations of the propane molecule adsorbed over H-FAU zeolite were discussed: The most stable propane adsorption complex (**Ads_Stable**), the adsorption of propane over H-FAU zeolites: at the primary (1°) carbon (**Ads_Pri**), and the adsorption of propane over H-FAU zeolites: at the secondary (2°) carbon (**Ads_Sec**). The details of three configurations are presented below.

1.1 The adsorption of propane over H-FAU zeolites: the most stable propane adsorption complex (**Ads_Stable**)

The most stable configuration of propane adsorbed over H-FAU is illustrated in Figure 12a and denoted as **Ads_Stable**. In this configuration, propane molecule weakly adsorbs over the H-FAU zeolite via the van der Waals interaction between the Brønsted acid site of zeolite (Hz) and the terminal methyl group (C1) of propane (primary carbon position). The structures of propane molecule and the zeolite were slightly changed, with respect to the isolated systems, due to the weak interaction during the adsorption (see Table 2). As can be seen, the Al-O1 bond distance decreases from 195.4 to 194.3 pm while and the Al-O2 bond distance slightly increases from 171.4 to 171.6 pm. The O1-Hz bond distance of the active region is increased by 0.7 pm as compared with the bare H-FAU zeolite. The C1-C2 bond distance of the propane molecule is increased slightly from 153.1 to 153.5 pm, as compared with the isolated propane molecule. The intermolecular distance Hz···C1 is 232.9 pm and the O1-Hz···C1 bond angle is 173.2^{o}. The adsorption energy is predicted to be -6.2 kcal/mol (Figure 15) and is in good agreement with the experimental measurement of heat of adsorption, -6.4 kcal/mol (Eder *et al.*, 1997).

1.2 The adsorption of propane over H-FAU zeolites: at the primary (1°) carbon (**Ads_Pri**)

In this system, the Brønsted acid site of zeolite (Hz) is also directly bound to the propane molecule at the primary carbon position the same as in the **Ads_Stable** system. The structures of the **Ads_Pri** are slightly different from that of the **Ads_Stable**. The **Ads_Pri** and **Ads_Stable** used the terminal methyl group of propane (C1) interacted with the Brønsted acid site of zeolite. But, the ethyl group (C2C3) of **Ads_Pri** is out of the plane of the 12-memebered-ring window of H-FAU zeolite (see Figure 12b). The Hz···C1 adsorption distances are slightly changed (232.9 pm for **Ads_Stable** and 233.5 pm for **Ads_Pri**). However, the O1-Hz bond distances and the O1-Hz···C1 bond angles were not changed (see Table 2). In addition, the Hz···C1-C2 bond angles and the O2···H(C1) are different. In **Ads_Stable**, the Hz···C1-C2 bond angles and the O2···H(C1) intermolecular distances are 145.8^{o} and 279.7 pm, respectively, while, the Hz···C1-C2 bond angles and the O2···H(C1) intermolecular distances of **Ads_Pri** are 113.9^{o} and 268.7 pm, respectively. The O2···H(C1) intermolecular distances of **Ads_Pri** are shorter than that of the **Ads_Stable**. The **Ads_Pri** structure is suitable for the hydrogen exchange reaction at the primary carbon of propane. However, the adsorption energy of the **Ads_Pri** complex is calculated to be -5.7 kcal/mol, which is slightly less stable than that of the **Ads_Stable** by 0.5. kcal/mol (Figure 15).

1.3 The adsorption of propane over H-FAU zeolites: at the secondary (2°) carbon (**Ads_Sec**)

The hydrogen exchange reaction at the secondary carbon of propane over H-FAU is indicated by **Ads_Sec** and is illustrated in Figure 12c. The acidic proton of the Brønsted site of zeolite (Hz) is interacted to the secondary carbon atom of the propane molecule. As a result, the propane molecule is located across the 12-memebered-ring window of H-FAU zeolite by the C1-C2 bond of propane aligned almost perpendicular to the O2-Al-O1-Hz plane of the Brønsted acid site (see Figure 12c). However, the O1-Hz bond distance and the structure of zeolite of **Ads_Sec** are very similar to that of the **Ads_Stable** and the **Ads_Pri**. The C2···Hz and O2···H(C2) intermolecular distance of the **Ads_Sec** are shorter than that of the **Ads_Stable**. The adsorption energy for the **Ads_Sec** is calculated to be -4.6 kcal/mol, which is less stable than the most stable propane adsorption complex (**Ads_Stable**) by 1.6 kcal/mol (Figure 15).

In all the cases, the adsorption energies of propane over H-FAU are in the order of **Ads_Stable** > **Ads_Pri** > **Ads_Sec**.

The Mulliken charges for **Ads_Stable**, **Ads_Pri**, and **Ads_Sec** are displayed in Figure 12 (right). Upon the three configurations of the propane molecule adsorbed over the acid site, the changes in the Mulliken charge on the acidic proton and bridging oxygen are minute. The propane molecule in **Ads_Stable**, **Ads_Pri**, and **Ads_Sec** are slightly positive charges of 0.033 *e*, 0.030 *e*, and 0.033 *e*, respectively. In **Ads_Stable** and **Ads_Pri**, the Mulliken charges at the C1 atom of the propane molecule are slightly increased by -0.060 *e* and -0.073 *e*, compared with the isolated propane molecule, respectively. The Mulliken charges at the C2 and C3 atoms of propane are slightly changed compared with the isolated propane molecule, respectively. Furthermore, the H(C1) atom shows the highest positive charge among all the hydrogen atoms in the propane molecule (see Figures 12a and 12b) because, it interacts with the O2 atom surface of zeolite. This indicates the polarization of the propane molecule due to interaction with the zeolite.

For **Ads_Sec**, the polarization of the propane molecule can be explained in the same fashion as already discussed in **Ads_Stable** and **Ads_Pri**. The Mulliken charge at the C2 atom of the propane molecule increased by -0.081 *e* compared with the isolated propane molecule. The H(C2) atom is the highest positive charge among all the hydrogen atoms in the propane molecule (See Figure 12c). This also indicates the polarization of the propane molecule due to interaction with the zeolite.

Table 2 The optimized geometric parameters (distances in pm and angles in degrees) of bare zeolite cluster, the most stable propane adsorption complex (**Ads_Stable**), adsorption of the primary carbon (**Ads_Pri**), and the secondary carbon (**Ads_Sec**) of propane over H-FAU obtained from the ONIOM(B3LYP/6-31G(d,p):UFF) method.

Parameters	**H-FAU**	**C_3H_8/H-FAU**		
	Bare cluster	**Ads_Stable**	**Ads_Pri**	**Ads_Sec**
Distances (pm)				
O1-Hz	97.1	97.8	97.8	97.5
O1-Si1	170.8	170.3	170.2	170.5
Al-O1	195.4	194.3	194.6	194.8
O2-Al	171.4	171.6	171.5	171.5
O2-Si2	163.6	163.5	163.5	163.4
C1-C2	153.1[*]	153.5	153.3	153.4
C2-C3	153.1[*]	153.1	153.1	153.4
C1···Hz	-	232.9	233.5	-
C2···Hz	-	-	-	260.0
O2···H(C1)	-	279.7	268.7	-
O2···H(C2)	-	582.2	-	273.8
Angles (degrees)				
∠Hz···C1-C2	-	145.8	113.9	65.6
∠Si1-O1-Al	129.4	129.3	129.3	129.1
∠Si2-O2-Al	137.5	137.9	137.9	138.2

[*] optimized geometric parameters of propane molecule

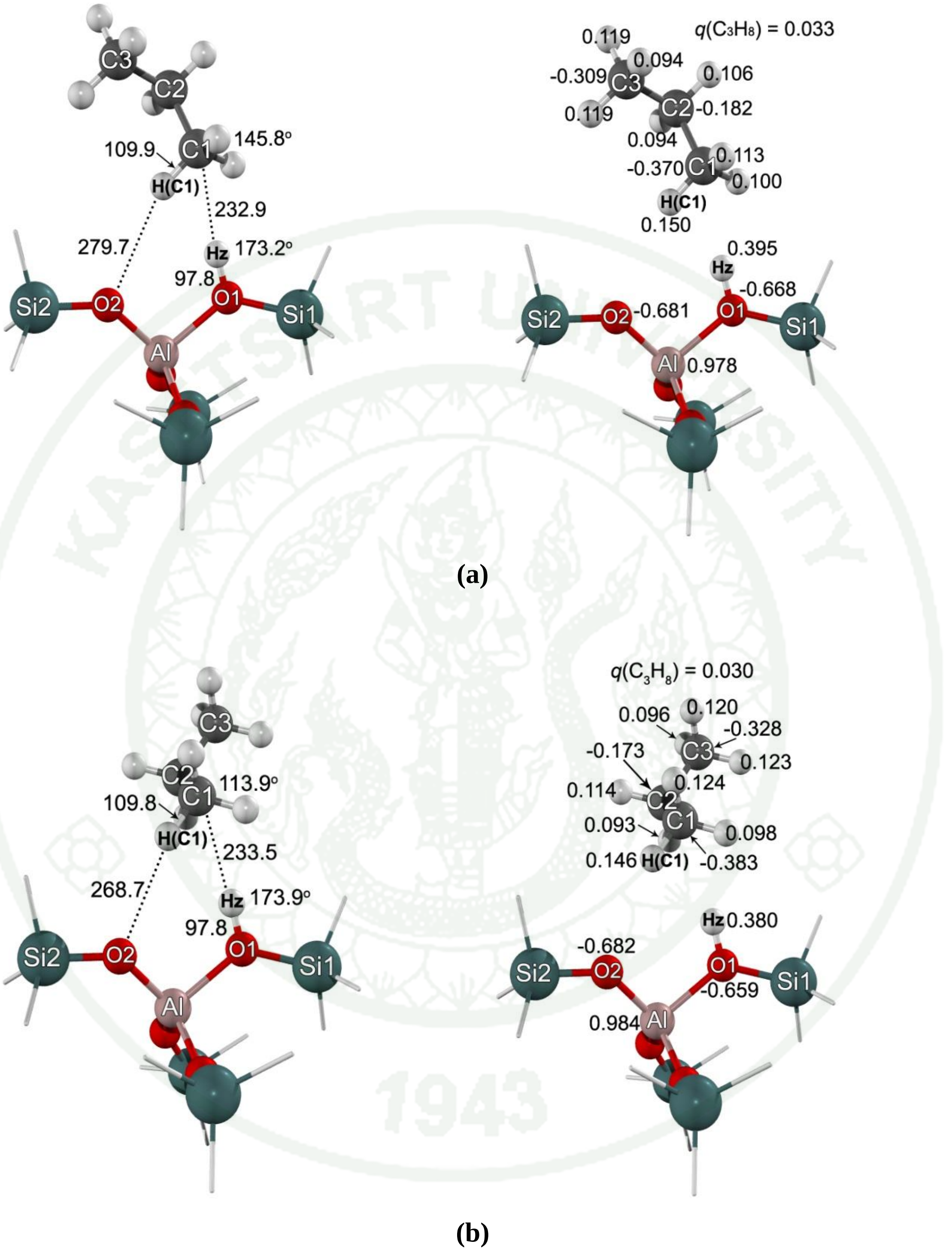

Figure 12 The optimized structure parameters (left) and the Mulliken charges (right) of (a) the most stable propane adsorption complex (**Ads_Stable**), (b) adsorption of the primary carbon (**Ads_Pri**), and (c) the secondary carbon (**Ads_Sec**) of propane over H-FAU.

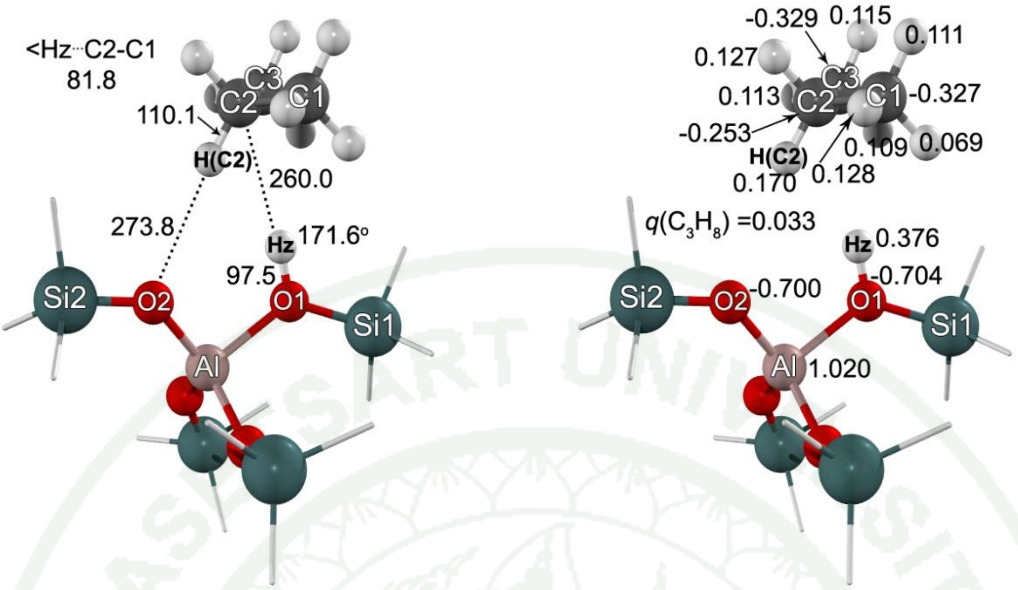

(c)

Figure 12 (Continued)

2. The H/H Exchange Reaction of Propane over H-FAU Zeolite

The H/H exchange of propane adsorbed over H-FAU zeolite has been investigated using the ONIOM(B3LYP/6-31G(d,p):UFF) method. The H/H exchange between the adsorbed propane and the Brønsted acid of zeolite was found to occur in two routes: via the adsorption at the primary carbon (**Ads_Pri**) and at the secondary carbon (**Ads_Sec**) of the propane molecule as described by the following schemes:

<u>*Scheme I*</u> : **Ads_Pri**

$CH_3CH_2\underline{\textit{C}}H_3 + \equiv SiO(Hz)Al(OSi\equiv)_2OSi\equiv \rightarrow CH_3CH_2\underline{\textit{C}}H_2Hz + \equiv SiOAl(OSi\equiv)_2O(HC1)Si$

<u>*Scheme II*</u> : **Ads_Sec**

$CH_3\underline{\textit{C}}H_2CH_3 + \equiv SiO(Hz)Al(OSi\equiv)_2OSi\equiv \rightarrow CH_3\underline{\textit{C}}HHzCH_3 + \equiv SiOAl(OSi\equiv)_2O(HC2)Si$

The italic underlined carbon atom indicates the place where the hydrogen exchange takes place. The details of these mechanisms will be discussed in the following sections:

2.1 The hydrogen exchange reaction mechanism at the primary carbon of propane

The hydrogen exchange reaction mechanism at the primary carbon of propane initially exists via the **Ads_Pri** complex. Then, the weakly adsorbed propane over H-FAU zeolite can be protonated by the Brønsted acid site of zeolite. Figure 13a (left) shows the corresponding transition state (TS) and the arrows in the figure represent the movement of the atom according to the reaction coordinate (corresponding to the imaginary frequency mode at –953 cm^{-1}). At the transition state (**TS_Pri**) the proton at the Brønsted acid of zeolite transfers to propane, resulting in the lengthening of the O1-Hz bond from 97.8 to 149.1 pm and the shortening of the Hz···C1 intermolecular distance to 125.9 pm. Concurrently, the C1-H(C1) bond distances between the primary hydrogen atom and the primary carbon (C1 position) of propane are elongated from 109.8 pm to 126.0 pm, while the corresponding H(C1)···O2 distance is 152.6 pm. Therefore, the primary hydrogen atom of propane, H(C1) and an acidic proton, Hz, locate rather close to the primary carbon, indicating the C1-Hz bond formation and C1-H(C1) bond breaking (see Figure 13a). The C1 carbon atom then becomes a non-classical pentacoordinated structure, resulting in the forming of the proponium cation ($C_3H_9^+$). In this situation, the zeolite cluster plays roles as the Brønsted acid (protonating a proton or hydrogen) and the Lewis base (receiving the proton or hydrogen) nature of the active site. The C1-C2 bond distance is slightly changed compared to that of the **Ads_Pri** complex. Our finding for the **TS_Pri** shows the effect of the zeolite frame work on the TS structure as compared to the previous theoretical studies using small clusters (Blaszkowski *et al.*, 1996; Zheng and Blowers, 2005a) in which they reported that the hydrogen atoms are nearly half-way between the carbon and the zeolitic oxygen atoms.

From Figure 15, the calculated apparent activation energy and the corresponding actual activation energy (E_a^{Pri}) are calculated to be 27.3 and 33.0 kcal/mol, respectively. The apparent activation energy obtained in this work is lower than the previous theoretical results: 32.2 kcal/mol [3T with B3LYP/6-31G(d,p)] (Esteves *et al.*, 1999); 40.5 kcal/mol [5T using BH&HLYP/6-31++G(d,p)] (Ryder *et* *al.*, 2000); 30.4 kcal/mol [3T using the CBS-QB3//B3LYP/6-31G(d)] (Zheng *et al.*, 2005a). However, no experiment activation energy of the hydrogen exchange of propane over H-FAU zeolite is available in the literature, so a comparison with the hydrogen exchange of propane over H-ZSM-5 zeolite will be made. We mention here that it is difficult to compare the activation energy obtained from different types of zeolites due to their different properties, such as acidity, pore size and channel, which properties directly affect to activation energy. The experimental activation energy for the hydrogen exchange reaction at the primary carbon of propane in H-ZSM-5 zeolite was reported to be 25.8±1.7 kcal/mol (Stepanov *et al.*, 1998). Our calculated apparent activation energy is in good agreement with the experiment. Moreover, the influence of the zeolitic framework plays significant roles on the activation energy for the hydrogen exchange reaction as described by our results compared to the studies using the small cluster model (Esteves *et al.*, 1999; Ryder *et al.*, 2000; Zheng *et al.*, 2005a).

Figure 13a (right) gives the Mulliken charges. The positive charge on the organic fragment ($C_3H_9^+$) of the **TS_Pri** is 0.639 *e*. This indicated the formation of the carbonium ion-like transition state. The $C_3H_9^+$ fragment can be divided in two parts. The $C_2H_7^+$ is nearly neutral (0.038 *e*). The two hydrogens (Hz, H(C1)) between the carbon and the bridging oxygen atoms of zeolite are positively charged. This displays the interaction of two hydrogens and the bridging oxygen atoms of zeolite as strong proton acceptors. This result agrees with the previous theoretical calculation (Blaszkowski *et al.*, 1996).

Finally, the product (**Prod_Pri)** of the hydrogen exchange reaction mechanism is the propane molecule adsorbed over the other oxygen atom (O2) of the surface of zeolite. In the product formation shown in Figure 13b (left), H(C1)···C1 becomes the intermolecular distance (247.5 pm). The obtained propane product interacted to the Brønsted acid site of zeolite by the primary carbon atom is the same as for the **Ads_Pri** complex. The Mulliken charge for this step is shown in Figure 13b (right). The charge distribution on propane and the acidic faujasite can be explained in a similar way as in the **Ads_Pri** complex.

Table 3 The optimized geometric parameters (distances in pm and angles in degrees) of transition state (TS) and product (Prod) of hydrogen exchange reaction of propane at primary position (Pri) and secondary position (Sec) over H-FAU zeolite using ONIOM(B3LYP/6-31G(d,p):UFF).

Parameters	**C_3H_8/H-FAU**			
	TS_Pri	**TS_Sec**	**Prod_Pri**	**Prod_Sec**
Distances (pm)				
O1-Hz	149.1	151.0	258.4	247.0
O1-Si1	165.5	165.4	162.6	162.6
Al-O1	181.2	1814	172.6	172.6
O2-Al	180.1	179.8	193.2	193.2
O2-Si2	166.8	166.5	172.7	172.6
C1-C2	154.0	153.3	153.2	153.2
C2-C3	153.1	153.7	153.1	153.3
C1···Hz	125.9	-	109.7	-
C1···H(C1)	126.0	-	247.9	-
O2···H(C1)	152.6	-	97.9	-
C2···Hz	-	126.7	-	110.1
C2···H(C2)	-	125.8	-	247.5
O2···H(C2)	-	156.3	-	98.0
Angles (degrees)				
∠Hz···C1-C2	99.8	35.4	-	-
∠Si1-O1-Al	128.6	128.6	127.2	127.3
∠Si2-O2-Al	137.7	138.2	138.3	138.3

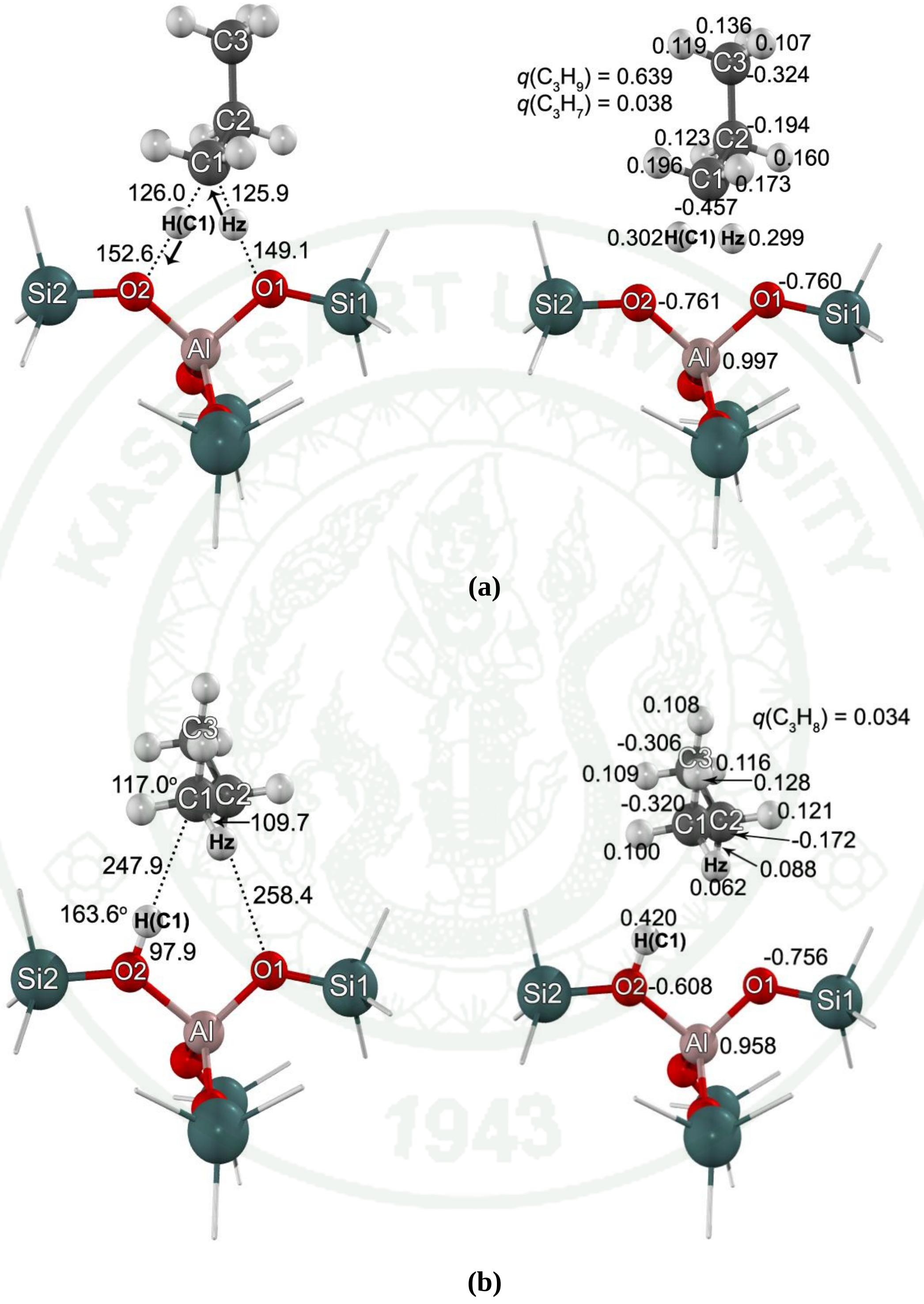

Figure 13 The optimized structures parameters (left) and the Mulliken charges (right) for (a) the transition state (**TS_Pri**) and (b) the product (**Prod_Pri**) of the hydrogen exchange reaction at the primary carbon of propane over H-FAU zeolite.

2.2 The hydrogen exchange reaction mechanism at the secondary carbon of propane

According to the **Ads_Sec** complex as already discussed in section 2.1.3, the reaction proceeds via the **TS_Sec** transition state structure (Figure 14a). At the transition state, the proton at the Brønsted acid of zeolite transfers to the secondary carbon atom of propane at the C2 position, which induces the extending of the O1-Hz bond from 97.5 (in **Ads_Sec** complex) to 151.0 pm and the shortening of the Hz···C2 intermolecular distance from 260.0 to 126.7 pm. At the same time, the C2-H(C2) bond distance is lengthened from 110.1 pm to 125.8 pm and correspondingly the H(C2)···O2 distance is shortened to 156.3 pm. Therefore, the secondary hydrogen atom of propane, H(C2) and the Brønsted proton, Hz, are placed rather close to the secondary carbon (see Figure 14a (left)). Hence, the proponium cation ($C_3H_9^+$) is proposed as a TS structure in the **TS_Sec**. This cation exists due to the generation of a non-classical pentacoordinated structure at C2. The C1-C2 and C2-C3 bond distances of propane are slightly changed with respect to the **Ads_Sec** complex. The transition state geometry is confirmed by the imaginary frequency of -834 cm^{-1} which corresponds to the H/H exchange.

The activation energy of this reaction is shown in Figure 15. The actual activation energy (E_a^{Sec}) and the apparent activation energy are calculated to be 31.1 and 26.5 kcal/mol, respectively. The computed apparent activation energy is lower than that of the previous theoretical results for the hydrogen exchange reaction mechanism at the secondary carbon of propane: 39.2 kcal/mol [5T, BH&HLYP/ 6-31++G(d,p)] (Ryder *et al.*, 1999); 33.3 kcal/mol [3T, B3LYP/6-31G(d,p)] (Esteves *et al.*, 2000); 29.8 kcal/mol [3T using the CBS-QB3//B3LYP/6-31G(d)] (Zheng *et al.*, 2005a). Our calculated apparent activation energy is in good agreement with the experimental apparent activation energy for the hydrogen exchange reaction mechanism at the secondary carbon of propane in H-ZSM-5 zeolite, 28.0±1.7 kcal/mol (Stepanov *et al.*, 1998). As a result, the framework effects of zeolite, included in our study, play a vital role in the stabilization of the TS as compared to the higher activation energies obtained from the small clusters reported in the literature (Esteves *et al.*, 1999; Ryder *et al.*, 2000; Zheng *et al.*, 2005a).

Figure 14a (right) gives the Mulliken charges. For **TS_Sec**, the formation of a carbonium ion-like transition state is indicated by the positive charge of the organic fragment ($C_3H_9^+$), 0.655 *e*. In addition, the $C_3H_9^+$ fragment can be divided into two parts. The $C_2H_7^+$ is nearly neutral (0.074 *e*). The two hydrogens (Hz, H(C1)) between the carbon and the bridging oxygen atoms of zeolite are positively charged, showing the strong proton acceptor behaviors of two hydrogens and the bridging oxygen atoms of zeolite. Our result agrees with the previous theoretical calculation (Blaszkowski *et al.*, 1996).

At the final step, the propane adsorption, resembling the **Ads_Sec** configuration, exists as a product by the following steps: The propane molecule adsorbed over the new Brønsted acid site H(C2), at the O2 position of the zeolite. In the product formation shown in Figure 14b (left), the H(C2)···C2 intermolecular distance was computed to be 247.5 pm. The Mulliken charges are given in Figure 14b (right). The charge in this step can be explained in the same way as for the **Ads_Sec** complex.

Now we will discuss the H/H exchange reaction mechanism. From section 2.1 and 2.2, we found that the apparent activation energies for the hydrogen exchange mechanism at the primary carbon atom and secondary carbon atom of propane were computed to be 27.3 and 26.5 kcal/mol, respectively, which are in good agreement with experiment. Since the activation energies for both systems are virtually identical, we confirm that the hydrogen exchange reaction of propane over acid zeolite can take place for both at the primary- and secondary carbon positions of the propane molecule, which are in good agreement with the previous theoretical and experimental investigations. Therefore, the hydrogen exchange reactions of propane over acidic zeolite are competitive reactions between two investigated routes as already discussed.

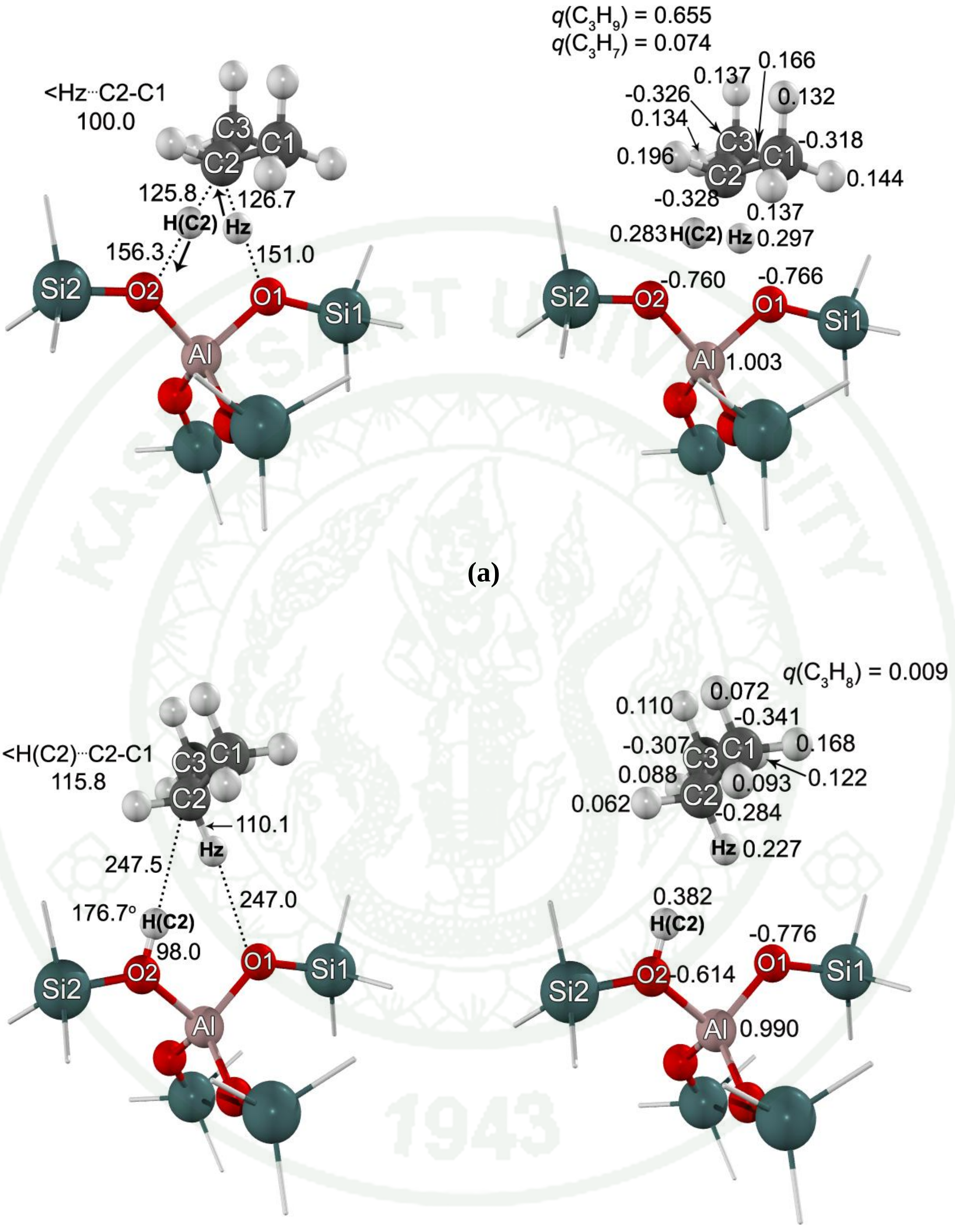

(a)

(b)

Figure 14 The optimized structure parameters (left) and the Mulliken charges (right) for (a) the transition state (**TS_Sec**) and (b) the product (**Prod_Sec**) of the hydrogen exchange reaction at the secondary carbon of propane over H-FAU zeolite.

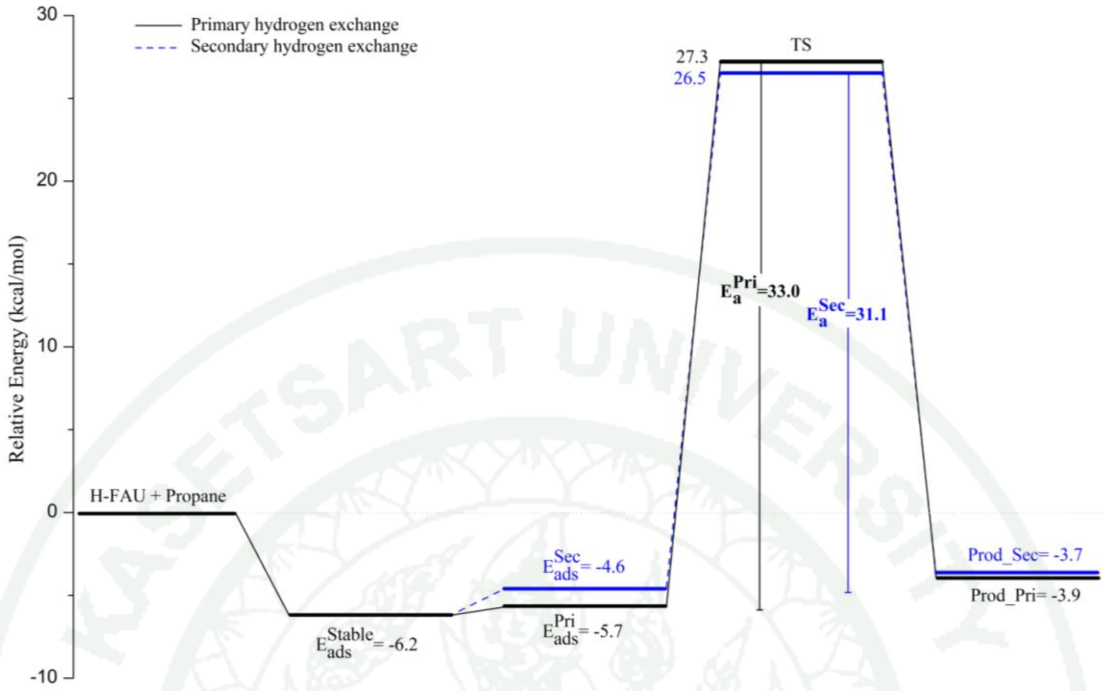

Figure 15 Calculated energy profiles (kcal/mol) for the hydrogen exchange reaction at the primary carbon (solid line) and the secondary carbon (dash line) of propane over H-FAU zeolite carried out by the ONIOM(B3LYP/6-31G (d,p):UFF) method.

Propane Cracking Reaction over Different Types of Nanostructured Zeolites: A Newly Developed DFT Approach

In this section, the propane cracking reaction over H-FAU and H-MOR zeolites is carried out by the ONIOM(B3LYP/6-31G(d,p):UFF) and ONIOM(M06-L/ 6-31G(d,p):UFF) methods which are discussed in four sections. Firstly, in section 1, we start with the discussion of the propane adsorption over H-FAU and H-MOR zeolites. In sections 2 and 3, the propane cracking reaction over H-FAU and H-MOR are discussed, respectively. Finally in section 4, the comparison of the propane cracking reaction over both zeolites as well as the efficiency of the density functional between B3LYP and M06-L are made.

1. Adsorption of propane over H-Zeolites

Two adsorption configurations of propane can exist in the cracking process for both the zeolites, *i.e.*, the most stable form (**Ads_Stable**) and the cracking form (**Ads_Crack**). As far as the stability is concerned, the **Ads_Stable** shows the greater stability compared to the **Ads_Crack** complex in both zeolites, However, the **Ads_Crack** complexes are suitable for the cracking reactions due to their appropriate configuration on the forming of the transition state structure. The details of these configurations are presented below.

1.1 Adsorption of propane over H-FAU zeolite

For the propane/H-FAU complex, the most stable adsorption complex and the cracking adsorption complex are noted as **Ads_Stable_FAU** (see Figure 16a) and **Ads_Crack_FAU** (see Figure 16b), respectively.

1.1.1 The most stable propane/H-FAU zeolite complex (**Ads_Stable_FAU**)

For the **Ads_Stable_FAU**, the O1-Hz bond distance is increased with a correspondingly slightly decrease of the Al-O1 bond and lengthening of the Al-O2 bond. The O1-Hz bond distance is increased from 97.1 to 97.8 pm for ONIOM(B3LYP/6-31G(d,p):UFF); and from 96.7 to 97.6 pm for ONIOM(M06-L/ 6-31G(d,p):UFF). The C1-C2 bond distance of the propane molecule is slightly increased as compared to the isolated molecule. The Hz···C1 adsorption distances are 232.9 and 227.9 pm for ONIOM(B3LYP/6-31G(d,p):UFF) and ONIOM(M06-L/6-31 G(d,p):UFF), respectively while the corresponding O1-Hz···C1 bond angles are 173.2^o and 175.1^o (see Figure 16a).

As for the adsorption energy, the calculation obtained from the B3LYP:UFF approach (-6.2 kcal/mol) is found to be lower than that of the M06-L: UFF method (-8.8 kcal/mol), Table 5. The B3LYP:UFF result is in good agreement with the experimental values of -6.4 (Eder *et al.*, 1997) and -7.4 kcal/mol (Xu *et al.*, 2006). On the other hand, the M06-L:UFF result is not as close to the experimental values.

1.1.2 The propane/H-FAU zeolite complex in the cracking form (**Ads_Crack_FAU**)

For the cracking reaction, the propane molecule in the **Ads_Stable_FAU** reorients itself to form the **Ads_Crack_FAU** structure. The differences in these complexes are related to the Hz···C1-C2 bond angles and the C2···Hz intermolecular distances (see Figure 16b). In the **Ads_Stable_FAU** complex, the Hz···C1-C2 bond angles are 145.8^{o}and 145.8^o for B3LYP:UFF and M06-L:UFF, respectively, while the corresponding, C2···Hz intermolecular distances are 370.1 and 364.0 pm. As for the **Ads_Crack_FAU** complex, the Hz···C1-C2 bond angles are determined to be 84.5^o and 90.5^o for B3LYP:UFF and M06-L:UFF, respectively. The C2···Hz intermolecular distances are shorter than those of the **Ads_Stable_FAU** which are calculated to be 295.4 pm (B3LYP:UFF) and 283.6 pm (M06-L:UFF). The intermolecular C1···Hz distances are 267.5 pm (B3LYP:UFF) and 237.8 pm (M06-L: UFF). Moreover, the O1-Hz bond length decreases by 0.3 pm for both predictions

(B3LYP:UFF and M06-L:UFF approaches), resulting in less stability of the **Ads_Crack_FAU** complex compared to the **Ads_Stable_FAU** by 1.2 kcal/mol (from -6.2 to -5.0 kcal/mol for B3LYP:UFF) and 0.4 kcal/mol (from -8.8 to -8.4 kcal/mol for M06-L:UFF) (see Table 5). The C1-C2 bond lengths of the propane molecule are almost unchanged (152.3 pm for B3LYP:UFF and 153.4 pm for M06-L:UFF), Figure 16.

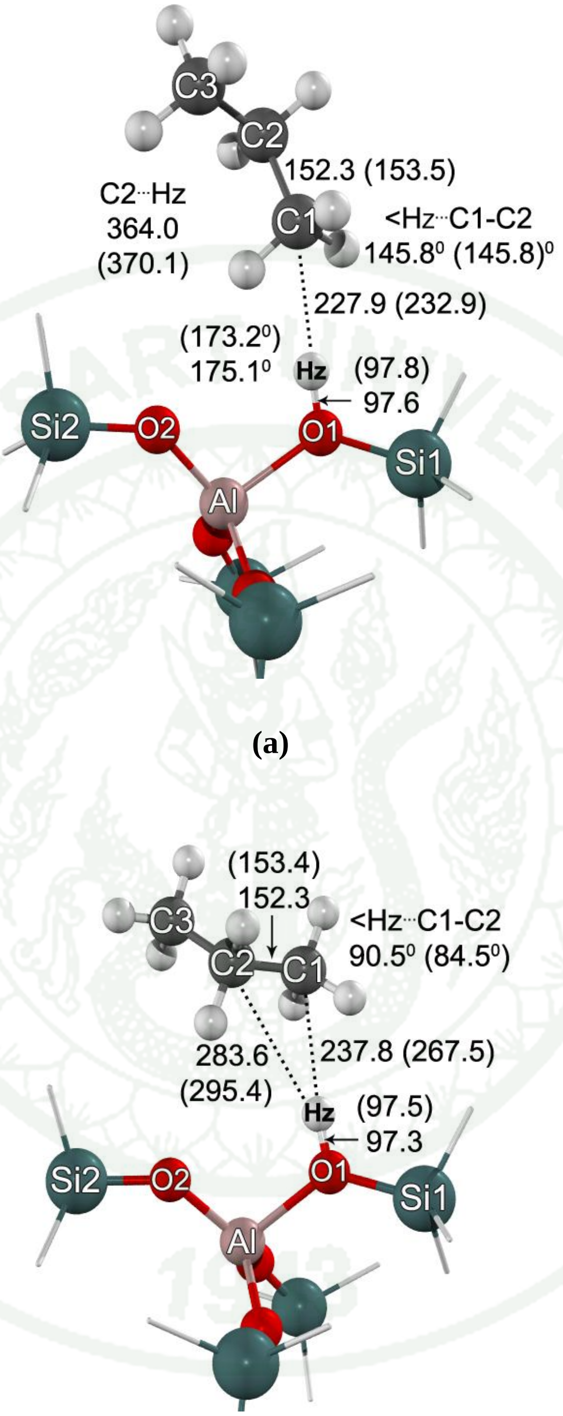

(a)

(b)

Figure 16 The selected structural parameters for (a) **Ads_Stable_FAU** and (b) **Ads_Crack_FAU** obtained from the ONIOM(B3LYP:UFF) and ONIOM(M06-L:UFF) methods. Values in parentheses represent the results obtained from ONIOM(B3LYP:UFF) method.

	B3LYP	M06-L
H1	0.150	0.138
H2	0.100	0.113
H3	0.113	0.136
H4	0.094	0.123
H5	0.106	0.132
H6	0.119	0.144
H7	0.094	0.108
H8	0.119	0.144

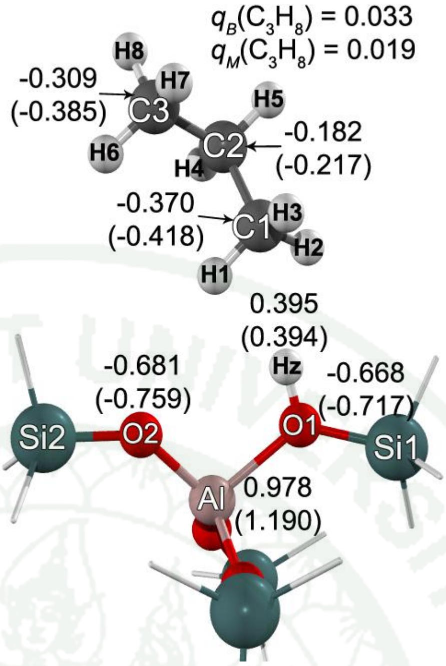

(a)

	B3LYP	M06-L
H1	0.121	0.149
H2	0.098	0.089
H3	0.130	0.127
H4	0.175	0.126
H5	0.108	0.119
H6	0.101	0.122
H7	0.087	0.111
H8	0.124	0.146

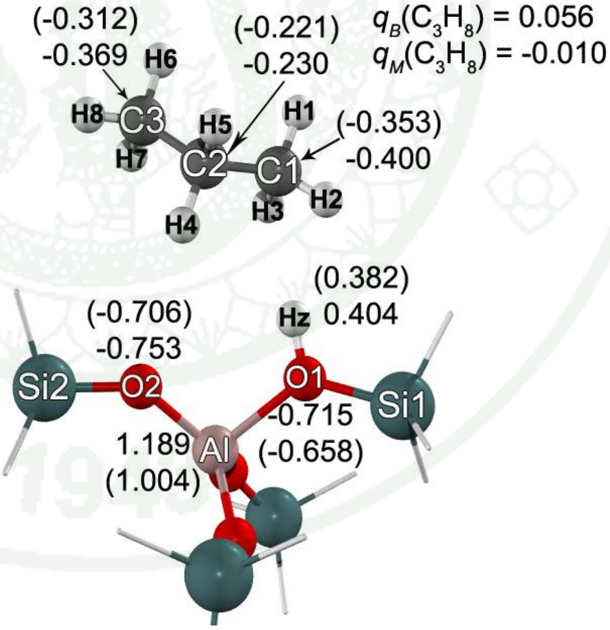

(b)

Figure 17 The Mulliken charges for (a) **Ads_Stable_FAU** and (b) **Ads_Crack_FAU** obtained from the ONIOM(B3LYP:UFF) and ONIOM(M06-L:UFF) methods. Values in parentheses represent the results obtained from ONIOM(B3LYP:UFF) method.

Table 4 The optimized geometric parameters of bare zeolites cluster, **Ads_Stable_FAU**, **Ads_Crack_FAU**, **Ads_Stable_MOR**, and **Ads_Crack_MOR** obtained from the ONIOM(B3LYP/6-31G(d,p):UFF) and ONIOM(M06-L/6-31G(d,p):UFF). Values in parentheses represent the results obtained from ONIOM(B3LYP/6-31G(d,p):UFF).

Parameters	**H-FAU**	**C_3H_8/H-FAU**		**H-MOR**	**C_3H_8/H-MOR**	
	Bare Cluster	**Ads_Stable_FAU**	**Ads_Crack_FAU**	**Bare Cluster**	**Ads_Stable_MOR**	**Ads_Crack_MOR**
Distances (pm)						
O1-Hz	96.7 (97.1)	97.6 (97.8)	97.3 (97.5)	96.5 (96.9)	97.3 (97.4)	97.1 (97.3)
O1-Si1	170.5 (170.8)	169.9 (170.3)	170.1 (170.6)	167.4 (167.7)	166.8 (167.4)	166.9 (167.5)
Al -O1	196.1 (195.4)	195.0 (194.3)	195.5 (195.0)	180.5 (180.1)	179.8 (179.7)	179.9 (179.8)
O2-Al	171.0 (171.4)	171.3 (171.6)	171.0 (171.4)	164.5 (164.8)	167.2 (165.1)	164.8 (165.2)
O2-Si2	163.3 (163.6)	163.2 (163.5)	163.0 (163.3)	156.9 (157.2)	157.2 (157.3)	157.1 (157.3)
C1-C2	151.9 (153.1)[*]	152.3 (153.5)	152.3 (153.4)	151.9 (153.1)[*]	152.1 (153.3)	152.3 (153.3)
Al···Hz	251.1 (250.3)	247.6 (250.1)	254.7 (252.3)	241.9 (242.0)	240.9 (241.6)	240.4 (242.0)
C1···Hz	-	227.9 (232.9)	237.8 (267.5)	-	230.1 (251.3)	232.0 (255.7)
C2···Hz	-	364.0 (370.1)	283.6 (295.4)	-	311.3 (350.0)	269.3 (337.0)
Angles (degrees)						
∠Si1-O1-Al	130.0 (129.4)	130.0 (129.4)	129.3 (129.0)	128.0 (127.3)	128.6 (127.4)	128.4 (127.3)
∠Si2-O2-Al	137.8 (137.5)	138.1 (137.9)	138.6 (138.1)	149.0 (149.3)	147.6 (148.7)	147.4 (148.5)

[*] the optimized geometrical parameters of propane molecule

Table 5 The breakdown of the ONIOM adsorption energy (kcal/mol) of propane over H-FAU and H-MOR zeolites.

Adsorption complexes	B3LYP/6-31G(d,p):UFF			M06-L/6-31G(d,p):UFF		
	14T QM	120T UFF	Total	14T QM	120T UFF	Total
Ads_Stable_FAU	-3.8	-2.4	-6.2	-6.2	-2.6	-8.8
Ads_Crack_FAU	-2.5	-2.5	-5.0	-5.9	-2.5	-8.4
Ads_Stable_MOR	-2.5	-7.7	-10.2	-7.7	-7.3	-15.0
Ads_Crack_MOR	-2.0	-8.2	-10.2	-7.5	-6.1	-13.6

1.2 Adsorption of propane over H-MOR zeolite

In the propane/H-MOR system, the notations **Ads_Stable_MOR** and **Ads_Crack_MOR** are named for the most stable adsorption complex and the cracking adsorption complex, respectively. The details for such structures are explained below.

1.2.1 The most stable propane/H-MOR zeolite complex (**Ads_Stable_MOR**)

The optimized structures of bare H-MOR zeolite and its propane adsorption complex (**Ads_Stable_MOR**) are portrayed in Table 4. Behavior similar to that of the adsorption in **Ads_Stable_FAU** can be observed. The propane molecule weakly adsorbs on H-MOR zeolite via the van der Waals interaction by the terminal methyl group (C1) of propane which interacts with the Brønsted acid of H-MOR zeolite (Hz). During the adsorption process, the O1-Hz bond lengths of the active region increases by 0.5 and 0.8 pm for B3LYP:UFF and M06-L:UFF, respectively, compared to the bare H-MOR zeolite. The intermolecular distances between C1···Hz are 251.3 pm and 230.1 pm. The corresponding bond angles of O1-Hz···C1, calculated with ONIOM(B3LYP/6-31G(d,p):UFF) and ONIOM(M06-L/6-31G(d,p):UFF) approaches are 152.8^o and 150.2^o, respectively (Figure 18a). The adsorbate molecule shows the slight elongation of the C1-C2 bond lengths as compared with the isolated molecule (from 153.1 to 153.3 pm for B3LYP:UFF and from 151.9 to 152.1 pm for M06-L:UFF).

The adsorption energies investigated from the ONIOM(B3LYP/6-31G(d,p):UFF) and ONIOM(M06-L/6-31G(d,p):UFF) are calculated to be -10.2 and -15.0 kcal/mol, respectively. Our results show that the better result is obtained from the B3LYP and the UFF combination since the experimental observation is about -9.8 kcal/mol (Eder *et al.*, 1997). The M06-L:UFF approach provides the overestimated adsorption energy from the experiment by 5.2 kcal/mol, Table 5.

1.2.2 The propane/H-MOR zeolite complex in the cracking form (**Ads_Crack_MOR**)

Similarly, the cracking form of propane (**Ads_Crack_MOR**), the propane molecule interacts with the Brønsted acid of H-MOR zeolite (Hz) by the methyl group (C1) (see Figure 18b). The geometrical parameters are tabulated in Table 4. The O1-Hz bond lengths slightly decrease by 0.1 and 0.2 pm for B3LYP:UFF and M06-L:UFF approaches, respectively. The intermolecular C1···Hz distances are 255.7 and 232.0 pm for B3LYP:UFF and M06-L:UFF, respectively. The dihedral angles of Hz···C1-C2-C3 are calculated to be 128.8^{o} (B3LYP:UFF) and 121.6^{o} (M06-L:UFF). In contrast, the dihedral angles of Hz···C1-C2-C3 are predicted to be -116.2^{o} (B3LYP:UFF) and -123.4^{o} (M06-L:UFF) for **Ads_Stable_MOR**. In addition, the C1-C2 bond length of the propane molecule is unchanged when using B3LYP:UFF (153.3 pm) and slightly increases by 0.2 pm for the calculation of the M06-L:UFF approach (152.3 pm).

1.3 The effects of the UFF on the adsorption energies

In order to validate the method, the adsorption energy from the ONIOM approaches the calculations were broken up into two parts: High level and low level of theory. The high level of theory calculation was performed for the 14T QM cluster whilst the adsorption energies for the **Ads_Stable_FAU**, **Ads_Crack_FAU**, **Ads_Stable_MOR** and **Ads_Crack_MOR** were discussed (Table 5).

For the **Ads_Stable_FAU**, the adsorption energies determined by the M06-L and the B3LYP functional are -6.2 and -3.8 kcal/mol, respectively (see Table 5), which contain 70% and 61% of the total adsorption energy calculated from the ONIOM method. In the **Ads_Crack_FAU** case, the adsorption energies are calculated to be -2.5 kcal/mol for the B3LYP functional and -5.9 kcal/mol for the M06-L functional. The QM part of adsorption energies in the 14T high level are 70% and 50% of the total adsorption energy for M06-L:UFF and B3LYP:UFF methods. The UFF shows the very strong contributions to the adsorption energy for the **Ads_Stable_MOR** and **Ads_Crack_MOR** systems, in which the contributions are up to ~80% and ~50% of the total adsorption carried out from the B3LYP:UFF and M06-L:UFF methods.

From the Table 5, the reason that the adsorption energy of propane over H-MOR zeolite shows larger values than those of the H-FAU zeolite may be due to the combination of the acidity and confinement effect (Derouane, 1986; Zicovich-Wilson *et al.*, 1994). The idea of the confinement effect says that molecules and the environment of the zeolite pore are interacted in a manner that maximizes their van der Waals attraction energy. This effect should be of more importance when the sizes of pore zeolite and the probe molecule are becoming closer. In considering the propane molecule inside the two different types of zeolite, in the present study, the propane molecule is trapped within a 12-membererd-ring window (cage window) connected by two supercages (7.4 Å for a cage window and 13 Å for supercage) for H-FAU zeolite. Unlike H-FAU zeolite, the propane molecule inside the H-MOR zeolite is located along the 12-membererd-ring window of straight channel and the 8-membererd-ring window opening to the side pockets (6.5 Å x 7.0 Å for the 12-membererd-ring window and 5.7 Å x 2.6 Å for the 8-memberer-ring window) (Figures 16 and 18). This difference in pore diameters and the propane molecule inside nanocluster zeolite can explain the better ability of H-MOR to adsorb propane.

The corrections of the adsorption energy were performed using the single point calculation of the 120T cluster at M06-L/6-31G(d,p)//ONIOM(M06-L/6-31 G(d,p):UFF) level of theory (Figure 27). The calculated adsorption energies were evaluated to be: -7.1 and -7.6 kcal/mol for **Ads_Stable_FAU** and **Ads_Crack_FAU**, respectively. In **Ads_Stable_MOR** and **Ads_Crack_MOR**, the calculated adsorption energies were calculated to be -11.2 and -9.9 kcal/mol, respectively. The obtained results are in good agreement with previous experimental studies (Eder *et al.*, 1997; Xu *et al.*, 2006).

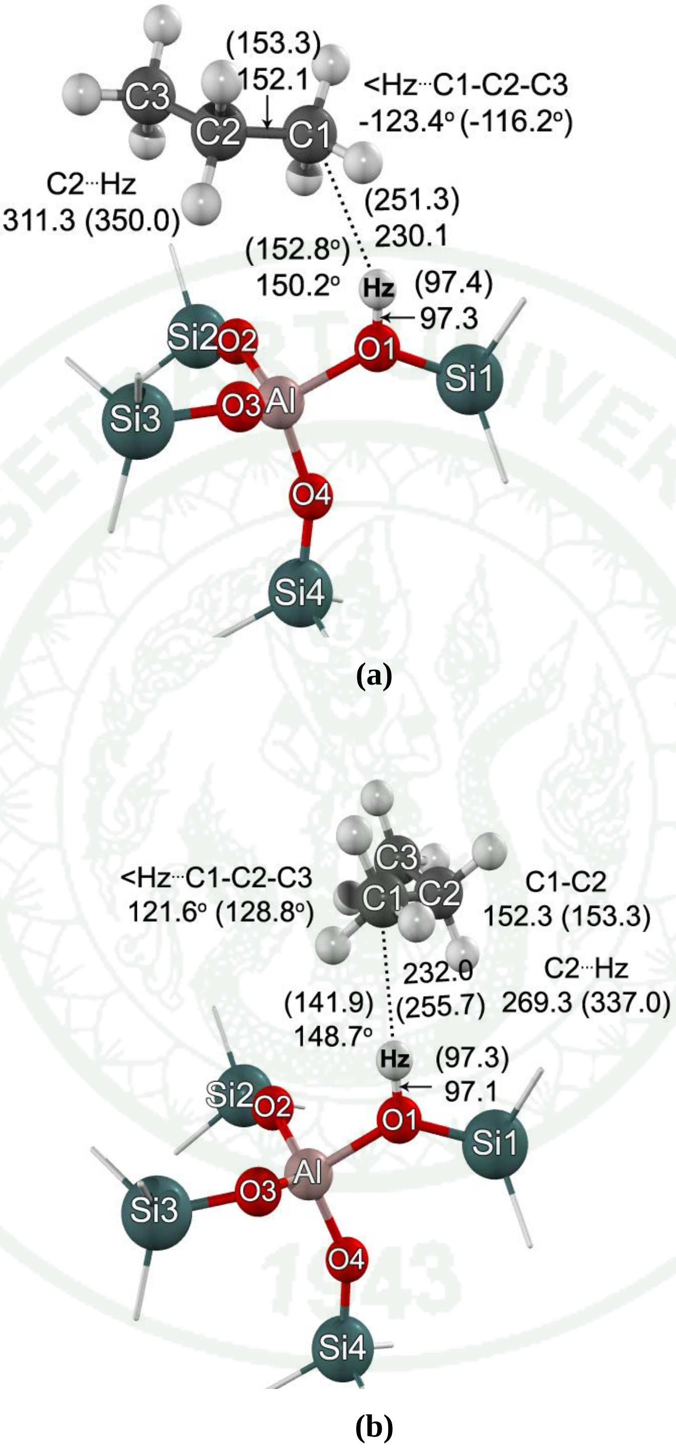

Figure 18 The selected structural parameters for (a) **Ads_Stable_MOR** and (b) **Ads_Crack_MOR** obtained from the ONIOM(B3LYP:UFF) and ONIOM(M06-L:UFF) methods. Values in parentheses present the results obtained from ONIOM(B3LYP:UFF) method.

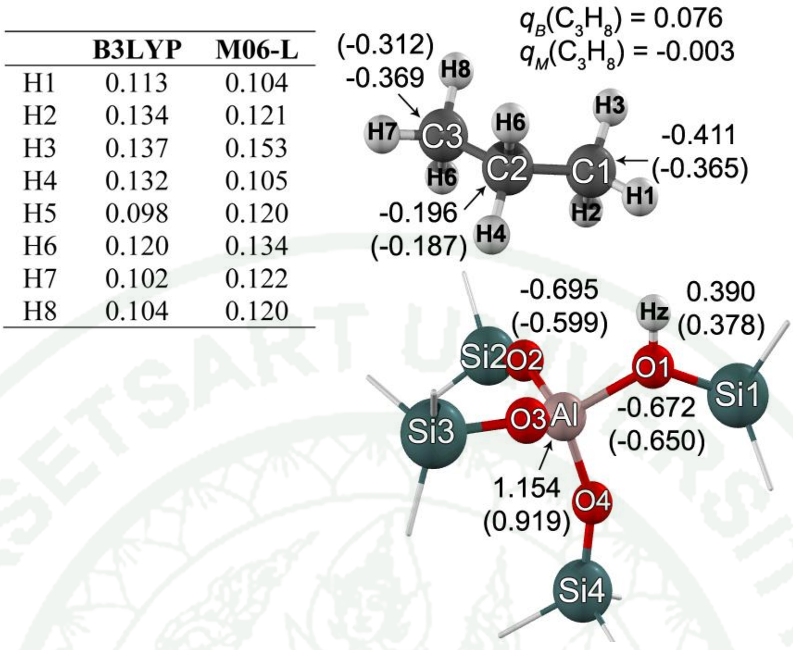

	B3LYP	M06-L
H1	0.113	0.104
H2	0.134	0.121
H3	0.137	0.153
H4	0.132	0.105
H5	0.098	0.120
H6	0.120	0.134
H7	0.102	0.122
H8	0.104	0.120

(a)

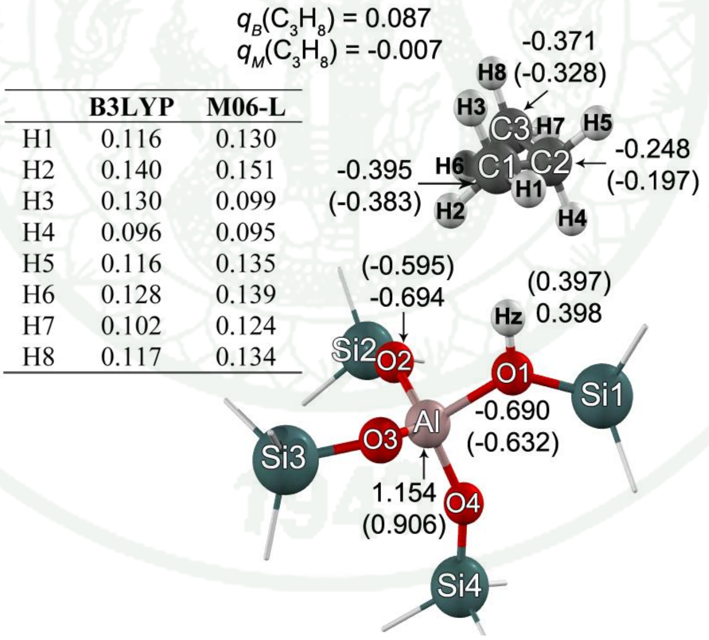

	B3LYP	M06-L
H1	0.116	0.130
H2	0.140	0.151
H3	0.130	0.099
H4	0.096	0.095
H5	0.116	0.135
H6	0.128	0.139
H7	0.102	0.124
H8	0.117	0.134

(b)

Figure 19 The Mulliken charges for (a) **Ads_Stable_MOR** and (b) **Ads_Crack_MOR** obtained from the ONIOM(B3LYP:UFF) and ONIOM(M06-L:UFF) methods. Values in parentheses represent the results obtained from ONIOM(B3LYP:UFF) method.

2. Propane cracking reaction over H-FAU

The reaction mechanism of the propane cracking reaction over H-FAU zeolite is proposed via the Haag-Dessau mechanism (Haag and Dessau, 1984:305). In this mechanism, the propane is protonated by the Brønsted acid of zeolite to form the carbonium-like ion transition state which would crack into methane (alkane) and ethoxide (alkoxide) intermediates. Following this, methane is desorbed, the ethoxide intermediate is then deprotonated the proton back to the zeolite framework, resulting in the formation of the ethylene product adsorbed on zeolite (Figure 20).

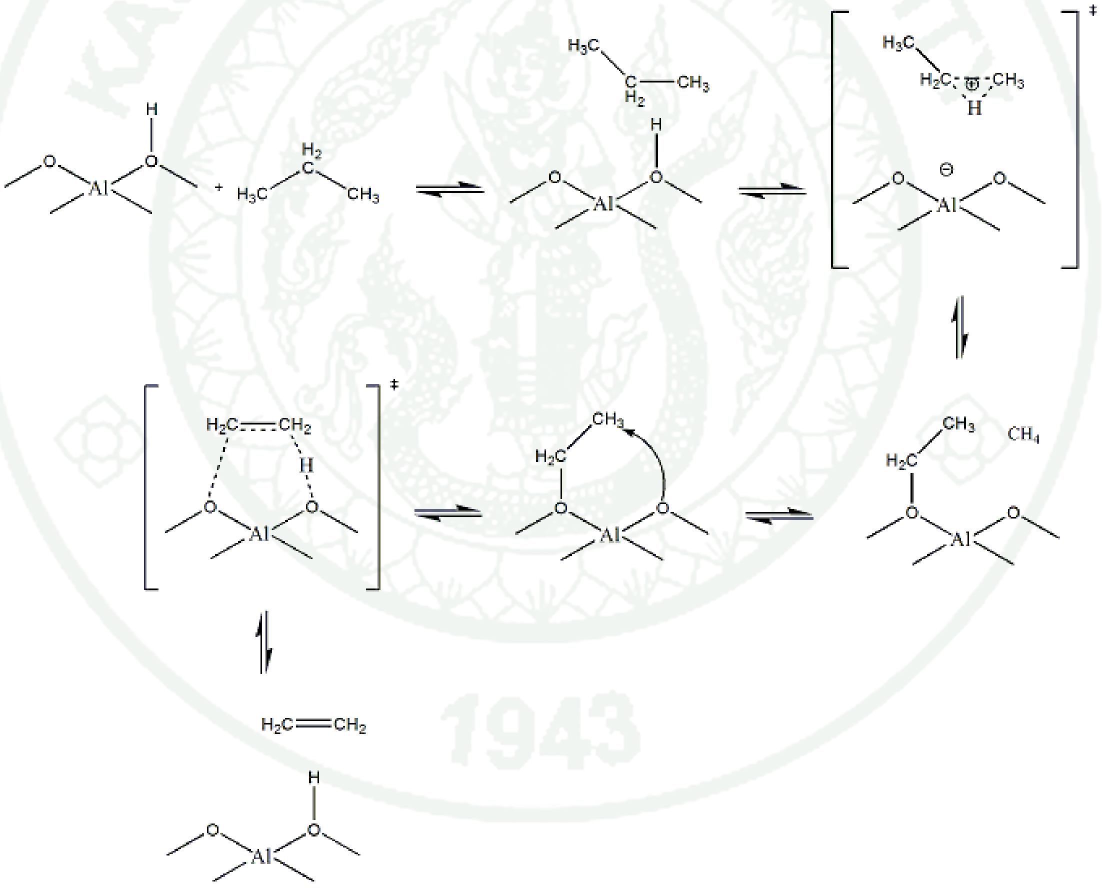

Figure 20 The reaction mechanism of propane cracking reaction over acidic zeolite.

Two adsorption configurations existed, i.e., **Ads_Stable_FAU** and **Ads_Crack_FAU**, during the adsorption process. The cracking reaction proceeds via the **Ads_Crack_FAU** complex. Initially, the acidic proton (Hz) is transferred to the C-C single bond between the methyl group (C1) and the ethyl group (C2C3) of propane. A C1-C2 bond of propane is weakened, leading to their longer atomic distances, when these atoms are protonated by an acidic proton from the zeolite. Both the carbon atoms are then chemically bonded to the proton, resulting in three-center/two-electron complexes (C-H-C) to form the $C_3H_9^+$ proponium ion (carbonium-like ion) (Figure 21a).

At the first transition state, **TS1_FAU**, the carbonium-like ion is found to be the transition state rather than the stable intermediates. The proponium cationic transition state in the channel of zeolite forms an ion pair complex ($C_3H_9^+\cdots{}^-OZ$). This ion-pair complex is stabilized by electrostatic interactions and van der Waals stabilization of the organic molecule ($C_3H_9^+$) in the transition state. In this step, the O1-Hz distances, obtained from the B3LYP:UFF and M06-L:UFF combined methods, are 183.0 and 183.4 pm, respectively. The C1-C2 bond distances of propane lengthened from 153.5 to 179.0 pm for B3LYP:UFF and from 152.3 to 169.4 pm for M06-L:UFF while correspondingly the acidic proton (Hz) moves closer to the C1 and C2 atom. The distances are 128.2 and 131.9 pm for the B3LYP:UFF (130.2 and 130.2 pm for the M06-L:UFF). The C1···Hz···C2 bond angle in the proponium ion is computed to be 87.0^{o} (B3LYP:UFF) and 81.2^{o} (M06-L:UFF). The transition state is confirmed by the frequency calculation with one imaginary frequency at -177 cm^{-1} for B3LYP:UFF and -171 cm^{-1} for M06-L:UFF which related to the movement of the acidic proton (Hz) of zeolite to the C1-C2 bond and breaking of C1-C2 bond of the propane molecule. This step is well known as the protonation step. The activation energy barriers (and the corresponding apparent activation energies) calculated with B3LYP:UFF (E_a^{1B}) and M06-L:UFF (E_a^{1M}) are 48.7 (43.7) and 47.1 (38.7) kcal/mol, respectively (see Figure 23), which are in agreement with the energy barrier and apparent activation energy of the previous experimental values of 46.9 and 39.4 kcal/mol (Xu *et al.*, 2006), respectively. However, in previous theoretical studies in the literature, the activation energies of the propane cracking reaction in a 3T cluster model are 68.0 kcal/mol with the MP2/6-31G(d)//HF/3-21G (Rigby *et al.*, 1997) and

62.1 and 62.6 kcal/mol for two different transition states calculated at CBS-QB3// B3LYP/6-31G(d) level of theory (Blowers 2005a).

Subsequently, the carbonium-like ion in the **TS1_FAU** leads to the formation of the $C_2H_5^+$ carbenium ion (the alkyl fragment) and methane side product. This step is noted as **Int_FAU** (Figure 21b). The carbenium ion ($C_2H_5^+$) is not a stable species within the zeolite channel (Zygmunt *et al.*, 2000; Bates and van Santen, 1998); hence, it is immediately transformed to stabilized alkoxide intermediate by forming a covalent bond to one of the bridging oxygen atoms (O2) of the zeolite framework, while the methane molecule locates far away from the active site. As for the ethoxide intermediate, the covalent bond distances (C2-O2) are 153.7 (B3LYP:UFF) and 152.4 pm (M06-L:UFF). The formation of the covalent bond significantly changes the structure of the zeolite framework as compared to the bare H-FAU zeolite. The Al-O1 and Si1-O1 bond distances are decreased by 22.5 pm (B3LYP:UFF) / 23.6 pm (M06-L:UFF) and 9.4 pm (B3LYP:UFF) / 9.4 pm (M06-L:UFF). The Si2-O2-Al bond angle is decreased by 3.5^o for B3LYP:UFF (and 2.8^o for M06-L:UFF). While, the Al-O2 and Si2-O2 bond distances are increased by 21.4 pm (B3LYP:UFF) / 22.1 pm (M06-L:UFF) and 9.5 pm (B3LYP:UFF) / 9.8 pm (M06-L:UFF). The Si1-O1-Al bond angle is increased by 1.0^o for B3LYP:UFF and 0.2^o for M06-L:UFF (See table 6). The changes of the zeolite structure tend to stabilize the alkoxide intermediate, which is in agreement with the report of Boronat *et al.* (2001) who stated that the stability of alkoxide intermediate formed in the zeolite structure is very sensitive to the local geometry of the active site. The adsorption energy of the complex (methane side product and the ethoxide intermediate complexes on zeolite) computed with B3LYP:UFF and M06-L:UFF are 6.9 and 3.2 kcal/mol (Figure 23), which are less stable than the adsorption of the propane/zeolite complex.

Figure 22a shows the Mulliken charges of the **TS1_FAU**. The proponium cation ($C_3H_9^+$) can retain the positive charge of 0.772 *e* and 0.769 *e* computed by the B3LYP and M06-L methods, respectively. The proton (Hz) of the $C_3H_9^+$ fragment holds the positive charge of 0.318 *e* (B3LYP) and 0.325 *e* (M06-L). Because of the interaction of the bridging Hz atom on $C_3H_9^+$ fragment with the O1 atom surface of the zeolite cluster, the $C_2H_5^+$ carbenium ion is more positively charged than the CH_3^+ carbenium ion group (0.256 *e* vs 0.234 *e* for B3LYP and 0.198 vs 0.209 *e* for the M06-L method). Thus, the carbonium ion-like transition state ($C_3H_9^+$) dissociated by the abstraction of methane and the $C_2H_5^+$ carbenium ion form a covalent bond with the O2 bridging oxygen atom of zeolite. In essence, it is difficult to compare the charge obtained with the two different methods, because the Mulliken charge analysis is a rather arbitrary method. However, these results indicated the formation of the carbonium ion-like transition state.

After that, the methane side product is desorbed from the zeolite structure (**Ds_Met_FAU**, Figure 21c) with a required energy of 1.9 kcal/mol for B3LYP:UFF (and 4.0 kcal/mol for M06-L:UFF) (see Figure 23). At this step, the structures of the active site of zeolite are almost unchanged (less than 0.2 pm and 1.0^o for changes in the bond distances and bond angles, respectively). The covalent bond distances (C2-O2) are decreased to be 0.3 pm (B3LYP:UFF) and 0.2 pm (M06-L:UFF) as compared with the previous **Int_FAU** step. The alkoxide species is an active species, then it prompts to be deprotonated for the next reaction step.

At the deprotonation step, a proton from the alkoxide species is transferred back to the bridging oxygen atom (O1) of zeolite via the transition state (**TS2_FAU**) to produce an ethylene product adsorbed on zeolite via a π-interaction (**Prod_Eth_FAU**). As compared with the methane desorption step, at the **TS2_FAU**, the covalent bonds between the ethoxide species (C2) and the O2 framework of zeolite are elongated to 227.7 pm and 236.1 pm (M06-L:UFF) (Figure 21d). The C2-C3 bond distances are decreased by 10.4 pm (B3LYP:UFF) and 10.6 pm (M06-L: UFF). Protons from the alkoxide species at C3, H(C), are extended by 119.0 pm (B3LYP:UFF) and 119.9 pm (M06-L:UFF) with the corresponding H(C)···O1 distances of 152.8 and 148.7 pm, respectively. The transition state is confirmed by the frequency calculation with one imaginary frequency at -284 cm^{-1} (B3LYP:UFF) and -187 cm^{-1} (M06-L:UFF). This is related to the movement of a proton from the alkoxide species to the bridging oxygen atom (O1) of the zeolite structure. The activation energies of the second transition state (**TS2_FAU**) are 27.8 kcal/mol

(B3LYP:UFF) and 27.9 kcal/mol (M06-L:UFF) (Figure 23). We found that the deprotonation step requires less energy than the protonation step. This finding agrees well with the experimental work in which it was stated that the protonation step is the rate-limiting step for the propane cracking reaction (Narbeshubet *et al.*, 1995).

For the ethylene product step (**Prod_Eth_FAU**; Figure 21e), a proton from the alkoxide species is transferred back to the zeolite framework, the C3-H(C) bond is broken and the hybridization of C3 changes from tetrahedral (sp^3) to planar (sp^2), produced the ethylene product adsorbed on the acidic proton. The reaction energies for this step are calculated to be 12.7 kcal/mol for B3LYP:UFF (and 15.0 kcal/mol for M06-L:UFF). Finally, the adsorbed ethylene product is endothermically desorbed by the energy of 10.9 kcal/mol for B3LYP:UFF (and 11.8 kcal/mol for M06-L:UFF**)**. The desorption energies of ethylene on H-FAU are in good agreement with a previous experimental study in which the ethylene adsorption on H-FAU is reported to be -9.1 kcal/mol (Cant and Hall, 1972), Figure 23.

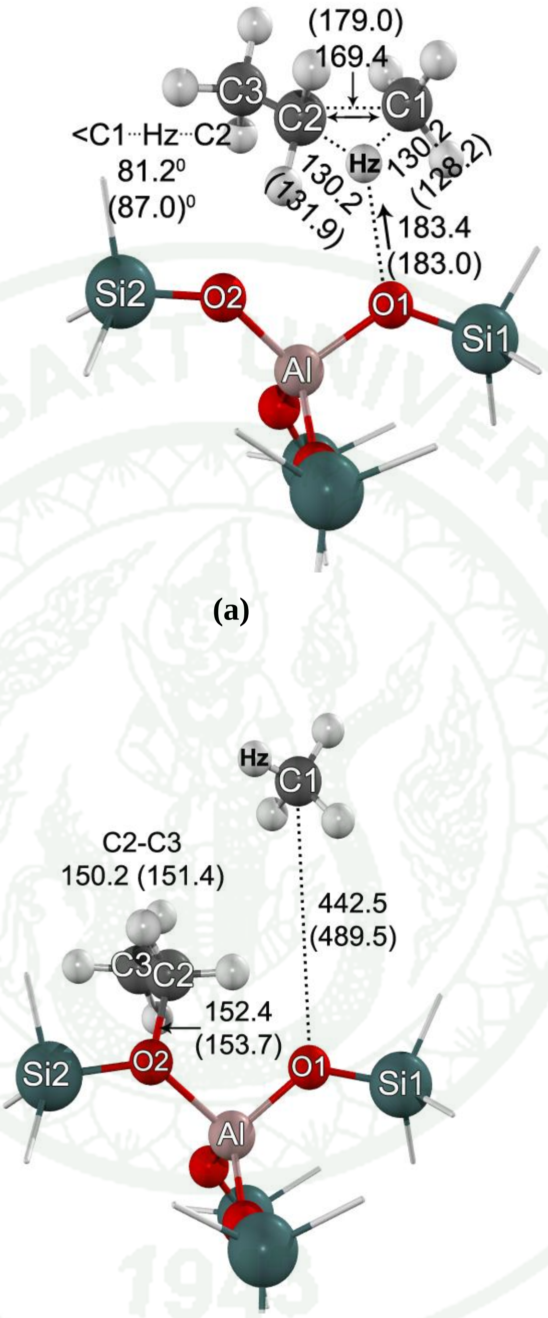

(a)

(b)

Figure 21 The optimized structure parameters for (a) first transition state (**TS1_FAU**), (b) intermediate (**Int_FAU**), (c) methane desorption (**Ds_Met_FAU**), (d) second transition state (**TS2_FAU**), and (e) ethylene product (**Prod_Eth_FAU**) of propane cracking reaction over H-FAU zeolite by ONIOM(B3LYP:UFF) and ONIOM(M06-L:UFF). Values in parentheses present the results obtained from ONIOM(B3LYP:UFF).

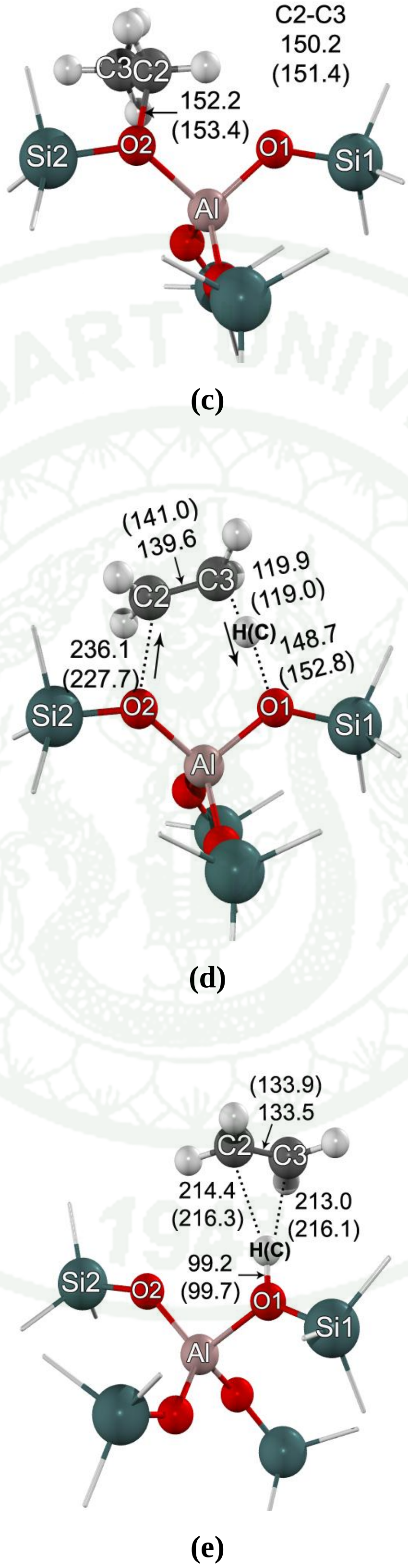

(c)

(d)

(e)

Figure 21 (Continued)

	B3LYP	M06-L
H1	0.195	0.228
H2	0.237	0.248
H3	0.200	0.218
H4	0.256	0.260
H5	0.198	0.231
H6	0.125	0.139
H7	0.172	0.179
H8	0.157	0.178

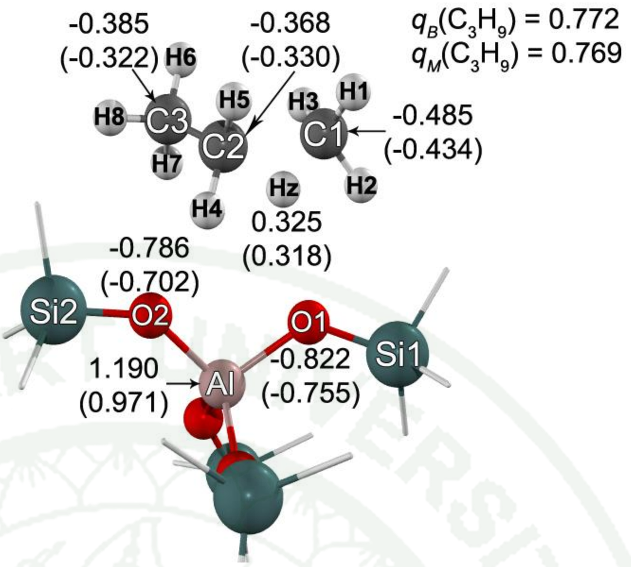

(a)

	B3LYP	M06-L
H1	0.147	0.162
H2	0.140	0.154
H3	0.101	0.116
H4	0.166	0.189
H5	0.203	0.222
H6	0.167	0.175
H7	0.124	0.136
H8	0.140	0.166

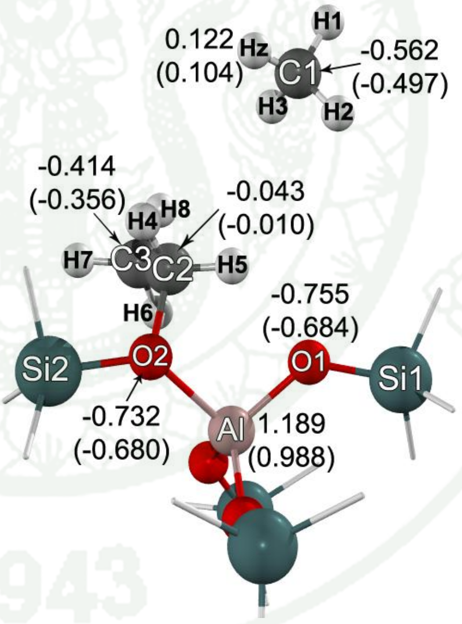

(b)

Figure 22 The Mulliken charges for (a) first transition state (**TS1_FAU**), (b) intermediate (**Int_FAU**), (c) methane desorption (**Ds_Met_FAU**), (d) second transition state (**TS2_FAU**), and (e) ethylene product (**Prod_Eth_FAU**) of propane cracking reaction over H-FAU zeolite by ONIOM(B3LYP:UFF) and ONIOM(M06-L:UFF). Values in parentheses present the results obtained from ONIOM(B3LYP:UFF).

	B3LYP	M06-L
H4	0.168	0.189
H5	0.202	0.224
H6	0.171	0.175
H7	0.124	0.136
H8	0.136	0.167

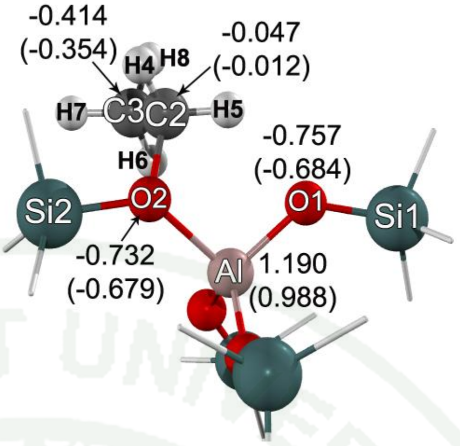

(c)

	B3LYP	M06-L
H4	0.191	0.205
H5	0.219	0.226
H7	0.173	0.215
H8	0.170	0.209

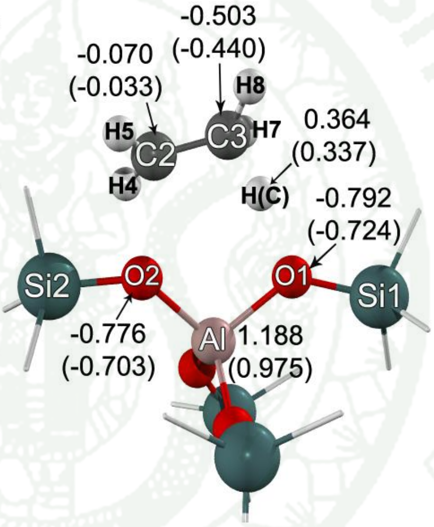

(d)

	B3LYP	M06-L
H4	0.160	0.199
H5	0.132	0.153
H7	0.132	0.164
H8	0.136	0.173

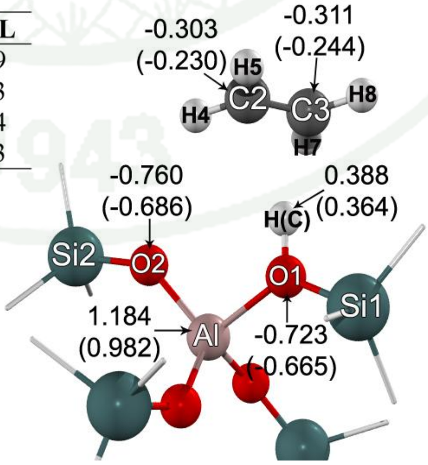

(e)

Figure 22 (Continued)

Table 6 The optimized geometric parameters of first transition state (**TS1_FAU**), intermediate (**Int_FAU**), methane desorption (**Ds_Met_FAU**), second transition state (**TS2_FAU**), and ethylene product (**Prod_Eth_FAU**) of propane cracking reaction over H-FAU zeolite by ONIOM(B3LYP/6-31G(d,p):UFF) and ONIOM(M06-L/6-31G(d,p):UFF). Values in parentheses present the results obtained from ONIOM(B3LYP/6-31G(d,p):UFF).

Parameters	**C_3H_8/H-FAU**				
	TS1_FAU	**Int_FAU**	**Ds_Met_FAU**	**TS2_FAU**	**Prod_Eth_FAU**
Distances (pm)					
O1-Hz	183.4 (183.0)	-	-	-	-
O1-Si1	163.3 (163.7)	161.1 (161.4)	161.2 (161.5)	163.8 (163.8)	169.3 (169.6)
Al -O1	182.4 (181.9)	172.5 (172.9)	172.4 (173.0)	180.5 (179.1)	193.2 (192.9)
O2-Al	175.6 (176.0)	193.1 (192.8)	193.3 (192.8)	178.8 (180.0)	171.5 (171.8)
O2-Si2	162.2 (163.2)	173.1 (173.1)	173.2 (173.3)	165.1 (166.1)	162.9 (163.1)
C1-C2	169.4 (179.0)	-	-	-	-
C1···Hz	130.2 (128.2)	-	-	-	-
C2···Hz	130.2 (131.9)	-	-	-	-
C2-O2	-	152.4 (153.7)	152.2 (153.4)	236.1 (227.7)	-
C2-C3	-	150.2 (151.4)	150.2 (151.4)	139.6 (141.0)	133.5 (133.9)
O1-H(C)	-	-	-	148.7 (152.8)	99.2 (99.7)

Table 6 (Continued)

Parameters	**C_3H_8/FAU**				
	TS1_FAU	**Int_FAU**	**Ds_Met_FAU**	**TS2_FAU**	**Prod_Eth_FAU**
Distances (pm)					
C3···H(C)	-	-	-	119.9 (119.0)	213.0 (216.1)
C2···H(C)	-	-	-	-	214.4 (216.3)
Angles (degrees)					
∠Si1-O1-Al	127.0 (126.7)	130.2 (130.4)	130.2 (130.3)	131.0 (130.8)	130.2 (129.2)
∠Si2-O2-Al	143.3 (142.4)	135.0 (134.0)	135.1 (134.0)	139.2 (137.6)	138.7 (138.7)

Discussion of the reaction pathways and the energy profiles for M06-L

From sections 1 and 2 the predictions of the adsorption energy and the activation energy in the protonation step calculated with ONIOM(M06-L/6-31G (d,p):UFF) are in good agreement with experimental study reported in the literature. In order to obtain more reliable reaction energies, the single point calculation was carried out at the M06-L/6-31G(d,p)//ONIOM(M06-L/6-31G(d,p):UFF) level of theory. The obtained results show that the reaction energy of adsorption and the all intermediates are increased in the range of 0.2-1.8 kcal/mol (see Figure 27) and the activation energies are decreased by 3.4 and 3.2 kcal/mol, with respect to the ONIOM(M06-L/6-31G(d,p):UFF) results. The activation energies for the protonation step and the deprotonation step calculated at the M06-L/6-31G(d,p)//ONIOM(M06-L/6-31G(d,p):UFF) level of theory are 43.7 and 24.7 kcal/mol, respectively (see Figure 27). This computed activation energy for the protonation step is slightly underestimated as compared to the experimental value of 46.9 kcal/mol (Xu *et al.*, 2006). These results indicate that the combined method between the newly DFT functional, M06-L, and the UFF force field is quite suitable for studying the structure, the adsorption energy, and the activation energy for the reaction mechanism of an alkane over the zeolite.

In previous theoretical studies, several groups studied the reaction of alkane cracking on zeolite using various models: 1T (Collins and O’Malley, 1995a; Kazansky *et al.*, 1999), 3T (Blaszkowski *et al.*, 1996), 5T (Zygmunt *et al.*, 2000; Boronat and Corma, 2008) and bigger clusters of 11T and 27T (Boronat and Corma, 2008). They found that the the carbonium-like ion can be either the transition state or the stable intermediate depending on the cluster size used in the calculations. For this work, we study the propane cracking reaction over a 120T zeolite cluster model of H-FAU zeolite with B3LYP:UFF and M06-L:UFF methods. We found the carbonium-like ion as a transition structure. Thus, attempts have been made to find the carbonium-like ion as a stable intermediate. However, we did not find this structure located on a local minimum of energy surface. This suggests that the zeolite structure directly affects the stability of the transition state and the intermediate species on the zeolite channel. Therefore, we propose that the propane cracking reactions on zeolite proceed via the carbonium-like ion as the transition state which would crack into methane and ethoxide intermediates. Our pathway is also confirmed by several quantum chemical calculations (Blaszkowski *et al.*,1996; Kazansky *et al.*, 1999; Zygmunt *et al.*, 2000; Zheng and Blowers, 2005a) and the experimental study (Ivanova *et al.*, 1998). The difference in the reaction pathway for alkane cracking between our study and those in literature (Collins and O'Malley, 1995a, 1995b; Boronat and Corma, 2008) is mainly due to the model used in the study. Since the small cluster size of zeolite does not represent the real zeolite structure and the size of probe molecule (propane) is small so that the steric effect is not taken into account as it has a strong effect in the channel of H-FAU (Kotrel et al., 2000, Boronat *et al.*, 2004).

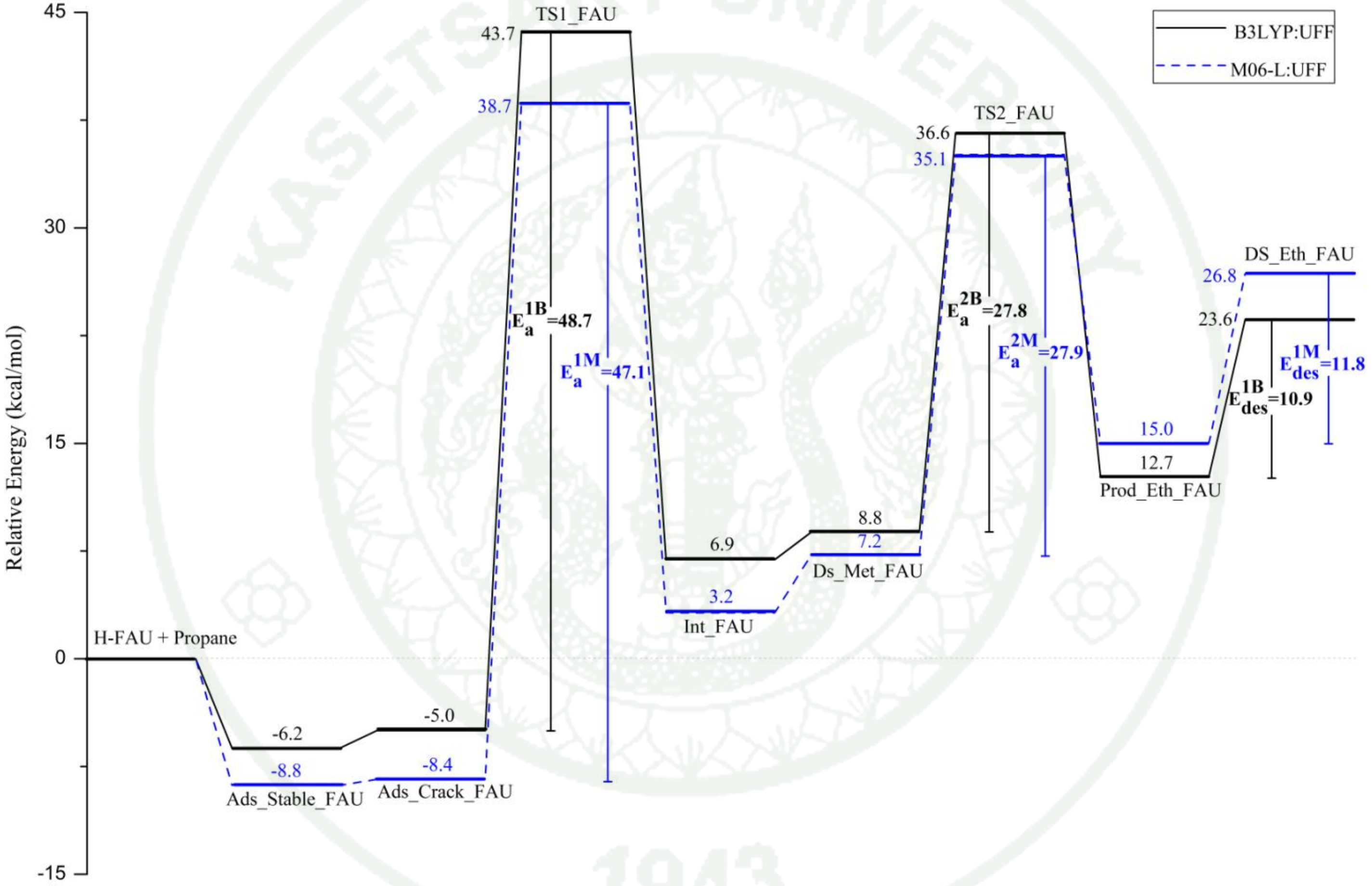

Figure 23 Calculated energy profiles (kcal/mol) for the propane cracking reaction mechanism over H-FAU zeolite by ONIOM(B3LYP/6-31G(d,p):UFF) (solid line) and ONIOM(M06-L/6-31G(d,p):UFF) (dash line).

3. Propane cracking reaction over H-MOR

The cracking reaction of propane on H-MOR zeolite proceeds via the same mechanism as already discussed for the H-FAU system. The adsorbed propane can be protonated by the acidic proton to form the carbonium-like ion transition state and then transformed to methane and ethoxide intermediates. As methane is desorbed, the ethoxide intermediate is then deprotonated. The corresponding proton is eventually transferred back to the zeolite framework. The final product is ethylene adsorbed on the Brønsted acid site (Figure 20).

Initially, the weakly adsorbed propane for the cracking reaction (**Ads_Crack_MOR**) can be protonated by the zeolite acid. The acidic proton (Hz) is then transferred to the C-C single bond between the methyl group (C1) and the ethyl group (C2C3) of propane. At the first transition state, **TS1_MOR**, the C1-C2 bond of propane molecule is weakened, when these atoms are protonated by an acidic proton from the zeolite, their atomic distances lengthen. Both the carbon atoms are then chemically bonded to the proton, resulting in three-center/two-electron complexes (C-H-C) to form the $C_3H_9^+$ proponium ion (carbonium-like ion). The selected geometric parameters are shown in Table 7. In this step, the distances O1-Hz are 222.8 pm (B3LYP:UFF) and 193.3 pm (M06-L:UFF). The C1-C2 bond distances of propane are lengthened from 153.3 to 211.2 pm for B3LYP:UFF (and 152.1 to 193.1 pm for M06-L:UFF) while the corresponding C1···Hz and C2···Hz distances are 122.3 and 129.2 pm for the B3LYP:UFF, respectively (122.3 and 130.3 pm for the M06-L: UFF). The C1···Hz···C2 bond angle in the proponium ion is computed to be 114.2^o (B3LYP:UFF) and 99.7^o (M06-L:UFF) (see Figure 24a). The transition state is confirmed by the frequency calculation with one imaginary frequency at -93 cm^{-1} for B3LYP:UFF and -97 cm^{-1} for M06-L:UFF, related to the movement of the acidic proton (Hz) of zeolite to the C1-C2 bond and the breaking of C1-C2 bond of the propane molecule. This step is called the protonation step. The activation energy barrier (and the corresponding apparent activation energy) calculated with B3LYP:UFF (E_a^{3B}) and M06-L:UFF (E_a^{3M}) are 54.1 (43.9) kcal/mol and 52.1 (38.4) kcal/mol, respectively (Figure 26), which are overestimated as compared to the experimental values (Xu *et al.*, 2006) of the energy barrier (45.0 kcal/mol) and apparent activation energy (35.0 kcal/mol). However, from the previous theoretical study using the 3T model of zeolite, the activation energy is about 62-68 kcal/mol (Rigby *et al.*, 1997, Zheng and Blowers, 2005a) which is significantly far from the experiment result. This can be explained by the lack of the framework effect on the adsorption energy as well as the activation energy. Thus, our results, with a better cluster model, provide reasonable values of the activation energy barrier and the corresponding apparent activation energy.

Then, the proponium ion is transformed into the ethoxide intermediate (**Int_MOR**) (see Figure 24b) and the methane side product is located in the zeolite channel. These complexes are stabilized by the zeolite framework. The ethoxide intermediate formed a covalent bond with O2 of the framework zeolite. Considering the structural parameter in comparison to the bare H-MOR zeolite, the covalent bond distances (C2-O2) are 153.6 pm (B3LYP:UFF) and 152.2 pm (M06-L:UFF). The Al-O1 and Si1-O1 bond distances are decreased by 14.9 pm (15.5 pm; M06-L:UFF) and 9.7 pm (9.5 pm; M06-L:UFF) from the B3LYP:UFF, respectively. The Si2-O2-Al bond angles are decreased by 15.4^{o} (B3LYP:UFF) and 13.4^{o} (M06-L:UFF). While, the Al-O2 and Si2-O2 bond distances are increased by 16.6 pm (17.5 pm; M06-L: UFF) and 10.9 pm (10.6 pm; M06-L:UFF) for B3LYP:UFF, respectively. The Si1-O1-Al bond angles are increased by 4.7^{o} (B3LYP:UFF) and 3.9^{o} (M06-L:UFF) (see Table 7). The adsorption energies of the intermediate complexes on zeolite computed with B3LYP:UFF and M06-L:UFF methods are 9.5 and 3.5 kcal/mol (Figure 26), respectively, which are less stable than the adsorption of the propane/ H-MOR complex.

Figure 25a gives the Mulliken charges for the **TS1_MOR**, the organic fragment ($C_3H_9^+$) holds the positive charge of 0.834 *e* (B3LYP) and 0.788 *e* (M06-L). From the $C_3H_9^+$ fragment, the proton (Hz) contributes the positive charges up to 0.243 (B3LYP) and 0.300 *e* (M06-L). Because of the interaction of the bridging Hz atom on the $C_3H_9^+$ fragment with the O1 atom surface of zeolite cluster, the $C_2H_5^+$ carbenium ion is more positively charged than that of the CH_3^+ carbenium ion group (0.699 *e* vs

0.661 *e* for B3LYP and 0.250 *e* vs 0.229 *e* for M06-L methods). Thus, the carbonium ion-like transition state ($C_3H_9^+$) dissociated by abstraction of methane and the $C_2H_5^+$ carbenium ion form the covalent bond with the O2 bridging oxygen atom of zeolite. These results indicated the formation of a carbonium ion-like transition state.

Subsequently, the methane side product is desorbed, **Ds_Met_MOR**, (Figure 24c) from the zeolite structure with a required energy of 4.3 kcal/mol for B3LYP:UFF (and 6.6 kcal/mol for M06-L:UFF) (Figure 26). This step slightly changes the structure of the active site of zeolite by less than 0.1 pm and 0.2^o for changes in the bond distance and bond angles, respectively. The covalent bond distance (C2-O2) is almost unchanged (Table 7). This alkoxide complex is an active species for the deprotonation step.

In the deprotonation step, a proton from the alkoxide species is transferred back to the bridging oxygen atom (O1) of the zeolite structure via the second transition state, **TS2_MOR**, which produces an ethylene product adsorbed on zeolite via a π-interaction (**Prod_Eth_MOR**). At the second transition state TS2_MOR (Figure 24d), the covalent bond between the ethoxide species (C2) and the O2 framework of zeolite is broken and a proton from the alkoxide species at C3, H(C), are extended by 116.1 and 115.7 pm, correspondingly the distance between a proton, H(C), and one from the bridging oxygen atom (O1) of the zeolite structure predicted by B3LYP:UFF and M06-L:UFF are about 158.5 and 158.3 pm, respectively. The imaginary frequency at -296 cm^{-1} from the B3LYP:UFF method (and -185 cm^{-1} for M06-L:UFF), is confirmed as the transition structure. This frequency is related to the movement of a proton from the ethoxide species to the bridging oxygen atom (O1) of the zeolite structure. The activation energies of the second transition state (**TS2_MOR**) are 24.8 and 25.1 kcal/mol calculated with the B3LYP:UFF and M06-L: UFF methods, respectively (Figure 26). Similar to the propane cracking on H-FAU zeolite, we found that the deprotonation step requires less energy than the protonation step. This finding agrees well with an experimental work which stated that the protonation step is the rate-limiting step for the propane cracking reaction (Narbeshuber *et al.*, 1995).

Subsequently, the reaction continues by the following steps. From **TS2_MOR**, a proton is transferred from the alkoxide species to the zeolite framework, resulting in the broken C3-H(C) bond and the hybridization of C3 is changed from tetrahedral (sp^3) to planar (sp^2), which produced the ethylene product adsorbed on the acidic proton (**Prod_Eth_MOR**), Figure 24e. The reaction energies for this step are calculated to be 13.0 kcal/mol for B3LYP:UFF (and 12.2 kcal/mol for M06-L:UFF). Finally, the adsorbed ethylene product is endothermically desorbed by energies of 10.6 kcal/mol (B3LYP:UFF) and 14.6 kcal/mol (M06-L:UFF) (see Figure 26).

The single point calculations at M06-L/6-31G(d,p)//ONIOM(M06-L/6-31G (d,p):UFF) level of theory are carried out in order to obtain more reliable reaction energies, are carried out. These results show that the reaction energies for all the complexes along the reaction pathway, compared to the M06-L:UFF energies, are increased in the range of 0.1-3.8 kcal/mol (see Figure 27) and the activation energies are decreased by 10.8 and 6.6 kcal/mol for the protonation step and deprotonation step, respectively. The activation energies obtained from the M06-L/6-31G(d,p)// ONIOM(M06-L/6-31G(d,p):UFF) are 41.3 and 18.5 kcal/mol for the protonation step and the deprotonation step, respectively. This computed activation energy for the protonation step is slightly underestimated in comparison with the experimentally measured energy by about ~4 kcal/mol (expt. = 45 kcal/mol; Xu *et al.*, 2006).

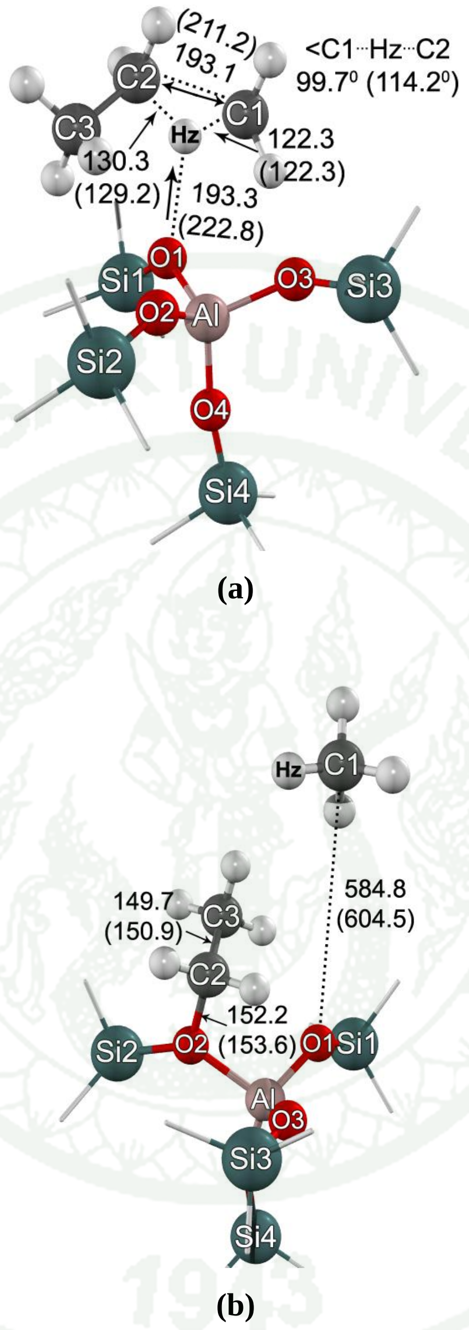

Figure 24 The optimized structure parameters for (a) first transition state (**TS1_MOR**), (b) intermediate (**Int_MOR**), (c) methane desorption (**Ds_Met_MOR**), (d) second transition state (**TS2_MOR**), and (e) ethylene product (**Prod_Eth_MOR**) of propane cracking reaction over H-MOR zeolite by ONIOM(B3LYP:UFF) and ONIOM(M06-L:UFF). Value in parentheses present the results obtained from ONIOM(B3LYP:UFF).

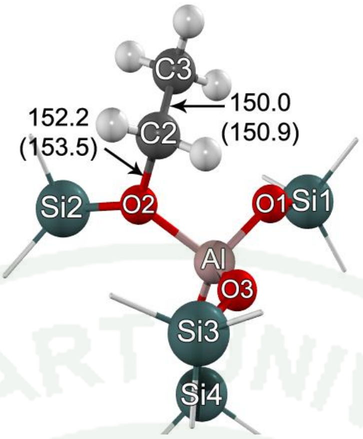

(c)

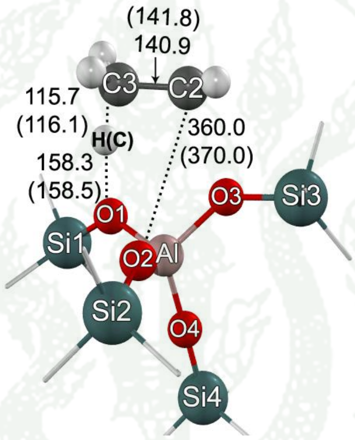

(d)

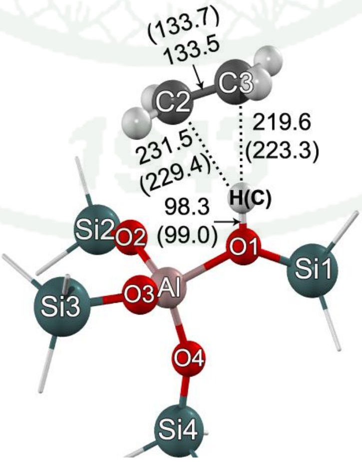

(e)

Figure 24 (Continued)

	B3LYP	M06-L
H1	0.219	0.231
H2	0.268	0.242
H3	0.168	0.199
H4	0.217	0.223
H5	0.190	0.215
H6	0.193	0.168
H7	0.152	0.172
H8	0.203	0.209

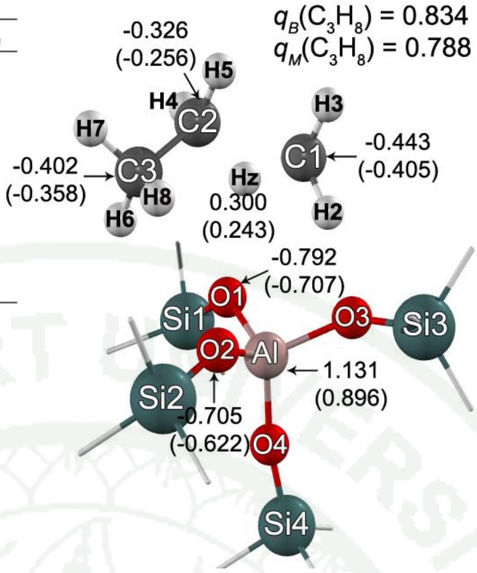

(a)

	B3LYP	M06-L
H1	0.125	0.137
H2	0.119	0.135
H3	0.142	0.150
H4	0.146	0.176
H5	0.176	0.191
H6	0.178	0.166
H7	0.138	0.167
H8	0.136	0.137

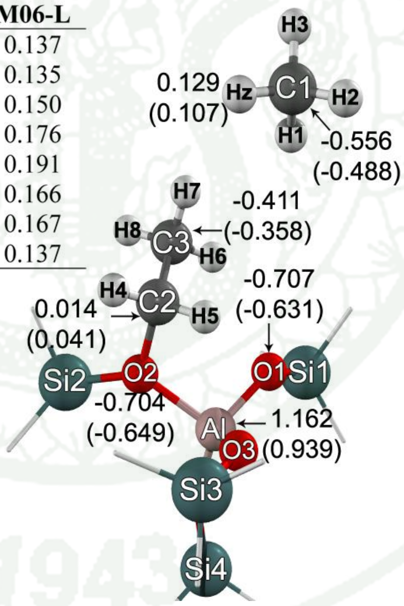

(b)

Figure 25 The Mulliken charges for (a) first transition state (**TS1_MOR**), (b) intermediate (**Int_MOR**), (c) methane desorption (**Ds_Met_MOR**), (d) second transition state (**TS2_MOR**), and (e) ethylene product (**Prod_Eth_MOR**) of propane cracking reaction over H-MOR zeolite by ONIOM (B3LYP:UFF) and ONIOM(M06-L:UFF). Values in parentheses present the results obtained from ONIOM(B3LYP:UFF).

	B3LYP	M06-L
H4	0.157	0.158
H5	0.182	0.177
H6	0.172	0.180
H7	0.139	0.166
H8	0.131	0.148

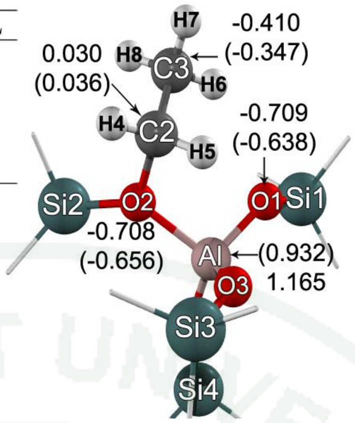

(c)

	B3LYP	M06-L
H4	0.215	0.202
H5	0.197	0.215
H7	0.207	0.204
H8	0.200	0.201

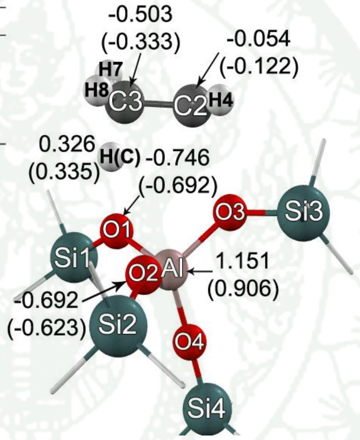

(d)

	B3LYP	M06-L
H4	0.160	0.181
H5	0.144	0.156
H7	0.140	0.147
H8	0.128	0.154

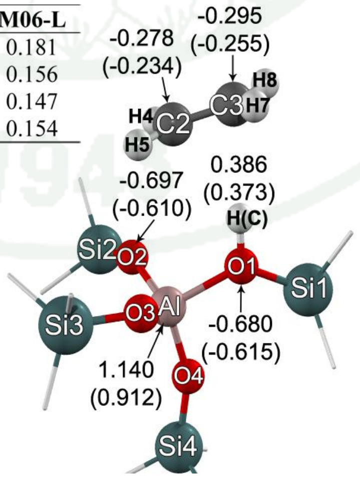

(e)

Figure 25 (Continued)

Table 7 The optimized geometric parameters of first transition state (**TS1_MOR**), intermediate (**Int_MOR**), methane desorption (**Ds_Met_MOR**), second transition state (**TS2_MOR**), and ethylene product (**Prod_Eth_MOR**) of propane cracking reaction over H-MOR zeolite by ONIOM(B3LYP/6-31G(d,p):UFF) and ONIOM(M06-L/6-31G(d,p):UFF). Values in parentheses present the results obtained from ONIOM(B3LYP/6-31G(d,p):UFF).

Parameters	**C_3H_8/H-MOR**				
	TS1_MOR	**Int_MOR**	**Ds_Met_MOR**	**TS2_MOR**	**Prod_Eth_MOR**
Distances (pm)					
O1-Hz	193.3 (222.8)	-	-	-	-
O1-Si1	158.9 (159.2)	157.9 (158.0)	157.8 (158.1)	159.0 (159.2)	166.3 (166.9)
Al -O1	170.2 (169.4)	165.0 (165.2)	165.0 (165.1)	168.6 (168.6)	178.9 (178.8)
O2-Al	167.4 (167.4)	182.0 (181.4)	182.0 (181.5)	165.6 (165.8)	165.0 (165.4)
O2-Si2	156.9 (156.9)	167.5 (168.1)	167.5 (168.1)	156.9 (156.9)	156.9 (157.1)
C1-C2	193.1 (211.2)	-	-	-	-
C1···Hz	122.3 (122.3)	-	-	-	-
C2···Hz	130.3 (129.2)	-	-	-	-
C2-O2	-	152.2 (153.6)	152.2 (153.5)	360.0 (370.0)	-
C2-C3	-	149.7 (150.9)	150.0 (150.9)	140.9 (141.8)	133.5 (133.7)
O1-H(C)	-	-	-	158.3 (158.5)	98.3 (99.0)

Table 7 (Continued)

Parameters	C_3H_8/H-MOR				
	TS1_MOR	**Int_MOR**	**Ds_Met_MOR**	**TS2_MOR**	**Prod_Eth_MOR**
Distances (pm)					
C3··· H(C)	-	-	-	115.7 (116.1)	219.6 (223.3)
C2··· H(C)	-	-	-	-	231.5 (229.4)
Angles (degrees)					
∠Si1-O1-Al	129.3 (127.9)	131.9 (132.0)	132.1 (132.1)	133.3 (132.7)	128.6 (127.3)
∠Si2-O2-Al	147.7 (147.6)	135.6 (133.9)	135.7 (133.9)	147.3 (149.0)	148.9 (149.1)

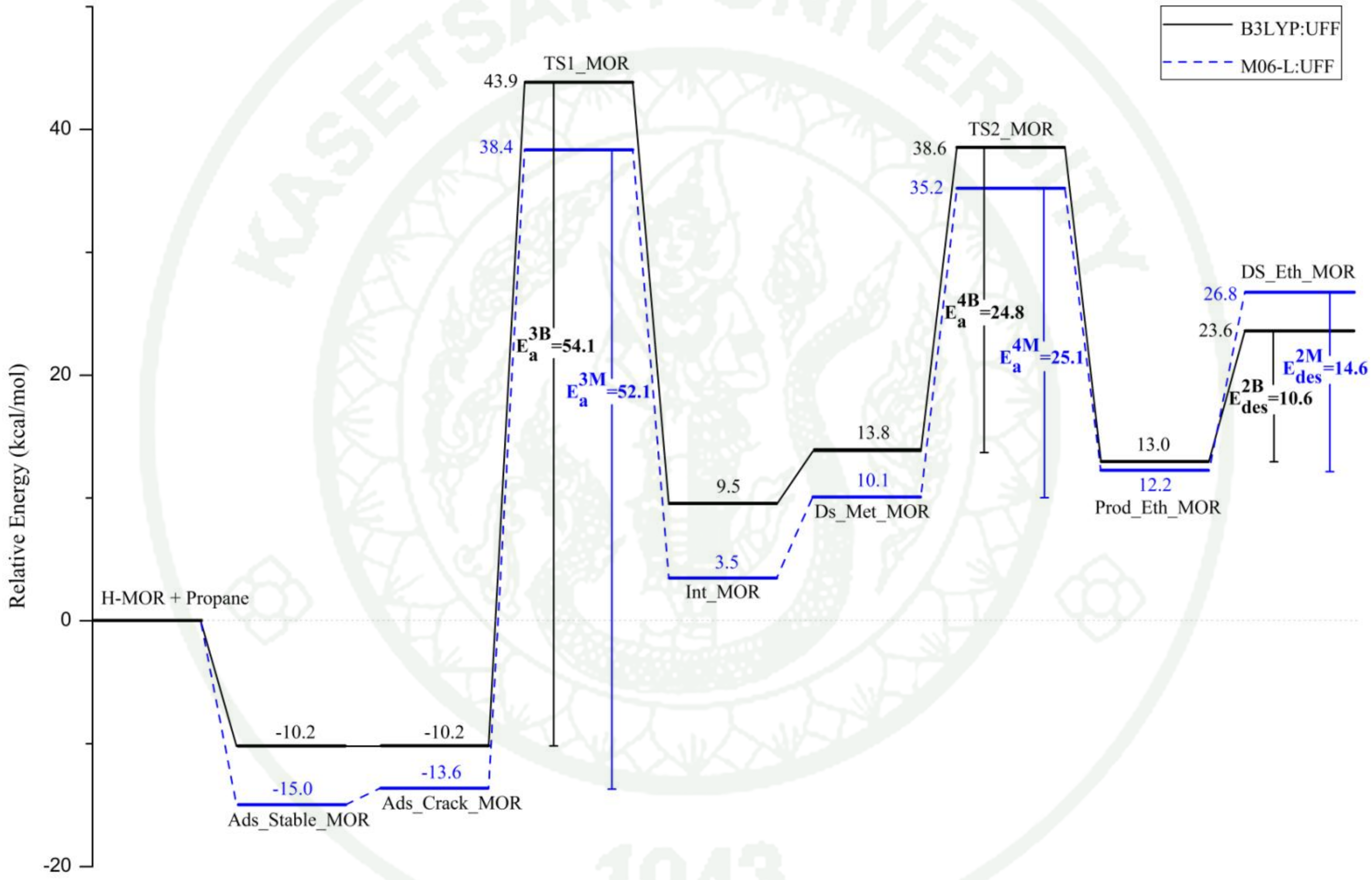

Figure 26 Calculated energy profiles (kcal/mol) for the propane cracking reaction mechanism over H-MOR zeolite by ONIOM (B3LYP/6-31G(d,p):UFF) (solid line) and ONIOM(M06-L/6-31G(d,p):UFF) (dash line).

4. The differences between C_3H_8/H-FAU and C_3H_8/H-MOR and the efficiency of density functional (B3LYP and M06-L)

The propane cracking reaction over H-FAU and H-MOR zeolites are carried out with the same procedure. The reaction proceeds via the Haag-Dessau mechanism, which is also known as the carbonium-like ion cracking mechanism. In this mechanism, the carbonium-like ion is the transition state which would crack into the methane side product and ethoxide intermediate formed covalent bond with the surface of zeolites. The first transition state is called the protonation step. Then, a methane side product is desorbed from the channel of zeolite. After that, the ethoxide is transferred proton back to the surface of zeolites resulting in the formation of the ethylene product adsorbed on the surface of the zeolites. The second transition state is known as the deprotonation step. From our data in sections 2 and 3, we found that the protonation step is the rate-limiting step which is in good agreement with experimental study (Narbeshuber *et al.*, 1995). From Figure 27, we found the adsorption energy of propane on H-MOR rather stronger than that of the H-FAU because of the stronger confinement effect (as discussed in section 1). However, the apparent activation barrier of the H-FAU is higher than that of the H-MOR. Because of, the transition state in the ion-pair complex is stabilized by electrostatic and van der Waals interaction from H-MOR> H-FAU zeolite. From the adsorption and the TS1 energetic profile, the actual activation energy barriers of propane on both zeolites are not different. This result suggests that the adsorption energy plays an important role in determining the cracking activity of the alkane on zeolite. The activation energy barrier of propane cracking is also insensitive to the size or structure of the selected zeolite in this work (Babitz *et al.*, 1999, van Bokhoven *et al.*, 2004; Xu *et al.*, 2006).

As for the method used, from sections 1-3, it is shown that the M06-L:UFF method predicted the structure, adsorption energy and activation energy of the propane cracking reaction on zeolites is better than the B3LYP:UFF, as can be seen from Figure 27 (as discussed in sections 1-3). However, reliable reaction energy is obtained from the single point calculation at M06-L/6-31G(d,p)//ONIOM(M06-L/ 6-31G(d,p):UFF). This method correctly predicted the adsorption energy as well as the activation energy barrier on both zeolites for the propane cracking reaction by providing closer values to the previous experiment values. From our data, we suggest that the M06-L functional is appropriate for predicting the propane cracking reaction over H-FAU and H-MOR zeolites than the B3LYP functional. The full quantum calculation treated by M06-L functional is highly recommended.

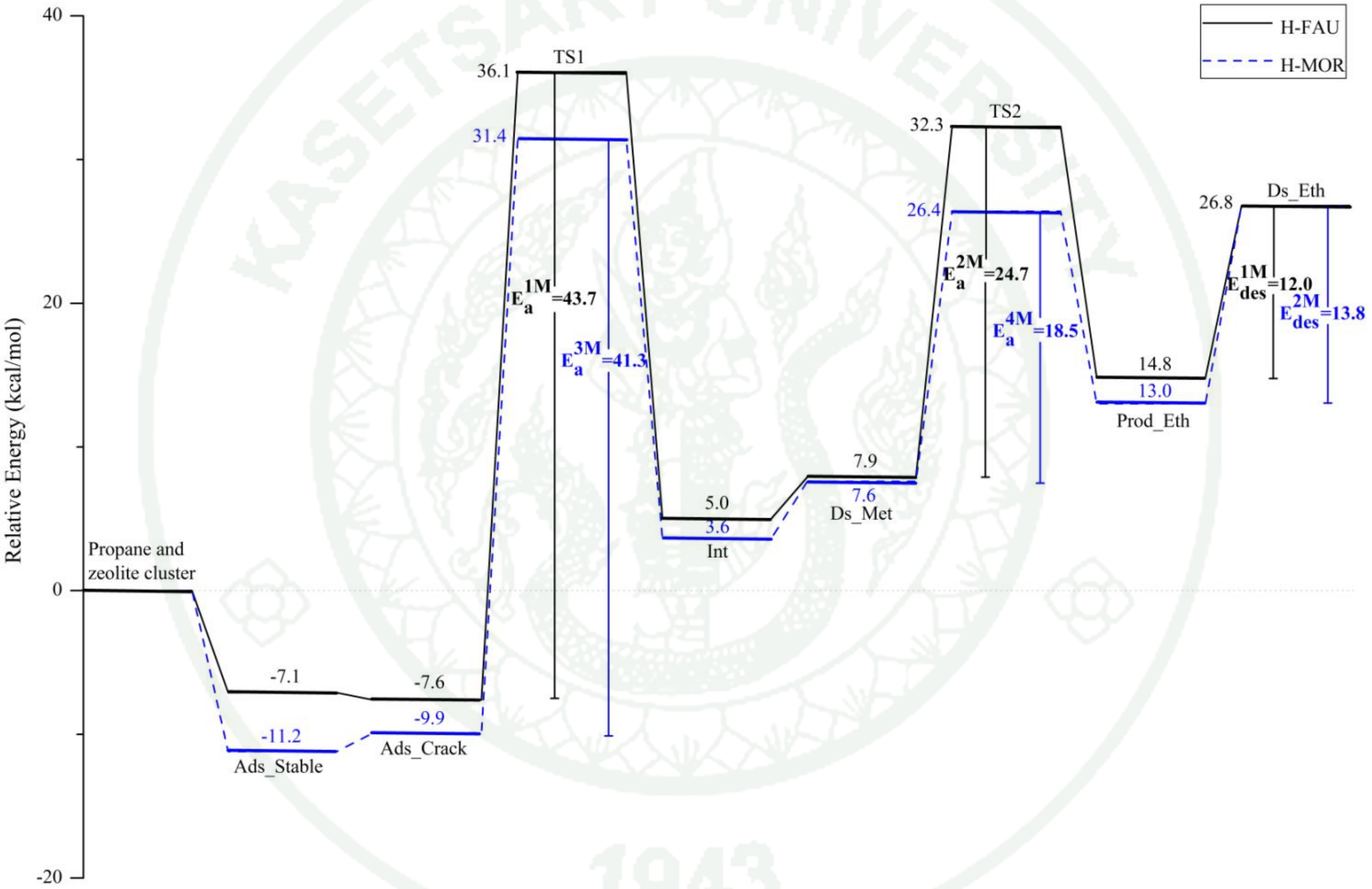

Figure 27 Calculated energy profiles (kcal/mol) for the propane cracking reaction mechanism over H-FAU (solid line) and H-MOR (dash line) zeolites by M06-L/6-31G(d,p)//ONIOM(M06-L/6-31G(d,p):UFF).

CONCLUSIONS

H/H Exchange Reaction of Propane Adsorbed over H-FAU Zeolite Investigated by the ONIOM method

The hydrogen exchange reactions of propane adsorbed over H-FAU zeolite were investigated by the ONIOM(B3LYP/6-31G(d,p):UFF) approach. Three different adsorption configurations of propane were obtained, dependent on the rearrangement of the propane molecule inside the nanocluster zeolite. The adsorption energies for the most stable, primary carbon, and secondary carbon propane/zeolite complex were predicted to be -6.2, -5.7, and -4.6 kcal/mol, respectively. The computed adsorption energy of the most stable propane/zeolite complex is in good agreement with the experimental observations. The H/H exchange reaction between the adsorbed propane molecule and the Brønsted acid of zeolite occur via both the primary- and the secondary hydrogen exchange mechanisms at the primary- and secondary carbon atoms of the propane molecule. These two exchange processes proceed via the carbonium ion-like transition state which is in agreement with the experiment study in literature. The corresponding apparent activation energies are calculated to be 27.3 and 26.5 kcal/mol for the primary- and secondary hydrogen exchange reactions, respectively, which are close to the previous experiment study of the H/H exchange reaction over H-ZSM-5 zeolite (to our knowledge, no experiment activation energy of H/H exchange reaction of propane over H-FAU zeolite is available in the literature). We find that the primary- and secondary hydrogen exchange of propane over acidic zeolite are competitive reactions. From our study, the calculated activation energies of the hydrogen exchange of propane adsorbed over zeolite show the influence of the zeolitic framework on the activation energy for the hydrogen exchange reaction. These results indicate that the ONIOM method is a practical tool for studying the activation energy properties of an alkane reaction on the framework zeolite.

Propane Cracking Reaction over Different Types of Nanostructured Zeolites: A Newly Developed DFT Approach

The propane cracking reactions over acidic faujasite and mordenite zeolites were studied at the molecular level using the ONIOM2 scheme. Two types of ONIOM models were utilized in this study, i.e., B3LYP/6-31G(d,p):UFF and M06-L/ 6-31G(d,p):UFF. The B3LYP and M06-L functionals were employed for the high level of calculation while the universal force field (UFF) molecular mechanic was selected to represent the low level. Our results show that the M06-L functional is the more appropriate method for the prediction of the propane cracking reaction over both the acidic zeolites than the B3LYP functional. Two major steps for cracking of propane are reported as the protonation and the deprotonation step. In the protonation step, the zeolite's proton transfers to a C-C bond of a propane molecule and forms the carbonium-like ion transition state (namely proponium ion) followed by the dissociation of methane and the ethoxide intermediate. Finally, one hydrogen atom of the ethoxide intermediate is deprotonated to the zeolite framwork, yeilding the ethylene product. The first step is found to be rate-determining step. The actual activation energies are computed to be 43.7 and 41.3 kcal/mol for H-FAU and H-MOR, respectively, which are close to the experimentally estimated of 46.9 (H-FAU) and 45.0 (H-MOR) kcal/mol. The second step required less activation energy: 24.7 kcal/mol for H-FAU and 18.5 kcal/mol for H-MOR. The predicted energy profiles were calculated at M06-L/6-31G(d,p)//ONIOM(M06-L/6-31G (d,p):UFF) level of theory. The results derived in the present study suggest that the propane cracking was insensitive to the type of selected zeolite structure.

LITERATURE CITED

Alberti, A. 1997. Location of Brønsted sites in mordenite. **Zeolites** 19(5-6):411-415.

______, P. Davoli and G.Z. Vezzalini. 1986. The crystal-structure refinement of a natural mordenite. **Kristallography** 175(3-4):249-256.

Allinger, N.L., Y.H. Yuh, and J-H Lii. 1989. Molecular Mechanics. The MM3 Force Field for Hydrocarbons. 1. **J. Am. Chem. Soc.** 111, 8551-8565.

Arzumanov, S.S., S.I. Reshetnikov, A.G. Stepanov, V.N. Parmon and D. Freude. 2005. In situ ^{1}H and ^{13}C MAS NMR kinetic study of the mechanism of H/D exchange for propane on zeolite H-ZSM-5. **J. Phys. Chem. B** 109(42):19748-19757.

Babitz, S.M., B.A. Williams, J.T. Miller, R.Q. Snurr, W.O. Haag and H.H. Kung. 1999. Monomolecular cracking of n-hexane on Y, MOR, and ZSM-5 zeolites. **Appl. Catal. A** 179(1-2):71-86.

Bates, S.P. and R.A. van Santen. 1998. The molecular basis of zeolite catalysis: A review of theoretical simulations. **Adv. Catal.** 42:1.

Becke, A.D. 1988. Density-functional exchange-energy approximation with correct asymptotic behavior. **Phys. Rev. A** 38: 3098-3100.

______. 1993. Density-functional thermochemistry. III. The role of exact exchange. **J. Chem. Phys.** 98(7):5648-5652.

Becker, K.A., H.G. Karge and W.D. Streubel. 1973. Benzene alkylation with ethylene and propylene over H-mordenite as catalyst. **J. Catal.** 28(3):403-413.

Blaszkowski, S.R., M.A.C. Nascimento and R.A. van Santen. 1996. Activation of C-H and C-C bonds by an acidic zeolite: A density functional study. **J. Phys. Chem.** 100(9):3463-3472.

Boronat, M. and A. Corma. 2008. Are carbenium and carbonium ions reaction intermediates in zeolite-catalyzed reactions?. **Appl. Catal. A** 336(1-2):2-10.

Boronat, M., P.M. Viruela and A. Corma. 2004. Reaction Intermediates in Acid catalysis by zeolites: prediction of the relative tendency to form alkoxides or carbocations as a function of hydrocarbon nature and active site structure. **J. Am. Chem. Soc.** 126(10):3300-3309.

______, C.M. Zicovich-Wilson, P. Viruela and A. Corma. 2001. Influence of the local geometry of zeolite active sites and olefin size on the stability of alkoxide intermediates. **J. Phys. Chem. B** 105(45):11169-11177.

Brändle, M. and J. Sauer. 1998. Acidity differences between inorganic solids induced by their framework structure. A combined quantum mechanics/molecular mechanics ab initio study on zeolites. **J. Am. Chem. Soc.** 120(7):1556-1570.

Brooks, B.R., R.E. Bruccoleri, B.D. Olafson, D.J. States, S. Swaminathan and Karplus M. 1983. "CHARMM: A program for macromolecular energy, minimization, and dynamics calculations". **J. Comp. Chem**. 4:187–217.

Cant, N.W. and W.K. Hall. 1972. Studies of hydrogen held by solids: XXI. The interaction between ethylene and hydroxyl groups of a Y-zeolite at elevated temperatures. **J. Catal.** 25(1):161-172.

Collins, S.J. and P.J. O’malley. 1995. A theoretical description for the monomolecular cracking of C-C bonds over acidic zeolites. **J. Catal.** 153(1):94-99.

Collins, S.J. and P.J. O’malley. 1995. The mechanism of alkane activation over zeolite Brønsted acid sites. A density-functional study. **Chem. Phys. Lett.** 246(6):555-561.

Corma, A. 2003. State of the art and future challenges of zeolites as catalysts. **J. Catal.** 216(1-2):298-312.

______, V. Martínez-Soria and E. Schnoeveld. 2000. Alkylation of benzene with short-chain olefins over MCM-22 zeolite: Catalytic behaviour and kinetic mechanism. **J. Catal.** 192(1):163-173.

______, J. Planelles, J. Sánchez-Marín and F. Tomás. 1985. The role of different types of acid site in the cracking of alkanes on zeolite catalysts. **J. Catal.** 93(1):30-37.

Cornell, W.D., P. Cieplak, C.I. Bayly, I.R. Gould, K.M. Merz, Jr., D.M. Ferguson, D.C. Spellmeyer, T. Fox, J.W. Caldwell, and P.A. Kollman. 1995. A Second Generation Force Field for the Simulation of Proteins, Nucleic Acids, and Organic Molecules. **J. Am. Chem. Soc.** 117, 5179-5197.

Dapprich, S., I. Komiromi, K.S. Byun, K. Morokuma, and M.J. Frisch. 1999. A new ONIOM implementation in Gaussian98. Part I. The calculation of energies, gradients, vibrational frequencies and electric field derivatives. **THEOCHEM** 461-462:1-21.

de Vries, A.H., P. Sherwood, S.J. Collins, A.M. Rigby, M. Rigutto and G.J. Kramer. 1999. Zeolite structure and reactivity by combined quantum-chemical-classical calculations. **J. Phys. Chem. B** 103(29):6133-6141.

Derouane, E.G. 1986. Shape selectivity in catalysis by zeolites: The nest effect. **J. Catal.** 100(2):541-544.

Eder, F., M. Stockenhuber and J.A. Lercher. 1997. Brønsted acid site and pore controlled siting of alkane sorption in acidic molecular sieves. **J. Phys. Chem. B** 101(27):5414-5419.

Engelhardt, J. and W.K. Hall. 1995. Peculiarities observed in H-D exchange between perdeuterioisobutane and H-zeolites. **J. Catal.** 151(1):1-9.

Esteves, P.M., M.A.C. Nascimento and C.J.A. Mota. 1999. Reactivity of alkanes on zeolites: A theoretical ab tnitio study of the H/H exchange. **J. Phys. Chem. B** 103(47):10417-10420.

Evleth, E.M., E. Kassab and L.R. Sierra. 1994. Calculation of the exchange mechanism of D_2 and CD_4 with a zeolite model. **J. Phys Chem.** 98(5):1421-1426.

Frisch, M.J., G.W. Trucks, H.B. Schlegel, G.E. Scuseria, M.A. Robb, J.R. Cheeseman, J.A. Montgomery, T. Vreven, K.N. Kudin, J.C. Burant, J.M. Millam, S.S. Iyengar, J. Tomasi, V. Barone, B. Mennucci, M. Cossi, G. Scalmani, N. Rega, G.A. Petersson, H. Nakatsuji, M. Hada, M. Ehara, K. Toyota, R. Fukuda, J. Hasegawa, M. Ishida, T. Nakajima, Y. Honda, O. Kitao, H. Nakai, M. Klene, X. Li, J.E. Knox, H.P. Hratchian, J.B. Cross, V. Bakken, C. Adamo, J. Jaramillo, R. Gomperts, R.E. Stratmann, O. Yazyev, A.J. Austin, R. Cammi, C. Pomelli, J.W. Ochterski, P.Y. Ayala, K. Morokuma, G.A. Voth, P. Salvador, J.J. Dannenberg, V.G. Zakrzewski, S. Dapprich, A.D. Daniels, M.C. Strain, O. Farkas, D.K. Malick, A.D. Rabuck, K. Raghavachari, J.B. Foresman, J.V. Ortiz, Q. Cui, A.G. Baboul, S. Clifford, J. Cioslowski, B.B. Stefanov, G. Liu, A. Liashenko, P. Piskorz, I. Komaromi, R.L. Martin, D.J. Fox, T. Keith, M.A. Al-Laham, C.Y. Peng, A. Nanayakkara, M. Challacombe, P.M.W. Gill, B. Johnson, W. Chen, M.W. Wong, C. Gonzalez and J.A. Pople. 2004. Gaussian 03, Gaussian Inc., Wallingford, CT.

Greatbanks, S.P., I.H. Hillier, N.A. Burton and P. Sherwood. 1996. Adsorption of water and methanol on zeolite Brønsted acid sites: An ab initio, embedded cluster study including electron correlation. **J. Chem. Phys.** 105(9):3770-3776.

Haag, W.O. and R.M. Desssau, in: Proceedings, 8th International Congress on Catalysis Berlin, 1984. Dechema, Frankfurt-am-Main, 1984, vol. 2:305.

______, ______, R.M. Lago, S.N. Tomoyuki lnui and T. Takashi. 1991. Kinetics and mechanism of paraffin cracking with zeolite catalysts. **Stud. Surf. Sci. Catal.** Vol. 60:255-265.

Haouas, M., S. Walspurger and J. Sommer. 2003. Regioselective H/D isotope exchange and skeletal rearrangement reactions of propane over strong solid acids. **J. Catal.** 215(1):122-128.

Haw, J.F., J.B. Nicholas, T. Xu, L.W. Beck and D.B. Ferguson. 1996. Physical organic chemistry of solid acids: Lessons from in situ NMR and theoretical chemistry. **Acc. Chem. Res.** 29(6):267.

______, B.R. Richardson, I.S. Oshiro, N.D. Lazo and J.A. Speed. 1989. Reactions of propene on zeolite H-Y catalyst studied by in situ variable-temperature solid-state nuclear magnetic resonance spectroscopy. **J. Am. Chem. Soc.** 111(6): 2052-2058.

Hill, J.R., C.M. Freeman and B. Delley. 1999. Bridging hydroxyl groups in faujasite: Periodic vs cluster density functional calculations. **J. Phy. Chem. A** 103(19): 3772-3777.

Hua, W., A. Sassi, A. Goeppert, F. Taulelle, C. Lorentz and J. Sommer. 2001. H/D exchange reaction between isobutane and acidic USY zeolite: A mechanistic study by mass spectrometry and in situ NMR. **J. Catal.** 204(2):460-465.

Hunter, K.C. and A.L.L. East. 2002. Properties of C-C bonds in n-alkanes: Relevance to cracking mechanisms. **J. Phys. Chem. A** 106(7):1346-1356.

Ivanova, I.I., E.B. Pomakhina, A.I. Rebrov and E.G. Derouane. 1998. ^{13}C MAS NMR mechanistic study of the initial stages of propane activation over H-ZSM-5 zeolite. **Top. Catal.** 6(1-4):49-59.

Jansang, B., T. Nanok and J. Limtrakul. 2007. Interaction of mordenite with an aromatic hydrocarbon: An embedded ONIOM study. **J. Mol. Catal. A:Chem.** 264(1-2):33-39.

______, ______, and ______. 2008. Structure and reaction mechanism of alkylation of phenol with methanol over H-FAU zeolite: An ONIOM study. **J. Phys. Chem. C** 112(2):540-547.

Jiang, G., L. Zhang, Z. Zhao, X. Zhou, A. Duan, C. Xu and J. Gao. 2008. Highly effective P-modified H-ZSM-5 catalyst for the cracking of C4 alkanes to produce light olefins. **App. Catal. A. Gen.** 340(2):176-182.

Kasuriya, S., S. Namuangruk, P. Treesukol, M. Tirtowidjojo and J. Limtrakul. 2003. Adsorption of ethylene, benzene, and ethylbenzene over faujasite zeolites investigated by the ONIOM method. **J. Catal.** 219(2):320-328.

Kazansky, V.B. 1999. Adsorbed carbocations as transition states in heterogeneous acid catalyzed transformations of hydrocarbons. **Catal. Today** 51(3-4):419-434.

______, M.V. Frash and R.A. van Santen. 1996. Quantumchemical study of the isobutane cracking on zeolites. **App. Catal. A: Gen.** 146(1):225-247.

Kazansky, V.B., I.N. Senchenya, M. Frash and R.A. van Santen. 1994. A quantum-chemical study of adsorbed nonclassical carbonium ions as active intermediates in catalytic transformations of paraffins. I. Protolytic cracking of ethane on high silica zeolites. **Catal. Lett.** 27(3-4):345-354.

Khaliullin, R.Z., A.T. Bell and V.B. Kazansky. 2001. An experimental and density functional theory study of the interactions of CH_4 with H-ZSM-5. **J. Phys. Chem. A** 105(45):10454-10461.

Klepel, O., A. Loubentsov, W. Böhlmann and H. Papp. 2003. Oligomerization as an important step and side reaction for skeletal isomerization of linear butenes on H-ZSM-5. **App. Catal. A: Gen.** 255(2):349-354.

Klinowski, J. 1991. Solid state NMR studies of molecular sieve catalysts. **Chem. Rev.** 91:1459-1479.

Kotrel, S., H. Knözinger and B.C. Gates. 2000. The Haag-Dessau mechanism of protolytic cracking of alkanes. **Micro. Meso. Mat.** 35-36:11-20.

Kramer, G.J. and R.A. Van Santen. 1995. An ab initio study of D/H exchange between CD_4 and the H-forms of zeolites FAU and MFI. **J. Am. Chem. Soc.** 117(6):1766-1776.

______, R.A. van Santen, C.A. Emeis and A.K. Nowak. 1993. Understanding the acid behaviour of zeolites from theory and experiment. **Nature** 363(6429):529-531.

Lee, B., J.N. Kondo, F. Wakabayashi and K. Domen. 1999. Infrared study of H/D isotope exchange reaction of alkanes and Brønsted acidic hydroxyl groups on FER zeolite. **Catal. Lett.** 59(1):51-54.

Lee, C., W. Yang and R.G. Parr. 1988. Development of the Colle-Salvetti correlation-energy formula into a functional of the electron density. **Phys. Rev. B** 37(2):785-789.

Lercher, J.A., R.A. van Santen and H. Vinek. 1994. Carbonium ion formation in zeolite catalysis. **Catal. Lett.** 27(1-2):91-96.

Limtrakul, J. 1995. Adsorption of methanol in zeolite, gallosilicate and SAPO catalysts. **Chem. Phys.** 193(1-2):79-87.

______, T. Nanok, S. Jungsuttiwong, P. Khongpracha and T.N. Truong. 2001. Adsorption of unsaturated hydrocarbons on zeolites: The effects of the zeolite framework on adsorption properties of ethylene. **Chem. Phys. Lett.** 349 (1-2):161-166.

______, P. Treesukol, C. Ebner, R. Sansone and M. Probst. 1997. Structures and potential energy surface of Faujasitic zeolite/water. **Chem. Phys.** 215(1):77-87.

Lins, J.O.M.A. and M.A.C. Nascimento. 1996. Theoretical investigation of the methane activation reaction on protonated zeolite from generalized valence-bond plus configuration interaction calculations. **J. Mol. Struct. THEOCHEM** 371:237-243.

Maihom, T., S. Namuangruk, T. Nanok and J. Limtrakul. 2008. Theoretical study on structures and reaction mechanisms of ethylene oxide hydration over H-ZSM-5: Ethylene glycol formation. **J. Phys. Chem. C** 112(33):12914-12920.

Martins, A., J.M. Silva, F.R. Ribeiro, M.F. Ribeiro and N.Z.a.P.N.J. Cejka. 2005. Isomerization of n-hexane on bifunctional catalysts Pt/HBEA and Pt/HMCM-22 with rare earth elements. **Stud. Surf. Sci. Catal.** 158(2):1875-1882.

Milas, I. and M.A. Chaer Nascimento. 2006. A density functional study on the effect of the zeolite cavity on its catalytic activity: The dehydrogenation and cracking reactions of isobutane over HZSM-5 and HY zeolites. **Chem. Phys. Lett.** 418(4-6):368-372.

Namuangruk, S., P. Khongpracha, P. Pantu and J. Limtrakul. 2006. Structures and reaction mechanisms of propene oxide isomerization on H-ZSM-5: An ONIOM study. **J. Phys. Chem. B** 110(51):25950-25957.

______, D. Tantanak and J. Limtrakul. 2006. Application of ONIOM calculations in the study of the effect of the zeolite framework on the adsorption of alkenes to ZSM-5. **J. Mol. Catal A: Chem.** 256(1-2):113-121.

Narbeshuber, T.F., A. Brait, K. Seshan and J.A. Lercher. 1997. Dehydrogenation of Light Alkanes over Zeolites. **J. Catal.** 172(1):127-136.

______, H. Vinek and J.A. Lercher. 1995. Monomolecular conversion of light alkanes over H-ZSM-5. **J. Catal.** 157(2):388-395.

Norman, L., and N.L. Allinger. 1977. Conformational analysis. 130. MM2. A hydrocarbon force field utilizing V1 and V2 torsional terms. **J. Am. Chem. Soc.** 99, 8127-8134.

Olah, G.A., G.K.S. Prakash and J. Sommer. 1995. **Superacids.** Wiley-Interscience, New York

______, ______, R.E. Williams, J.D. Field and D. Wade. 1987. **Hydrocarbon chemistry.** Wiley&Sons, New York.

Olson, D.H. and E. Dempsey. 1969. The crystal structure of the zeolite hydrogen faujasite. **J. Catal.** 13(2):221-231.

Pabchanda, S., P. Pantu and J. Limtrakul. 2005. Hydrolysis of methoxide species and regeneration of active site in Fe-ZSM-5 catalyst by the ONIOM method. **J. Mol. Catal. A: Chem.** 239(1-2):103-110.

Pantu, P., B. Boekfa and J. Limtrakul. 2007. The adsorption of saturated and unsaturated hydrocarbons on nanostructured zeolites (H-MOR and H-FAU): An ONIOM study. **J. Mol. Catal. A: Chem.** 277(1-2):171-179.

Perdew, J.P. 1986. Density-functional approximation for the correlation energy of the inhomogeneous electron gas. **Phys. Rev. B.** 33:8822–8824.

Poutsma, M.L. and J. A. Rabo. 1979. **In zeolite chemistry and catalysis.** Chapter 8. ACS No. 171, Washington, DC.

Rappé, A.K., C.J. Casewit, K.S. Colwell, W.A. Goddard III and W.M. Skiff. 1992. UFF, a full periodic table force field for molecular mechanics and molecular dynamics simulations. **J. Am. Chem. Soc.** 114(25):10024-10035.

Reddy, K.S.N., B.S. Rao and V.P. Shiralkar. 1993. Alkylation of benzene with isopropanol over zeolite beta. **App. Catal. A: Gen.** 95(1):53-63.

Rigby, A.M., G.J. Kramer and R.A. van Santen. 1997. Mechanisms of hydrocarbon conversion in zeolites: A quantum mechanical study. **J. Catal.** 170(1):1-10.

Rozanska, X., T. Demuth, R.A. van Santen, F. Hutschka and J. Hafner. 2002. A periodic structure density functional theory study of propylene chemisorption in acidic chabazite: Effect of zeolite structure relaxation. **J. Phys. Chem. B** 106(12):3248-3254.

Ryder, J.A., A.K. Chakraborty and A.T. Bell. 2000. Density functional theory study of proton mobility in zeolites: Proton migration and hydrogen exchange in ZSM-5. **J. Phys. Chem. B** 104(30):6998-7011.

Sauer, J. 1989. Molecular models in ab initio studies of solids and surfaces: From ionic crystals and semiconductors to catalysts. **Chem. Rev.** 89(1):199-255.

______, P. Ugliengo, E. Garrone and V.R. Saunders. 1994. Theoretical study of van der Waals complexes at surface sites in comparison with the experiment. **Chem. Rev.** 94(7):2095-2160.

Schoofs, B., J. Schuermans and R.A. Schoonheydt. 2000. Hydrogen-deuterium exchange reactions with isobutane over acid zeolites. **Micro. Meso. Mat.** 35-36:99-111.

Solans-Monfort, X., J. Bertran, V. Branchadell and M. Sodupe. 2002. Keto-enol isomerization of acetaldehyde in H-ZSM-5. A theoretical study using the ONIOM2 method. **J. Phys. Chem. B** 106(39):10220-10226.

Sommer, J., D. Habermacher, R. Jost, A. Sassi, A.G. Stepanov, M.V. Luzgin, D. Freude, H. Ernst and J. Martens. 1999. Activation of small alkanes on solid acids. An H/D exchange study by liquid and solid-state NMR: The activation energy and the inhibiting effect of carbon monoxide. **J. Catal.** 181(2):265-270.

______, M. Hachoumy, F. Garin, D. Barthomeuf and J. Vedrine. 1995. Alkene formation during low-temperature alkane activation on various solid acids or superacids. **J. Am. Chem. Soc.** 117(3):1135-1136.

Stepanov, A.G., S.S. Arzumanov, M.V. Luzgin, H. Ernst, D. Freude and V.N. Parmon. 2005. In situ ^{1}H and ^{13}C MAS NMR study of the mechanism of H/D exchange for deuterated propane adsorbed on H-ZSM-5. **J. Catal.** 235(1):221-228.

Stepanov, A.G., H. Ernst and D. Freude. 1998. In situ ^{1}H MAS NMR studies of the H/D exchange of deuterated propane adsorbed on zeolite H-ZSM-5. **Catal. Lett.** 54(3-4):1-4.

Svensson, M., S. Humbel, R.D.J. Froese, T. Matsubara, S. Sieber and K. Morokuma. 1996. ONIOM: A multilayered integrated MO + MM method for geometry optimizations and single point energy predictions. A test for Diels-Alder reactions and $Pt(P(t\text{-}Bu)_3)_2$ + H_2 oxidative addition. **J. Phys. Chem.** 100(50): 19357-19363.

Tal'roze, V.L. and A.L. Lyubimova. 1953. **Chem. Abstr.** vol. 47:2590.

van Bokhoven, J.A., M. Tromp, D.C. Koningsberger, J.T. Miller, J.A.Z. Pieterse, J.A. Lercher, B.A. Williams and H.H. Kung. 2001. An explanation for the enhanced activity for light alkane conversion in mildly steam dealuminated mordenite: The dominant role of adsorption. **J. Catal.** 202(1):129-140.

______, B.A. Williams, W. Ji, D.C. Koningsberger, H.H. Kung and J.T. Miller. 2004. Observation of a compensation relation for monomolecular alkane cracking by zeolites: The dominant role of reactant sorption. **J. Catal.** 224(1):50-59.

van Santen, R.A. and G.J. Kramer. 1995. Reactivity theory of zeolitic Brønsted acidic sites. **Chem. Rev.** 95(3):637-660.

Voorhis, T.V. and G.E. Scuseria. 1998. A novel form for the exchange-correlation energy functional. **J. Chem. Phys.** 109: 400-410.

Vosko, S.H., L. Wilk and M. Nusair. 1980. Accurate spin-dependent electron liquid correlation energies for local spin density calculations: a critical analysis. **Can. J. Phys.** 58(8):1200-1211.

Weitkamp, J. and Y. Traa. 1999. Isobutane/butene alkylation on solid catalysts. Where do we stand? **Catal. Today** 49(1-3):193-199.

Xu, B., S. Bordiga, R. Prins and J.A. van Bokhoven. 2007. Effect of framework Si/Al ratio and extra-framework aluminum on the catalytic activity of Y zeolite. **Appl. Catal. A: Gen.** 333(2):245-253.

______, F. Rotunno, S. Bordiga, R. Prins and J.A. van Bokhoven. 2006. Reversibility of structural collapse in zeolite Y: Alkane cracking and characterization. **J. Catal.** 241(1):66-73.

______, C. Sievers, S.B. Hong, R. Prins and J.A. van Bokhoven. 2006. Catalytic activity of Brønsted acid sites in zeolites: Intrinsic activity, rate-limiting step, and influence of the local structure of the acid sites. **J. Catal.** 244(2):163-168.

Zhao, Y., N.E. Schultz and D.G. Truhlar. 2005. Exchange-correlation functional with broad accuracy for metallic and nonmetallic compounds, kinetics, and noncovalent interactions. **J. Chem. Phys.** 123:161103-161106.

______, ______, and ______. 2006. Design of density functionals by combining the method of constraint satisfaction with parametrization for thermochemistry, thermochemical kinetics, and noncovalent interactions. **J. Chem. Theor. Comp.** 2(2):364-382.

______, and ______. 2006. Density functional for spectroscopy: No long-range self-interaction error, good performance for Rydberg and charge-transfer states, and better performance on average than B3LYP for ground states. **J. Phys. Chem. A** 110(49):13126-13130.

______, and ______. 2006. A new local density functional for main-group thermochemistry, transition metal bonding, thermochemical kinetics, and noncovalent interactions. **J. Chem. Phys.** 125(19): 194101-194118.

Zhao, Y. and D.G. Truhlar. 2008. Benchmark data for interactions in zeolite model complexes and their use for assessment and validation of electronic structure Methods. **J. Phys. Chem. C** 112(17):6860-6868.

______, and ______. 2008. Density functionals with broad applicability in chemistry. **Acc. Chem. Res.** 41(2):157-167.

______, and ______. 2008. The M06 suite of density functionals for main group thermochemistry, thermochemical kinetics, noncovalent interactions, excited states, and transition elements: Two new functionals and systematic testing of four M06-class functionals and 12 other functionals. **Theor. Chem. Acc.** 120(1-3):215-241.

Zheng, X. and P. Blowers. 2005. Reactivity of alkanes on zeolites: A computational study of propane conversion reactions. **J. Phys. Chem. A** 109(47):10734-10741.

______, and ______. 2005. A computational study of alkane hydrogen-exchange reactions on zeolites. **J. Mol. Catal. A: Chem.** 242(1-2):18-25.

______, and ______. 2005. An ab initio study of ethane conversion reactions on zeolites using the complete basis set composite energy method. **J. Mol. Catal A: Chem.** 229(1-2):77-85.

______, and ______. 2006. Reactivity of isobutane on zeolites: A first principles study. **J. Phys. Chem. A** 110(7):2455-2460.

Zicovich-Wilson, C.M., A. Corma and P. Viruela. 1994. Electronic confinement of molecules in microscopic pores. A new concept which contributes to explain the catalytic activity of zeolites. **J. Phys. Chem.** 98(42):10863-10870.

Zygmunt, S.A., L.A. Curtiss, P. Zapol and L.E. Iton. 2000. Ab initio and density functional study of the activation barrier for ethane cracking in cluster models of zeolite H-ZSM-5. **J. Phys. Chem. B** 104(9):1944-1949.

CURRICULUM VITAE

NAME : Mr. Sarawoot Impeng

BIRTH DATE : October 12, 1984

BIRTH PLACE : Sukhothai, Thailand

NATIONALITY : Thai

EDUCATION :

YEAR	INSTITUTION	DEGREE/DIPLOMA
2003-2007	Naresuan University	B.Sc. (Chemistry)

SCHOLARSHIPS : scholarship from the Commission on Higher Education, Ministry of Education, under the Postgraduate Education and Research Programs in Petroleum and Petrochemicals, and Advanced Materials (2007-2010)

CONFERENCES :

- **H/H Exchange Reaction of Propane Adsorbed over H-FAU Zeolite Investigated by ONIOM Method**
  Sarawoot Impeng, Thana Maihom, Somkiat Nokbin and Jumras Limtrakul. The Proceeding of 35th Congress on Science and Technology of Thailand, The Tide Resort, Bangsean Beach, Chonburi, Thailand, October 15-17, 2009. (Oral Presentation)

- **Propane Cracking reaction over Different Types of Nanostructured Zeolite: A Newly Developed DFT Approach**
  Sarawoot Impeng, Thana Maihom, Pipat Khongphacha, Somkiat Nokbin, and Jumras Limtrakul. Abstract of papers, the 239th ACS National Meeting

& Exposition, San Francisco, California, United State, March 21-25, 2010. (Poster Presentation)

- **Propane Cracking Reaction over H-FAU Zeolite: A Newly Developed DFT Study**

  Sarawoot Impeng, Thana Maihom, Pipat Khongphacha, Somkiat Nokbin, and Jumras Limtrakul. Abstract of papers, the 1st National Research Symposium on Petroleum, Petrochemicals, and Advanced Materials and the 16th PPC Symposium on Petroleum, Petrochemicals, and Polymers, Montien Hotel, Bangkok, Thailand, April 22, 2010. (Poster Presentation)